Caspase Regulation of Autophagy in *Drosophila melanogaster*

by

Lindsay Yvonne DeVorkin

B.Sc., University of British Columbia, 2008

Thesis Submitted In Partial Fulfillment of the
Requirements for the Degree of
Doctor of Philosophy

in the
Department of Molecular Biology and Biochemistry
Faculty of Science

© Lindsay DeVorkin 2013

SIMON FRASER UNIVERSITY

Spring 2013

All rights reserved.
However, in accordance with the *Copyright Act of Canada*, this work may be reproduced, without authorization, under the conditions for "Fair Dealing." Therefore, limited reproduction of this work for the purposes of private study, research, criticism, review and news reporting is likely to be in accordance with the law, particularly if cited appropriately.

Approval

Name: **Lindsay Yvonne DeVorkin**

Degree: **Doctor of Philosophy (Molecular Biology and Biochemistry)**

Title of Thesis: ***Caspase regulation of autophagy in Drosophila melanogaster***

Examining Committee: **Chair: Dr. Mark Brockman**
Associate Professor

Dr. Sharon Gorski
Senior Supervisor
Associate Professor

Dr. Nicholas Harden
Supervisor
Professor

Dr. Esther Verheyen
Supervisor
Professor

Dr. Gordon Rintoul
Internal Examiner
Associate Professor
Department of Biology

Dr. Kimberly McCall
External Examiner
Associate Professor
Biology, University of Boston

Date Defended/Approved: April 8th, 2013

Partial Copyright Licence

The author, whose copyright is declared on the title page of this work, has granted to Simon Fraser University the right to lend this thesis, project or extended essay to users of the Simon Fraser University Library, and to make partial or single copies only for such users or in response to a request from the library of any other university, or other educational institution, on its own behalf or for one of its users.

The author has further granted permission to Simon Fraser University to keep or make a digital copy for use in its circulating collection (currently available to the public at the "Institutional Repository" link of the SFU Library website (www.lib.sfu.ca) at http://summit/sfu.ca and, without changing the content, to translate the thesis/project or extended essays, if technically possible, to any medium or format for the purpose of preservation of the digital work.

The author has further agreed that permission for multiple copying of this work for scholarly purposes may be granted by either the author or the Dean of Graduate Studies.

It is understood that copying or publication of this work for financial gain shall not be allowed without the author's written permission.

Permission for public performance, or limited permission for private scholarly use, of any multimedia materials forming part of this work, may have been granted by the author. This information may be found on the separately catalogued multimedia material and in the signed Partial Copyright Licence.

While licensing SFU to permit the above uses, the author retains copyright in the thesis, project or extended essays, including the right to change the work for subsequent purposes, including editing and publishing the work in whole or in part, and licensing other parties, as the author may desire.

The original Partial Copyright Licence attesting to these terms, and signed by this author, may be found in the original bound copy of this work, retained in the Simon Fraser University Archive.

Simon Fraser University Library
Burnaby, British Columbia, Canada

revised Fall 2011

Abstract

Autophagy is an evolutionary conserved process whereby intracellular components are sequestered and delivered to lysosomes for degradation. Autophagy acts as a cell survival mechanism in response to stress, such as starvation, and also engages in a complex relationship with apoptosis. Understanding the crosstalk between autophagy and apoptosis is important, as it plays a critical role in the balance between survival and death, and has important implications in both normal development and human diseases.

To better understand the crosstalk between autophagy and apoptosis, I examined the role of the *Drosophila melanogaster* effector caspase Dcp-1 in starvation-induced autophagy during mid-oogenesis. I confirmed that Dcp-1 positively regulates starvation-induced autophagic flux in degenerating mid-stage egg chambers, and does so in a catalytically dependent manner. Dcp-1 candidate interactors/substrates, identified previously, were analyzed using *in vitro* autophagy assays to elucidate potential mechanisms related to Dcp-1-mediated autophagy. I identified 13 novel Dcp-1-associated regulators of starvation-induced autophagy, including the chloride intracellular channel protein Clic, the heat shock protein Hsp83, and the mitochondrial protein SesB. *In vivo* analyses revealed that Clic and Hsp83 act as negative regulators of autophagic flux following starvation during *Drosophila* oogenesis. Further investigation into the possible mitochondrial-related role of Dcp-1 in autophagy revealed that Dcp-1 partially localizes within the mitochondria where it functions to regulate mitochondrial network morphology and ATP levels, demonstrated both *in vitro* and *in vivo* during mid-oogenesis. Moreover, I found that the pro-form of Dcp-1 interacts with the adenine nucleotide translocase SesB, and as such, Dcp-1 does not cleave SesB but rather

affects its stability. In addition, I identified SesB as a novel negative regulator of autophagic flux during mid-oogenesis. Depletion of ATP or reduction of SesB levels rescued the autophagic defect in *Dcp-1* loss-of-function flies, and genetic interaction studies revealed that SesB acts downstream of Dcp-1 in the regulation of autophagy.

In conclusion, I found that non-apoptotic caspase activity is an important molecular mechanism underlying autophagy regulation and mitochondrial physiology *in vivo,* and have provided a foundation for further analyses involving Dcp-1-associated regulators of starvation-induced autophagy.

Keywords: *Drosophila*; autophagy; Dcp-1; oogenesis; cell death; mitochondria

To my dad,
whose too few years ignited my passion for research

Acknowledgements

First and foremost, I would like to thank my senior supervisor Dr. Sharon Gorski for her unwavering support, guidance, and advice throughout my graduate studies. It has been both a privilege and pleasure to have had the opportunity to develop scientifically in her laboratory. Thank you for your mentorship, patience and enthusiasm, and for the opportunity to work independently. I would also like to thank my committee members Drs. Nick Harden and Esther Verheyen for their valuable guidance, helpful comments and suggestions throughout my studies.

I would like to thank past and present members of the autophagy group at the Genome Sciences Center. In particular, I would like to thank Dr. Suganthi Chittaranjan for her support, advice and kindness, both professionally and personally. I would also like to thank Nancy Erro Go for all of her advice, help and expertise on several aspects of my thesis, and to Dudley Chung for his hard work optimizing *in vitro* assays. I thank Dr. Ian Bosdet for initially taking me on as a volunteer student in the Gorski lab, and to Dr. Claire Hou for teaching me many assays that have been instrumental to my studies. Thank you to all other Autophagy/PCD lab members for your advice and friendship.

I would like to thank Dr. Gregg Morin for advice and suggestions on my manuscript, and to the Sam Apricio lab, specifically John Fe and Elena Ostroumov, for confocal training and support.

Last but not least, I would like to thank my family and friends whose support and encouragement has made this work possible.

Table of Contents

List of Tables

List of Figures

List of Acronyms

ATP	Adenosine triphosphate
Atg	Autophagy-related
Bcl-2	B-cell lymphoma 2
Bax	Bcl-2-associated X protein
Bak	Bcl-2 activator or killer
CARD	Caspase activation recruitment domain
Caspase	Cysteine-dependent aspartate specific protease
CED	Cell death abnormal
CMA	Chaperon-mediated autophagy
DAPI	4'6-diamidino-2-phenylindole
Dcp-1	*Drosophila* Caspase-1
DED	Death effector domain
DEPTOR	DEP domain containing mTOR-interacting protein
DREDD	Death-related ced-3/Nedd-2-like
Dronc	Drosophila Nedd-2-like caspase
DRAQ5	1,5-bis{[2-(di-methylamino) ethyl]amino}-4, 8-dihydroxyanthracene-9,10-dione
Drice	*Drosophila* Interleukin-1β-Converting Enzyme
dsRNA	Double stranded ribonucleic acid
EGL	Egg laying defective
ER	Endoplasmic reticulum
FADD	Fas-associated protein with death domain
FBS	Fetal bovine serum
FIP200	200 kDa FAK family kinase-interacting protein
GFP	Green fluorescent protein
GST	Glutathione-S Transferase
Hsp	Heat shock protein
Hsc	Heat shock cognate
IAP	Inhibitor of apoptosis
JC-1	5,5',6,6'-tetrachloro-1,1',3,3' tetraethylbenzimidazolylcarbocyanine iodide
l(2)mbn	Lethal (2) malignant blood neoplasm
Lamp2a	Lysosome associated membrane protein type 2a
LC3	Microtubule-associated protein 1A/B light chain 3
LIR	LC3-interacting region
LTG	LysoTracker Green
LTR	LysoTracker Red
l(2)mbn	Lethal (2) malignant blood neoplasm
IP	Immuno-affinity purification
MDC	Monodansylcadaverine
MLST8/GβL	Mammalian LST8/G-protein-β-subunit like protein
MS	Mass spectrometry
NAO	10-nonyl acridine orange
PBS	Phosphate buffered saline
UAS	Upstream activating sequence
TUNEL	Terminal deoxynucelotidyl transferase dUTP nick end labelling
PCD	Programmed cell death

PE	Phosphatidylethanolamine
PI	Propidium iodide
PI3K	Phosphatidylinositol 3-kinase
PI3P	Phosphatidylinositol 3-phosphate
PRAS40	Proline-rich Akt/PKB substrate 40 kDa
PS	Phosphatidylserine
Ref(2)P	Refractory to sigma P
RFP	Red fluorescent protein
ROS	Reactive oxygen species
S2	Schenider 2
SesB	Stress sensitive B
Smac	Second mitochondrial-derived activator of caspase
TEM	Transmission electron microscopy
TOR	Target of rapamycin
UBD	Ubiquitin binding domain
Ulk1/2	Unc-51 like kinase 1/2
UVRAG	Ultraviolet irradiation resistance associated tumour suppressor gene
Vps	Vacuolar protein sorting

1. Introduction

1.1. Autophagy

Autophagy, a Greek term that literally means “self-eating”, is a cellular self-digestion process whereby long-lived proteins and organelles are degraded within lysosomes. Autophagy was first described more than 40 years ago (De Duve, 1963) and, to date, three forms of autophagy including microautophagy, chaperone-mediated autophagy (CMA) and macroautophagy have been described. Microautophagy involves the uptake of cytoplasmic material by direct invagination of the lysosome, or by the formation of arm-like extensions stemming from the lysosome (Ahlberg and Glaumann, 1985; Marzella et al., 1980). Little is known about the mechanism and regulation of microautophagy due to the current lack of approaches to detect the process aside from electron microscopy (Mijaljica et al., 2011). In CMA, all proteins to be degraded by the lysosome contain a pentapeptide KFERQ motif (Fred Dice, 1990) that is selectively recognized by the cytosolic chaperone Heat-shock cognate 70 (Hsc70) (Chiang et al., 1989). Hsc70 targets cytosolic proteins to the lysosome where lysosome-associated membrane protein type 2a (Lamp-2a) acts as a receptor for the substrate (Cuervo and Dice, 1996). Lysosomal Heat-shock cognate 73 (Hsc73) is required to translocate the substrate across the lysosomal membrane into the lysosomal matrix where the substrate is then degraded by lysosomal hydrolases (Cuervo et al., 1997). Macroautophagy, hereafter referred to as autophagy, is the most studied and well understood form of

Figure 1.1 Macroautophagy

The induction of macroautophagy (autophagy) involves the formation of a phagophore that sequesters cytoplasmic contents and organelles. Expansion and completion of the phagophore results in the formation of a double membrane structure called an autophagosome. Autophagosomes fuse with lysosomes, forming autolysosomes, where the cellular contents are degraded by acidic hydrolases and the resulting breakdown products are released back into the cell. The complete process of autophagy is referred to as autophagic flux.

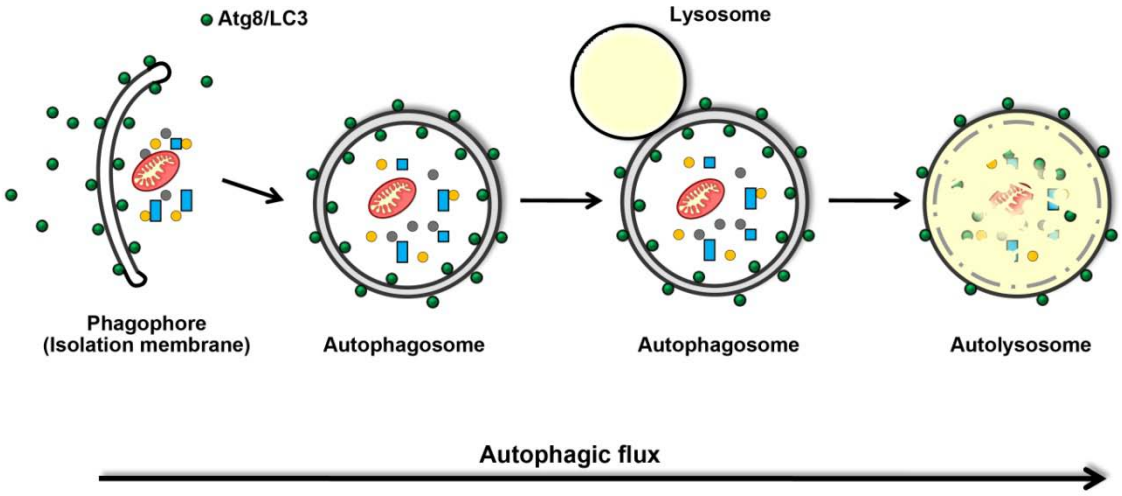
Atg8/LC3
Lysosome
Phagophore
(Isolation membrane)
Autophagosome
Autophagosome
Autolysosome
Autophagic flux

autophagy and will be the focus of this thesis. Using electron microscopy, the first morphological description of autophagy was performed by Clark (Clark, 1957) who observed cytoplasmic bodies and vacuoles in proximal tubules containing canalicular structures, altered mitochondria and dense lamellar inclusions. Subsequently, studies by Ashford and Porter revealed that sequestration of mitochondria by membrane structures led to their degradation in lysosomes in glucagon-treated hepatocytes (Ashford and Porter, 1962). The term “autophagy” was coined by Christian de Duve and colleagues (De Duve, 1963; de Duve and Wattiaux, 1966) who described the process of autophagy in rat liver hepatocytes following starvation. These studies, together with several others (Arstila and Trump, 1968; Dunn, 1990; Schworer and Mortimore, 1979), described the morphological aspects of autophagy, including the autophagosome and autolysosome (de Duve and Wattiaux, 1966). The process of autophagy involves the formation of double membrane structures called autophagosomes (Figure 1.1). Following fusion of autophagosomes with lysosomes to form autolysosomes, the cellular contents are degraded and the resulting breakdown products including amino acids, metabolites and metabolic precursors, are recycled back into the cell by lysosomal permeases (Rabinowitz and White, 2010; Yang and Klionsky, 2010). Autophagic flux, which refers to the complete process of autophagy, occurs at basal levels and is also upregulated in response to various cellular stresses, including nutrient deprivation (Filkins, 1970; Scott et al., 2004), chemotherapies (Bursch et al., 1996; Høyer-Hansen and Jäättelä, 2008; Kanzawa et al., 2003) and reactive oxygen species (ROS) (Chen et al., 2009; Scherz-Shouval et al., 2007). Autophagy provides constituents for energy production and protein synthesis during periods of stress to promote cell survival, and it removes toxic metabolites, harmful protein aggregates, and damaged organelles to maintain cellular integrity (Mizushima et al., 2011).

1.2. Molecular machinery of autophagy

Ohsumi and colleagues pioneered the molecular era of autophagy (Tsukada and Ohsumi, 1993). Proteinase deficient yeast accumulate autophagic bodies in vacuoles when transferred from nutrient rich media to nitrogen deficient media, and this accumulation can be monitored by light microscopy. Following EMS mutagenization, Ohsumi and colleagues screened for mutants unable to accumulate autophagic bodies following nitrogen starvation and identified 15 yeast mutants required for autophagy (Tsukada and Ohsumi, 1993). Further ultrastructural analysis revealed that the autophagic process is highly similar to that observed earlier in mammalian cells (Baba et al., 1994). Various screens were carried out to identify additional genes required for autophagy (Harding et al., 1995, 1996; Klionsky et al., 2003) and to date, more than 30 autophagy-related (Atg) genes have been identified (Klionsky et al., 2011), many of which are evolutionary conserved among higher eukaryotes. Atg genes encode proteins that are required for autophagy induction, autophagosome nucleation, vesicle expansion and completion (Mizushima, 2007) (Table 1.1, Figure 1.2). Although not completely understood, several models have now been proposed for the origin of the phagophore, the isolation membrane required to sequester cytoplasmic contents during autophagy. Following amino acid starvation, phosphatidylinositol 3-phosphate (PI(3)P)-rich membrane structures called omegasomes are in dynamic equilibrium with the endoplasmic reticulum (ER) and serve as a platform for autophagosome expansion and completion (Axe et al., 2008). In addition, the outer leaflet of the mitochondrial membrane (Hailey et al., 2010) and the plasma membrane (Ravikumar et al., 2010) were also proposed to be membrane sources for autophagosomes. The molecular

machinery of autophagy is well conserved from yeast to mammals and will be discussed in greater detail below.

1.2.1. Autophagy induction

Autophagy induction is a tightly regulated process involving an input of diverse signals including nutrients, growth factors and adenosine triphosphate (ATP). These signals often converge on the Target Of Rapamycin (TOR) kinase, a negative regulator of autophagy and positive regulator of cellular processes including ribosome biogenesis, protein synthesis and cell growth (Díaz-Troya et al., 2008). Autophagy induction is mediated by the conserved serine/threonine kinase Atg1 (Kamada et al., 2000). In yeast, under nutrient rich conditions TOR hyperphosphorylates Atg13 (which is bound to Atg17, Atg31 and Atg29), preventing its association with Atg1 and thereby inhibiting autophagy (Figure 1.2 A) (Chang and Neufeld, 2010; Kamada et al., 2010). TOR is inhibited following starvation leading to Atg13 dephosphorylation, Atg1 autophosphorylation and association of Atg1 with Atg13 (Kamada et al., 2010). Atg1 is required to recruit downstream Atg proteins to the pre-autophagosomal structure (PAS) to promote autophagosome formation (Kawamata et al., 2008). In *Drosophila*, a TOR-Atg1-Atg13 complex forms irrespective of nutrient status (Figure 1.2 A) (Chang and Neufeld, 2010). TOR phosphorylates Atg13 and hyperphosphorylates Atg1 under nutrient rich conditions to inhibit autophagy. Starvation inhibits TOR, leading to dephosphorylation of Atg1 and Atg13. In turn, Atg1 autophosphorylates itself and hyperphosphorylates Atg13 (Chang and Neufeld, 2010). Atg1 signaling in turn regulates the recruitment of PI(3)P to nascent autophagosomes (Juhász et al., 2008). In mammals, TOR is part of a complex referred to as mammalian TOR complex1 (mTORC1). mTORC1 is made up of regulatory-associated protein of mTOR (Raptor),

Table 1.1 Conservation of Atg genes involved in autophagosome induction, nucleation and expansion (Klionsky et al., 2011)

Yeast Gene	Drosophila Gene	Mammalian Gene	Function	Step in autophagy
Atg1	*DmAtg1*	*Ulk1, Ulk2*	Conserved serine/threonine kinase	Induction
Atg3	*DmAtg3*	*Atg3*	E2-like enzyme involved in Atg8 conjugation to PE	Expansion
Atg4	*DmAtg4*	*Atg4A, B, C, D*	Conserved cysteine protease that cleaves the C-terminal residue of Atg8 to expose a glycine residue. Also involved in deconjugation and recycling of Atg8 from the autophagosomal membrane	Expansion
Atg5	*DmAtg5*	*Atg5*	Undergoes conjugation with Atg12, forming a multi-protein complex together with Atg16 and required for autophagosome formation	Expansion
Atg6	*DmAtg6*	*Becn1*	Component of the Class III PI3K complex required for autophagosome formation	Nucleation
Atg7	*DmAtg7*	*Atg7*	E1-like enzyme that mediates the conjugation of Atg5 to Atg12 and Atg8 to PE	Expansion
Atg8	*DmAtg8a, DmAtg8b*	*LC3, GABARAP, GABARAPL2*	A ubiquitin like protein that is conjugated to PE and inserted into the autophagosomal membrane	Expansion
Atg10	*CG12821*	*Atg10*	E2-like enzyme involved in Atg5 conjugation to Atg12	Expansion
Atg12	*DmAtg12*	*Atg12*	Undergoes conjugation with Atg5, forming a multi-protein complex consisting of Atg12-Atg5-Atg16	Expansion
Atg13	*Atg13*	*HARBI1*	Component of the Atg1 kinase complex and is required for Atg1 kinase activity	Induction
Atg16	*CG31033*	*Atg16L1, Atg16L2*	Interacts with Atg5-Atg12 to form a Atg16-Atg5-Atg12 multiprotein complex required for autophagosome formation	Expansion
Atg17	-	-	Yeast component of the Atg1 kinase complex	Induction
Atg29	-	-	Yeast component of the Atg1 kinase complex required for autophagy	Induction
Atg31	-	-	Yeast component of the Atg1 kinase complex and is required for protein recruitment	Induction

mammalian LST8/G-protein β-subunit like protein (mLST8/GβL), Proline-rich Akt/PKB substrate 40 kDa (PRAS40) and DEP domain containing mTOR-interacting protein (DEPTOR). Under nutrient rich conditions, mTORC1 phosphorylates Atg13 and the mammalian homologues of yeast Atg1, Unc-51-like kinase 1/2 (Ulk1/2), leading to inhibition of Ulk kinase activity and a block in autophagy (Figure 1.2 A) (Jung et al., 2009). Several components make up the Ulk complex irrespective of nutrient status or mTOR activation, and include Ulk1 or Ulk2, Atg13, FIP200 and Atg101 (Ganley et al., 2009; Hosokawa et al., 2009). Atg13 binds Ulk1/2 to promote the interaction between Ulk proteins and FIP200 (Jung et al., 2009). Following induction of autophagy, mTOR is inhibited and dissociates from the Ulk complex, leading to Ulk1/2 and Atg13 dephosphorylation and phosphorylation of FIP200 by Ulk1 (Jung et al., 2009). It is speculated that FIP200 is the functional mammalian counterpart of yeast Atg17 (Ganley et al., 2009; Hara and Mizushima, 2009) however further studies are required to confirm this. Upon autophagy induction, the Ulk1 complex translocates from the cytoplasm to the ER to form a putative mammalian PAS (Itakura and Mizushima, 2010; Mizushima et al., 2011). The exact mechanism of how the Atg1 complex controls the PI3K complex required for vesicle nucleation remains to be elucidated (Mizushima et al., 2011).

1.2.2. Vesicle nucleation

Vesicle nucleation requires the Class III phosphatidylinositol 3-kinase (PI3K) Vps34 to generate PI(3)P in yeast, *Drosophila* and mammals (Juhász et al., 2008; Kihara et al., 2001; Petiot et al., 2000). In yeast and *Drosophila*, activation of Vps34 requires the formation of a multi-protein complex that includes Atg6, Vps15, Atg14 and Vsp34 (Figure 1.2 B) (Kihara et al., 2001; Vanhaesebroeck et al., 2010). In mammals, the multi-protein Class III PI3K complex composed of Beclin 1 (the mammalian homolog of yeast Atg 6),

Figure 1.2 Molecular machinery of autophagy.

Autophagy induction, vesicle nucleation and vesicle elongation are required for autophagosome formation, and the molecular machinery involved is evolutionarily conserved. **(A)** Autophagy induction is regulated by TOR kinase. TOR regulates the phosphorylation status of Atg13 and Atg1 to induce autophagy. Inhibition of TOR, for example by nutrient deprivation, leads to dephosphorylation of Atg13 in yeast, and to dephosphorylation of Atg13 and Atg1/Ulk1/Ulk2 in *Drosophila* and mammals, resulting in autophosphorylation of Atg1 and induction of autophagy. **(B)** Vps34, the Class III phosphatidylinositol 3 kinase (PI3K), generates phosphatidylinositol 3-phosphate (PI3P) and is required for vesicle nucleation. Activation of this complex is dependent on Atg6/Beclin 1 in yeast and mammals, as well as Ambra1 and UVRAG in mammals. **(C)** Two well conserved ubiquitin-like conjugation systems are required for autophagosome elongation. Atg12 is conjugated to Atg5, which in turn interacts with Atg16 to form an Atg12-Atg5-Atg16 complex that localizes to growing autophagosomes. In the second conjugation pathway, LC3, or the yeast homolog Atg8, is cleaved by the cysteine protease Atg4 to reveal a C-terminal glycine residue. This is followed by LC3 conjugation to phosphatidylethanolamine (PE), and localization of LC3 to autophagosomal membranes. Adapted from (Chen and Klionsky, 2011; Maiuri et al., 2007a; Meléndez and Neufeld, 2008).

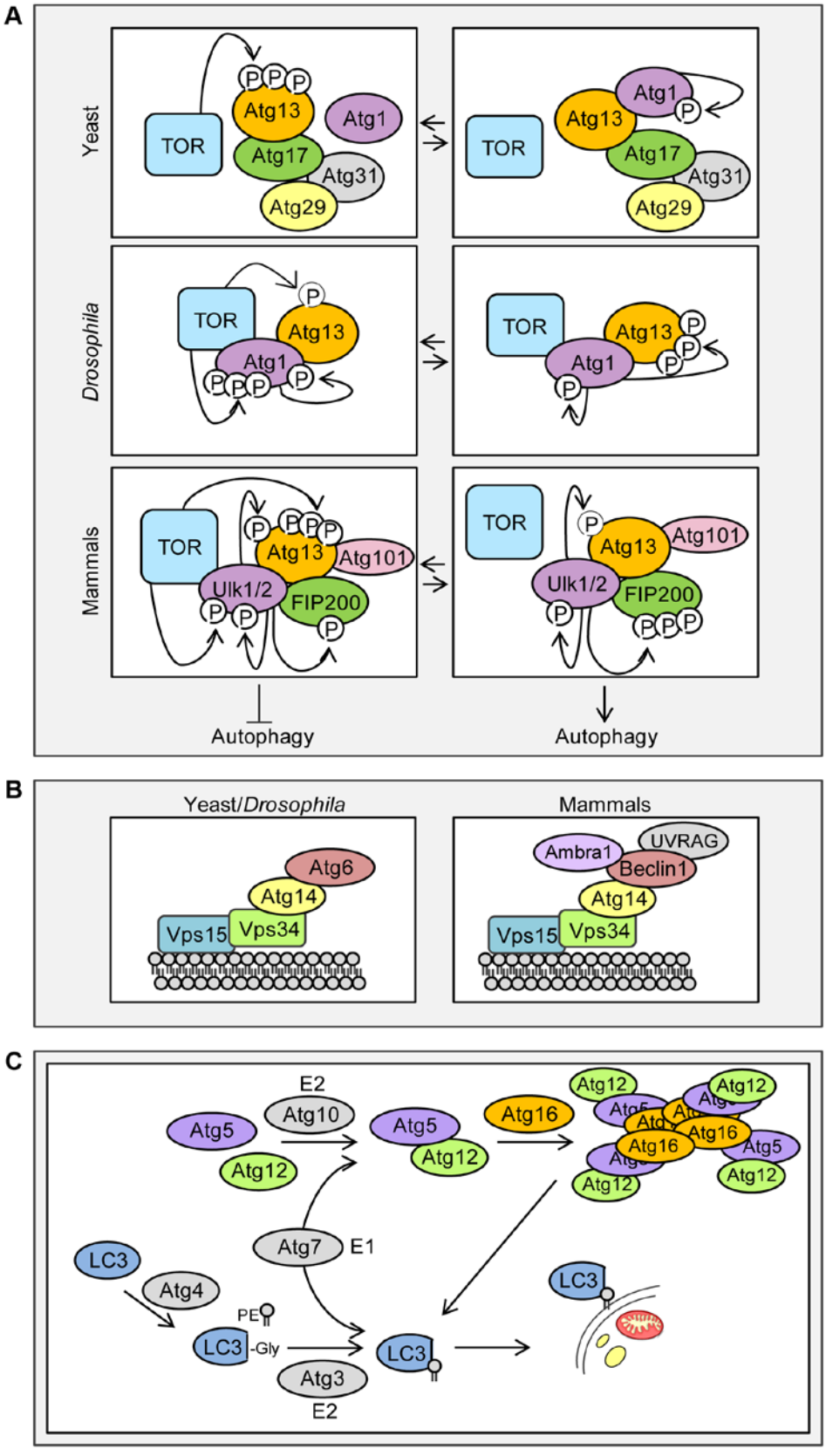
A
Yeast
TOR
Atg13
Atg1
Atg17
Atg31
Atg29
Drosophila
Mammals
Atg101
Ulk1/2
FIP200
Autophagy
B
Yeast/Drosophila
Mammals
Atg6
Atg14
Vps15
Vps34
Ambra1
UVRAG
Beclin1
C
E2
Atg10
Atg5
Atg12
Atg16
Atg7
E1
LC3
Atg4
PE
LC3-Gly
Atg3
E2

Vps34 and Vps15 functions at different steps in membrane formation (Funderburk et al., 2010). When Atg14L is bound to the Class III PI3K complex it promotes the formation of nascent autophagosomes (Matsunaga et al., 2009), whereas binding of UVRAG to Beclin 1 promotes autophagosome formation, autophagosome fusion with lysosomes and endocytic trafficking (Liang et al., 2008). Ambra1 is a Beclin 1 interacting protein, and upon autophagy induction, Ulk1 phosphorylates Ambra1 allowing translocation of the Beclin 1 complex to the ER to promote autophagosome formation (Bartolomeo et al., 2010), thereby linking autophagy induction to vesicle nucleation.

1.2.3. Vesicle expansion and completion

Two ubiquitin-like pathways exist to promote autophagosome elongation and completion (Figure 1.2 C). In one pathway, Atg12 is activated by the E1-like enzyme Atg7 and is transferred to the E2-like enzyme Atg10. Atg12 is then conjugated to Atg5, which in turn interacts with Atg16 forming an Atg12-Atg5-Atg16 multimeric complex that localizes to autophagosome assembly sites (Romanov et al., 2012; Shintani et al., 1999). In the second pathway, the cysteine protease Atg4 cleaves pro-Atg8/LC3 to expose a C-terminal glycine residue, forming Atg8/LC3-I (Kabeya et al., 2000; Tanida et al., 2004a). Atg8/LC3-I is activated by Atg7 and is transferred to the E2-like enzyme Atg3. Subsequently, Atg8/LC3-I is conjugated to phosphatidylethanolamine (PE), forming Atg8/LC3-II, and is inserted into the autophagosomal membrane (Ichimura et al., 2000; Kabeya et al., 2000). The Atg12-Atg5-Atg16 complex is required for Atg8/LC3 conjugation to PE and is involved in targeting Atg8/LC3 to the autophagosome membrane (Fujita et al., 2008; Hanada et al., 2007). Following vesicle completion, autophagosomes fuse with lysosomes, forming autolysosomes, and the sequestered components are degraded by lysosomal hydrolases. The digested components,

including building blocks for macromolecular synthesis and metabolites for energy production, are released into the cytosol by lysosomal efflux transporters (Mizushima, 2007). Atg8/LC3-II located within the autolysosome is also degraded in the hydrolytic compartment, whereas Atg8/LC3-II on the cytoplasmic side of the autolysosome is recycled in an Atg4 dependent manner (Tanida et al., 2004b).

1.3. Methods to detect autophagy in *Drosophila*

Drosophila melanogaster is a powerful model system to study the dynamic process of autophagy. Several advances in genetic and molecular tools in *Drosophila* have made this system amenable to the detection and manipulation of autophagy *in vivo*. Studies in *Drosophila* have also helped to elucidate the roles of autophagy in cell survival, cell death, development, immunity, aging and cellular homeostasis, aiding our understanding of the links between autophagy and human diseases (for review see (McPhee and Baehrecke, 2009). There are several techniques and assays now available in yeast, *Drosophila,* mammals and other organisms to monitor the induction of autophagy and flux through the autophagy process (Klionsky et al., 2012). Many tools used to monitor autophagy in *Drosophila* were derived from yeast and mammalian systems, and include LysoTracker/monodansylcadaverine staining, p62 analyses, GFP-Atg8/LC3, and GFP-RFP-Atg8/LC3 analyses, all of which are described in greater detail below.

LysoTracker and monodansylcadaverine (MDC) are acidotropic dyes that label both autolysosomes and lysosomes (Klionsky et al., 2012), and although LysoTracker has been beneficial for examining autophagic activity in *Drosophila* cell culture (Hou et al., 2008), as well as in several tissues including the fat body (Scott et al., 2004), midgut

(Ren et al., 2009), salivary gland (Berry and Baehrecke, 2007) and ovary (Barth et al., 2011; Hou et al., 2008), it is not specific for autophagy. Therefore, LysoTracker or MDC are useful as initial indicators of potential autophagy-associated lysosomal activity but must be used in combination with other autophagic flux markers.

Mammalian p62 is a multifunctional scaffold protein involved in various cellular signalling pathways including stress responses and autophagy (Moscat and Diaz-Meco, 2009). p62 contains a ubiquitin-binding domain (UBD) and an LC3-interacting region (LIR) that functions to target ubiquitinated proteins for degradation by autophagy (Geetha and Wooten, 2002; Pankiv et al., 2007). In the process, p62 is selectively degraded by autophagy and therefore serves as a marker of autophagic flux (Pankiv et al., 2007). The single *Drosophila* ortholog of p62, Refractory to sigma P (Ref(2)P), was first characterized for its ability to inhibit sigma rhabdovirus multiplication (Dezelee et al., 1989; Nezis et al., 2008; Wyers et al., 1993). Inhibition of autophagy leads to an accumulation of Ref(2)P positive protein aggregates (Bartlett et al., 2011; Cumming et al., 2008; Nezis et al., 2008), indicating that, like mammalian p62, it is a substrate of autophagy and can be used as a marker of autophagic activity. Caution must be used when examining Ref(2)P because Ref(2)P was shown to accumulate following genetic inhibition of the proteasome (Nezis et al., 2008), suggesting that Ref(2)P has a dual role in degrading ubiquitinated proteins by autophagy and the proteasome. In addition, Ref(2)P was transcriptionally upregulated in the larval fat body following starvation (Pircs et al., 2012), indicating that Ref(2)P should be used in conjunction with other autophagy assays to confirm autophagic flux.

Several *Drosophila* transgenic lines have been created that express Atg8a (DrAtg8a) or mammalian LC3 fused to GFP (Rusten et al., 2007), mCherry (Nezis et al.,

2009) or dual-tagged GFP-mCherry (Nezis et al., 2010). GFP fused to Atg8/LC3 has proven useful as a marker of autophagy in *Drosophila*. Under non-autophagy inducing conditions, GFP-LC3/Atg8 is dispersed throughout the cytoplasm (Hou et al., 2008). When autophagy is induced, for example by starvation, Atg8/LC3 becomes lipidated and inserted into the autophagosome, thus appearing as green puncta (Hou et al., 2008; Juhász et al., 2008). Although GFP-Atg8 is an indicator of autophagic activity, an increase in GFP-Atg8 puncta may represent an increase in flux through the system or a block in the fusion step between autophagosomes and lysosomes, thus leading to an accumulation of autophagosomes (Klionsky et al., 2012). To distinguish between these possibilities, a dual-tagged GFP-mCherry-Atg8a/LC3 can be used. GFP fluorescence is sensitive to acidic conditions and its fluorescence is quenched in the autolysosome, whereas mCherry (or RFP) fluorescence is more stable (Kimura et al., 2007). Therefore autophagosomes will fluoresce as yellow puncta (overlap of green and red fluorescence), whereas autolysosomes will fluoresce as red puncta (Nezis et al., 2010). The dual tagged GFP-mCherry-Atg8a reporter is advantageous because it enables both the detection of autophagy induction and flux through the system. In addition to the dual tagged reporter, the use of GFP-Atg8 in combination with LTR has been used to help assess the delivery of autophagosomes to autolysosomes (Rusten et al., 2004).

1.4. Autophagy in *Drosophila*

Autophagy contributes to multiple processes in *Drosophila*, including degradation of larval tissues such as the salivary gland (Berry and Baehrecke, 2007) and midgut (Denton et al., 2009), and elimination of the amnioserosa during embryogenesis (Mohseni et al., 2009). In *Drosophila*, autophagy also plays critical roles in innate

immunity (Shelly et al., 2009), protein aggregate clearance, neuronal homeostasis, and longevity (Juhasz and Neufeld, 2008; Simonsen et al., 2008). Autophagy is regulated by hormones and various signaling pathways during *Drosophila* development (Calamita and Fanto, 2011; Lee and Baehrecke, 2001; Rusten et al., 2004) and also by exogenous factors such as nutrients. During nutrient deprivation autophagy functions, at least in part, to remobilize nutrients to promote cell survival, and thus is considered an adaptive survival response to cell stress. Starvation-induced autophagy has been described in the larval fat body (Scott et al., 2004), the midgut (Wu et al., 2009) and the ovary (Barth et al., 2011; Hou et al., 2008). The focus of my thesis will be starvation induced autophagy in the ovary.

1.4.1. Drosophila oogenesis and autophagy

The *Drosophila* ovary is sensitive to nutritional cues and has been a beneficial system to examine the role of autophagy and its relationship with cell death. The *Drosophila* ovary is made up of 15-20 ovarioles, each containing a series of developing egg chambers that arise from the germarium and progress posteriorly through 14 well-defined stages (King, 1970) (Figure 1.3, Figure 1.6A). Germline stem cells are located in region 1 of the germarium and divide asymmetrically to produce one germline stem cell that remains in its niche and one daughter cytocyst. Following its posterior movement to region 2a of the germarium, the daughter cytoblast undergoes 4 rounds of mitosis with incomplete cytokinesis to form a 16-cell cyst that remains interconnected by ring canals (Spradling,1993). One cell in each cyst differentiates into an oocyte and the remaining 15 cells become polyploid nurse cells required to support the development of the oocyte. As the cyst continues to migrate posteriorly in the germarium, it flattens to form a lens shaped disc at the 2a/2b region where it is then encapsulated by a

Figure 1.3 *Drosophila* oogenesis

A schematic of *Drosophila* oogenesis. Anterior is to the left, posterior is to the right. Egg chambers arise from the germarium and progress through 14 well defined stages. Each egg chamber is made up of 15 germline nurse cells and one developing oocyte that is located at the posterior of the egg chamber. Egg chambers are surrounded by a layer of somatically derived follicle cells. Germline stem cells located at the anterior of the germarium divide asymmetrically giving rise to one stem cell that remains in its niche and one daughter cytocyst. The cytocyst undergoes 4 rounds of mitosis to form a 16 cell cyst that moves posteriorly through the germarium. At the region 2a/2b boundary, the cyst is encapsulated in follicle cells and in region 3, it exits the germarium as a stage 1 egg chamber.

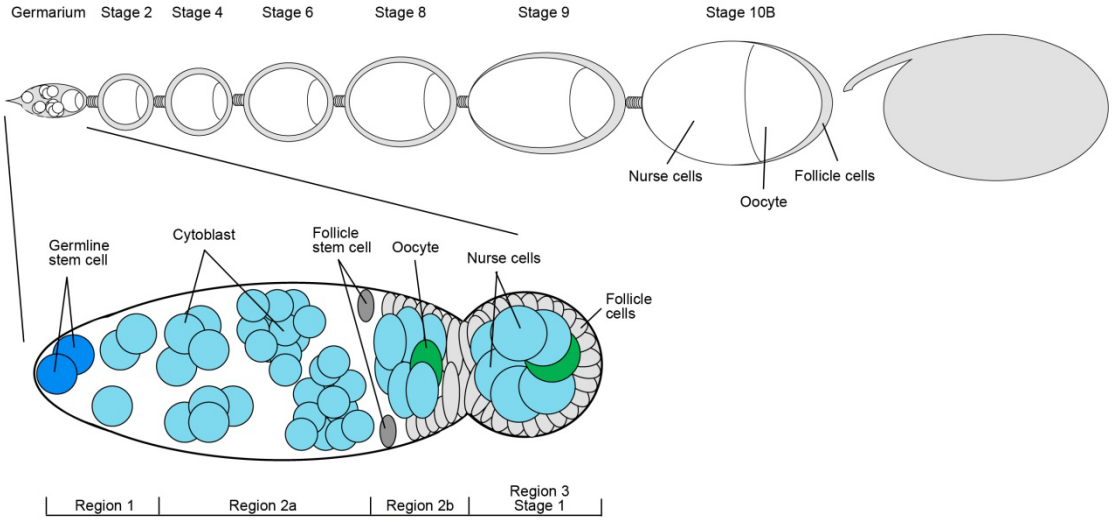
Germarium
Stage 2
Stage 4
Stage 6
Stage 8
Stage 9
Stage 10B
Nurse cells
Oocyte
Follicle cells
Germline stem cell
Cytoblast
Follicle stem cell
Oocyte
Nurse cells
Follicle cells
Region 1
Region 2a
Region 2b
Region 3 Stage 1

monolayer of somatically derived follicle cells. Two follicle stem cells (FSCs), one on each side of the ovary, divide asymmetrically to produce one FSC and one daughter follicle cell that will encase the developing cyst (Margolis and Spradling, 1995). Once encapsulated by follicle cells, the cyst enters an endoreplicative and growth phase and exits the germarium as a stage 1 egg chamber, consisting of 15 germline nurse cells and one oocyte surrounded by a layer of follicle cells (Spradling, 1993) (Figure 1.3). The germline nurse cells support the growth of the oocyte by transferring cytoplasmic contents to the oocyte as they progress through oogenesis. The oocyte begins to increase in volume at stage 8 and undergoes vitellogenesis, a process that involves yolk protein synthesis and uptake. During stage 10B, nurse cell cytoplasm is rapidly transported into the oocyte and by stage 14 when all of the nurse cell cytoplasm has been transferred, nurse cell nuclei condense and fragment, and nurse cell remnants are engulfed by the surrounding follicle cells (Foley and Cooley, 1998; Nezis et al., 2000). The fully developed oocyte is then encased in a vitelline membrane and chorion secreted by the follicle cells, and this is followed by follicle cell death (Nezis et al., 2002).

Using MDC staining and ultrastructural analyses, autophagy was first described to occur in mid-stage egg chambers (stage 7-9) undergoing spontaneous degeneration in *Drosophila virilis* (Velentzas et al., 2007). In *Drosophila melanogaster* oogenesis, autophagy occurs in both the germline and follicle cells under basal conditions and is upregulated in response to nutritional cues in the germarium and mid-stage egg chambers (Barth et al., 2011; Hou et al., 2008; Nezis et al., 2009). It has been proposed that autophagy is required for communication between follicle cells and the germline, as inhibition of autophagy in the follicle cells, but not the germline, leads to the formation of defective eggs (Barth et al., 2011). Autophagy also occurs during developmental cell

death during late stage oogenesis and is required for the normal maturation of the egg chambers. The focus of this thesis will be on starvation induced autophagy during mid-oogenesis.

1.5. Apoptosis

In contrast to the cell survival process of autophagy, apoptosis, a term derived from the Greek words “falling off”, refers to the morphological changes that occur during cellular self-destruction (Kerr et al., 1972). Apoptosis, or Type I programmed cell death (PCD), is a cellular homeostasis mechanism required to eliminate unnecessary cells during development and adulthood, and also occurs in response to a variety of cell death stimuli including starvation, ligation of cell surface receptors, growth factor withdrawal and DNA damage (Baehrecke, 2002). Apoptosis is morphologically characterized by cell shrinkage, nuclear fragmentation, chromatin condensation, membrane blebbing and the formation of apoptotic bodies (Kerr et al., 1972). Apoptotic bodies are phagocytosed by surrounding macrophages thereby preventing an inflammatory response and maintaining cellular integrity (Kerr et al., 1972).

Analysis of the genetic regulation of apoptosis in *Caenorhabditis elegans* led to the identification of 4 genes that control cell death, CED-3, CED-4, CED-9 and EGL-1 (Ellis and Horvitz, 1986; Gumienny et al., 1999; Sulston et al., 1983) (Figure 1.4). Cell death abnormal-3 (CED-3) is a cysteine-dependent aspartate-specific protease (caspase) that becomes activated following a cell death signal and is required for cell killing (Xue et al., 1996; Yuan et al., 1993). The pro-apoptotic protein CED-4 is an adaptor protein for CED-3 and is required for its activation (Yuan et al., 1993; Zou et al., 1997). CED-9, an anti-apoptotic B-cell lymphoma 2 (Bcl-2) family member, blocks cell

Figure 1.4 The apoptosis machinery is well conserved in *C. elegans*, *D. melanogaster* and mammals.

Functional homologs are indicated by the same colour across species. The inhibitor of apoptosis proteins (IAPs) negatively regulate apoptosis by inhibiting caspases. Caspase 9 in mammals and Dronc in *Drosophila* function as initiator caspases, whereas Caspase 3 and Caspase 7 in mammals, and Drice and Dcp-1 in *Drosophila* function as effector caspases. The IAP binding proteins Smac/Diablo in mammals and Reaper, Hid, Grim and Sickle in *Drosophila* activate apoptosis by inhibiting IAP proteins, thus allowing activation of caspases. CED-4, ARK and APAF-1 function as adaptor molecules for initiator caspases in *C. elegans*, mammals and *Drosophila,* respectively. *Drosophila* apoptosis can also be activated through the ligand Eiger and receptor Wengen. Apoptosis in mammalian cells is also mediated through the extrinsic, death receptor pathway. Adapted from (Riedl and Shi, 2004).

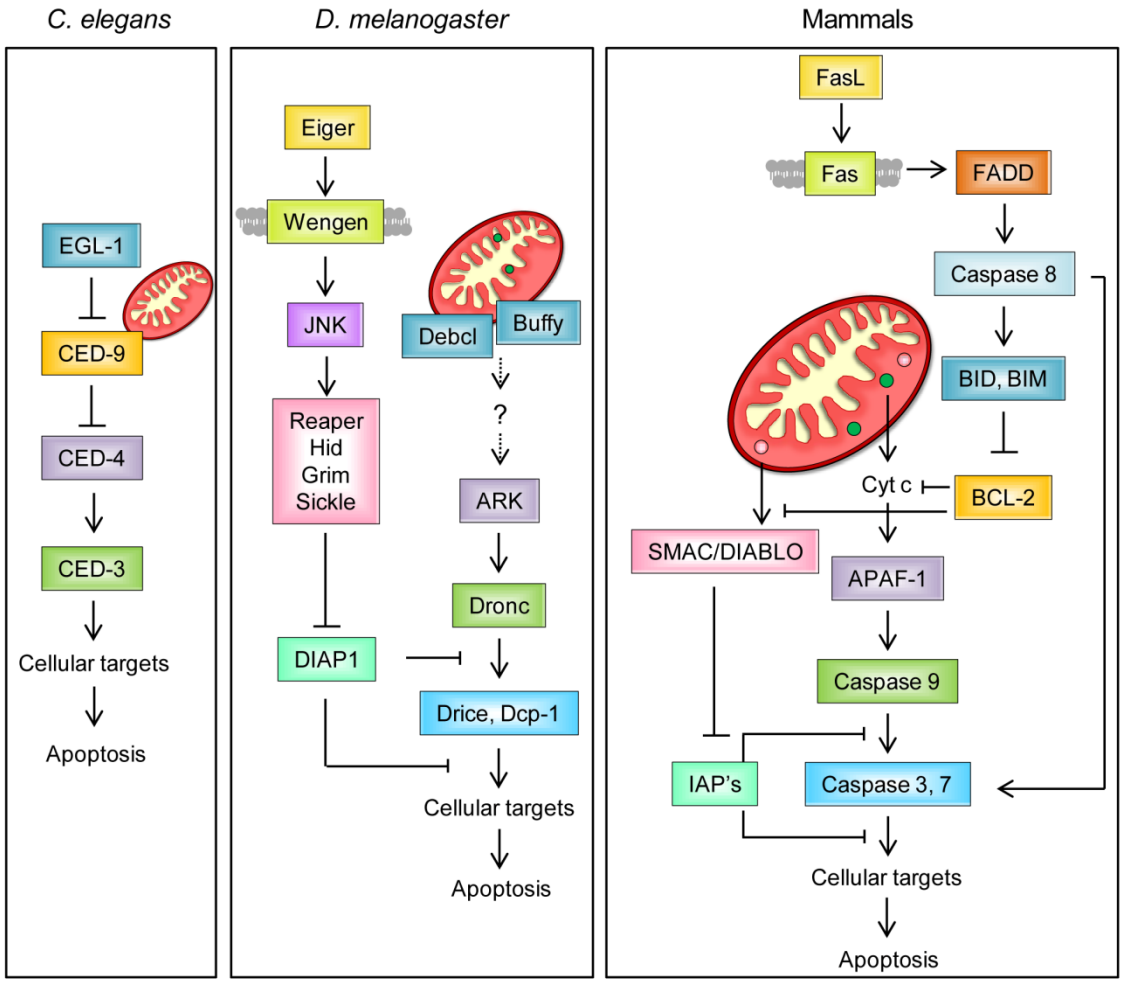
C. elegans
D. melanogaster
Mammals
EGL-1
CED-9
CED-4
CED-3
Cellular targets
Apoptosis
Eiger
Wengen
JNK
Reaper
Hid
Grim
Sickle
DIAP1
Debcl
Buffy
?
ARK
Dronc
Drice, Dcp-1
Cellular targets
Apoptosis
FasL
Fas
FADD
Caspase 8
BID, BIM
Cyt c
BCL-2
SMAC/DIABLO
APAF-1
Caspase 9
IAP's
Caspase 3, 7
Cellular targets
Apoptosis

death by sequestering CED-4 and thereby preventing CED-3 activation (Hengartner and Horvitz, 1994). In response to death inducing stimuli, the pro-apoptotic Bcl-2 family member Egg Laying Defecting (EGL)-1 disrupts the CED-4-CED-9 interaction, allowing the release of CED-4 and activation of CED-3 to induce cell death (Conradt and Horvitz, 1998). Subsequent studies in other organisms showed that these molecules are highly conserved regulators and effectors of apoptosis.

In *Drosophila*, the major initiators of cell death are the pro-apoptotic proteins Reaper, Hid, Grim and Sickle (Chen et al., 1996; Grether et al., 1995; Srinivasula et al., 2002; Wang et al., 1999; White et al., 1996) (Figure 1.4). Following a cell death signal, these proteins bind to the *Drosophila* inhibitor of apoptosis protein (IAP), DIAP1, via a well conserved IAP-binding tetrapeptide motif to induce DIAP1 degradation (Riedl and Shi, 2004; Yoo et al., 2002). DIAP1 is an E3-ubiquitin ligase and is required to restrain caspase activity in *Drosophila* cells by promoting the non-degradative ubiquitination of the initiator caspase Dronc (Wilson et al., 2002), and by binding and inhibiting the effector caspases *Drosophila* Interleukin-1β-Converting Enzyme (Drice) and *Drosophila* Caspase-1 (Dcp-1) (Tenev et al., 2005). DIAP1 is therefore essential for survival in *Drosophila* cells (Meier et al., 2000). Reaper, Hid and Grim have been shown to localize to mitochondria where they are required for the efficient induction of apoptosis (Krieser and White, 2009). Reaper, Hid, Grim and Sickle-mediated degradation of DIAP1 disrupts the DIAP1-caspase interaction allowing for caspase activation (Goyal et al., 2000). The initiator caspase Dronc interacts with Apaf-1 related killer (Ark), the *Drosophila* homolog of *C. elegans* CED-4 and mammalian apoptotic protease activating factor 1 (Apaf-1) leading to Dronc activation (Muro et al., 2004; Yuan et al., 2011). This activation is followed by Dronc mediated cleavage and activation of downstream effector

caspases including Drice and Dcp-1 to induce apoptosis. Two *Drosophila* Bcl-2 family members, Buffy and Debcl, were originally characterized to be anti- and pro-apoptotic proteins respectively (Colussi et al., 2000; Quinn et al., 2003), however more recent studies indicate that Buffy can act pro-apoptotically during microchaete and mid-stage ovarian cell death (Quinn et al., 2003; Tanner et al., 2011). Apoptosis can also be activated by the Drosophila TNF family ligand Eiger. Eiger binds to the receptor Wengen, leading to the activation of Misshapen (Msn). Activated Msn phosphorylates and activates Tak1, leading to activation of Hemipterous (Hep), which in turn phosphorylates and activates JNK leading to transcriptional upregulation of Hid and induction of cell death (Kanda and Miura, 2004).

In mammals, the process of apoptosis is controlled by an intrinsic or an extrinsic pathway both of which converge on the activation of effector Caspases 3 and 7. In the intrinsic pathway, activation of pro-apoptotic Bcl-2 associated X (Bax) or Bcl-2 antagonist or killer (Bak) leads to mitochondrial outer membrane permeabilization (MOMP) and release of pro-apoptotic proteins such as Cytochrome c and Second Mitochondrial-Derived Activator of Caspase (Smac)/Diablo from the mitochondrial intermembrane space (Degenhardt et al., 2002) (Figure 1.4). Cytochrome c along with ATP binds Apaf1 in the cytoplasm leading to the formation of the apoptosome (Jiang and Wang, 2000; Zou et al., 1997). Notably, Cytochrome c and mitochondrial outer membrane permeabilization do not seem to play a role in *Drosophila* apoptosis, however conflicting reports indicate that Cytochrome C may play an apoptotic role following overexpression of Reaper in *Drosophila* S2 cells (Kanuka et al., 1999; Tait and Green, 2010). The apoptosome recruits and activates initiator Caspase 9 which in turn cleaves downstream effector caspases to induce cell death (Saleh et al., 1999). Smac is an IAP binding

protein that binds XIAP1 via its IAP-binding tetrapeptide motif Ala-Val-Pro-Ile to relieve XIAP1 inhibition of Caspase 9 (Riedl and Shi, 2004). In the extrinsic pathway, ligand binding to death receptors induces death receptor ligation and recruitment of adaptor molecules such as FAS-associated death domain protein (FADD) (Bodmer et al., 2000; Kischkel et al., 2000). FADD then associates with pro-Caspase 8, an initiator caspase, via the death effector domain of FADD to form the death inducing signaling complex (DISC) (Kischkel et al., 1995). At the DISC, Caspase 8 undergoes autocatalytic activation leading to Caspase 8-mediated cleavage and activation of effector Caspase 3 and 7 in the absence of MOMP (Bodmer et al., 2000; Kischkel et al., 2000; Muzio et al., 1997; Stennicke et al., 1998). Mitochondrial apoptosis also occurs in a Caspase 8 dependent manner. Active Caspase 8 cleaves the pro-apoptotic Bcl-2 homology 3 (BH3)-interacting domain death agonist (Bid), leading to activation of Bid and its translocation to the mitochondria to induce MOMP (Li et al., 1998).

Although morphological features of apoptosis were first described in yeast in 1997 (Madeo et al., 1997), the validity of this finding has been under debate ever since. Nonetheless, it is well established that several components of the apoptotic machinery is conserved in yeast and a variety of intrinsic and extrinsic stimuli are capable of inducing apoptosis. For example, the yeast metacaspase Yca1p is required for cell death in response to oxygen stress, valproic acid and altered mRNA stability (Carmona-Gutierrez et al., 2010; Madeo et al., 2002; Mazzoni et al., 2005).

1.6. Caspases

Caspases are synthesized as inactive zymogens, also called pro-caspases, and are responsible for executing apoptosis following a cell death signal. Each caspase

consists of an N-terminal pro-domain of variable length followed by a large 20kDa (p20) and a small 10kDa (p10) subunit separated by a short linker region. The p20 subunit contains the catalytic active site consisting of the catalytic dyad residues Cys and His, whereas the p10 subunit contains several residues that form the substrate-binding groove (Pop and Salvesen, 2009). In *Drosophila*, there are 7 caspases that are divided into either initiator or effector caspases. Three initiator caspases, Death-related ced-3/Nedd2-like (Dredd), Drosophila Nedd-2-like caspase (Dronc) and Strica, have long N-terminal pro-domains that contain a caspase-activation recruitment domain (CARD) or a death effector domain (DED), whereas the four effector caspases Dcp-1, Drice, Decay and Damm, have short pro-domains (Hay and Guo, 2006). Initiator caspases are stable as monomers, and recruitment of initiator caspases to activation platforms including the apoptosome leads to increased caspase concentration and caspase activation by proximity-induced dimerization (Boatright and Salvesen, 2003). Activation of initiator caspases requires dimerization and occurs independently of cleavage of their interdomain region linking the p20 and p10 subunits (Boatright et al., 2003; Donepudi et al., 2003), although this is now a subject of debate as it was recently shown that both dimerization and cleavage are required for activation of the initiator Caspase 8 (Oberst et al., 2010). In contrast to initiator caspases, effector caspases are present as inactive zymogen dimers and activation requires cleavage of their interdomain linker (Boatright et al., 2003) (Figure 1.5 A-B). Cleavage of this linker region results in the rearrangement of essential loops (L1-L4) that function in substrate binding and favours the formation of the catalytic groove (Chai et al., 2001; Witkowski and Hardy, 2009) (Figure 1.5 B). Cleavage primes caspases for substrate or inhibitor binding, as shown for mammalian Caspase 7 (Chai et al., 2003). A caspase recognizes the substrate peptide sequence P_4-P_3-P_2-P_1-P_1', where P_1-P_1' is the scissile bond. Several factors determine whether a

Figure 1.5 Effector caspase processing.

(A) Shortly after synthesis, effector caspases dimerize in an inactive state. Cleavage between the p10 and p20 subunits allows for the rearrangement of essential loops and favours the formation of the catalytic active site. Removal of the N-terminal pro-domain stabilizes the active caspase. **(B)** A crystal structure of a Caspase 3 heterodimer bound to an inhibitor (shown in pink). The p20 and p10 subunits are shown in blue and orange ribbon representation, respectively. The N and C termni for the p20 and p10 subunits as well as the L1 to L4 loops are indicated Adapted with permission from Elsevier Limited: Mechanisms of caspase activation and Inhibition during apoptosis (Shi, 2002), copyright 2002. **(C)** A schematic representation of Dcp-1 and Drice. The red rectangle indicates the catalytic cysteine residue, and the four surface loops, N-terminal pro-domain, p20 and p10 subunits are indicated. The catalytic cysteine residue is located within the L2 loop and interdomain cleavage results in a conformational change of L2 promoting the formation of the catalytic active site. Interdomain cleavage sites of Dcp-1 and Drice are indicated by arrows.

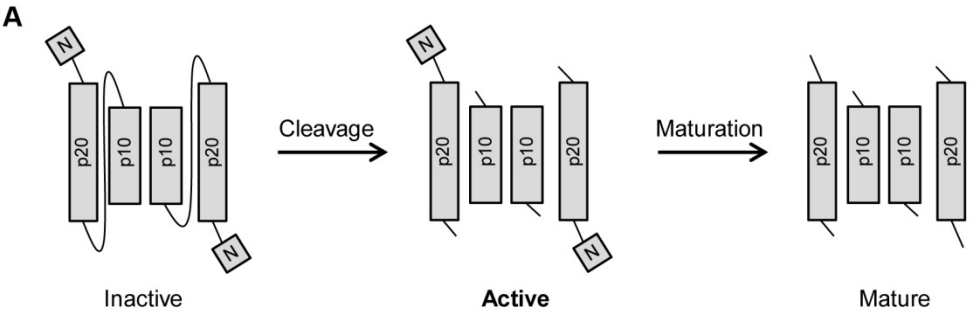
A
N
p20
p10
p10
p20
N
Cleavage
N
p20
p10
p10
p20
N
Maturation
p20
p10
p10
p20
Inactive
Active
Mature

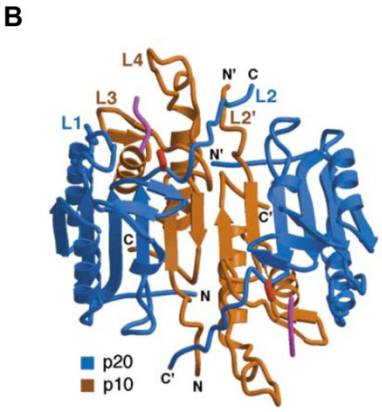
B
L4
N' C
L3
L2
L1
L2'
N'
C'
C
N
p20
p10
C'
N

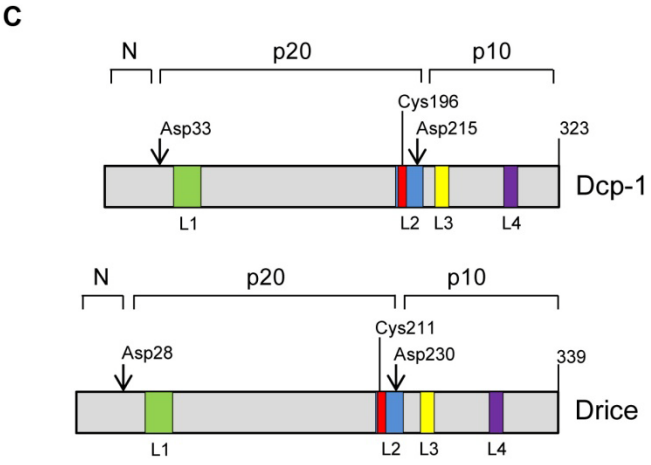
C
N
p20
p10
Cys196
Asp33
Asp215
323
Dcp-1
L1
L2
L3
L4
N
p20
p10
Cys211
Asp28
Asp230
339
Drice
L1
L2
L3
L4

.

protein will be a favourable caspase substrate. For example, P1 is usually an Asp residue, with the exception of Dronc which will cleave equally as well when P1 is a Glu (Hawkins et al., 2000; Stennicke et al., 1998). In addition, the P1' residue is a small, uncharged residue (Ser, Ala, Gly, Thr, Ser, Asn), and P_4-P_3-P_2 are residues that will interact favourably in the catalytic groove (Stennicke et al., 1998). For example, based on *in vitro* positional scanning peptide libraries, Caspase 3's preferred sequence is DEVD, however, it is now clear that Caspase 3 also cleaves at non-canonical sites (Thornberry et al., 1997; Nicholson, 1999). This suggests that although computational methods are useful for predicting caspase substrate preferences, the actual caspase substrate sequence may differ significantly and therefore must be validated. Maturation of caspases involves the removal of the N-terminal pro-domain resulting in caspase stability (Figure 1.5 A). Maturation occurs after activation and is a distinct process from caspase activation, as removal of the pro-domain without interdomain cleavage does not result in caspase activation (Pop and Salvesen, 2009).

1.6.1. Cell death in the *Drosophila* ovary

Cell death in the *Drosophila* ovary occurs at three developmental stages – the germarium, mid-oogenesis and late-oogenesis. Developmental cell death that occurs during late oogenesis is required for proper egg formation and involves the death of both the germline nurse cells and somatic follicle cells. The focus of this study will be on cell death during mid-oogenesis. The process of vitellogenesis is energy demanding and therefore a checkpoint exists during mid-oogenesis to prevent egg production in nutrient poor conditions (Drummond-Barbosa and Spradling, 2001). Mid-stage egg chambers undergoing cell death are characterized by nurse cell nuclei condensation and fragmentation (Figure 1.6C), engulfment of the nurse cell cytoplasm by the surrounding

follicle cells and follicle cell death (Giorgi and Deri, 1976) (Figure 1.6 D-E). In contrast to most other somatic tissues in *Drosophila*, the IAP binding proteins Reaper, Hid and Grim are not required for cell death in the ovary (Peterson et al., 2007), whereas the effector caspase Dcp-1 is required for cell death during mid-oogenesis. Nutrient deprived Dcp-1 null mutant flies (*Dcp-1*^{Prev1}) contain mid-stage egg chambers that are defective for cell death. These egg chambers have persisting, uncondensed nurse cell nuclei and follicle cells that undergo a pre-mature cell death (Laundrie et al., 2003) (Figure 1.6F). Although DIAP1 is downregulated during mid-oogenesis (Baum et al., 2007), it is not sufficient to induce cell death in a Dcp-1 wildtype background indicating that another upstream activator of Dcp-1, or downregulation of a negative regulator of Dcp-1, is required.

1.6.2. The Drosophila effector caspase Dcp-1

The *Drosophila* effector caspase Dcp-1 was first identified by degenerate PCR amplification from embryonic cDNA libraries (Song et al., 1997). Dcp-1 was found to be a 323 amino acid protein that undergoes proteolytic processing at Asp33 and Asp213 to form an active heterodimer (Song et al., 1997). Dcp-1 has a substrate specificity similarto that of mammalian Caspase 3 and *C. elegans* CED-3, and *in vitro* cleavage assays showed Dcp-1 can cleave caspase substrates including p35 and PARP (Song et al., 1997). Dcp-1 shares high sequence homology with the effector caspase Drice (57% amino acid identity (Song et al., 2000), which undergoes processing itself at Asp28 and Asp230 to form an active heterodimer (Figure 1.4C). Both Dcp-1 and Dronc have been shown to cleave Drice (Hawkins et al., 2000; Song et al., 2000), and unlike most other caspases, Dcp-1 can undergo auto-processing and activate itself (Song et al., 2000). Dcp-1 has been proposed to finely tune the apoptotic process, whereas Drice acts as the main executioner of cell death (Florentin and Arama, 2012). Overexpression of full-

Figure 1.6 Cell death occurs in mid-stage egg chambers following starvation. Ovaries were stained with anti-Armadillo (green) to visualize membranes, and Draq5 (blue) to visualize DNA. **(A)** Developing egg chambers arise from the germarium and progress though 14 well defined stages. Each egg chambers is made up of 15 germline nurse cells and one developing oocyte surrounded by a layer of somatic follicle cells. **(B)** Mid-stage egg chamber from a well fed w^{1118} control fly. **(C)** Following a cell death signal, nurse cell nuclei condense and fragment, and **(D)** nurse cells are taken up into the surrounding follicle cells. **(E)** Mid-stage egg chambers late in the death process contain mostly follicle cells, and this is followed by follicle cell death. **(F)** Dcp-1 is required for cell death in mid-stage egg chambers. Degenerating mid-stage egg chambers from *Dcp-1* loss-of-function ($Dcp\text{-}1^{Prev1}$) flies contain persisting nurse cell nuclei and a premature cell death of follicle cells. Scale bars: 25μm.

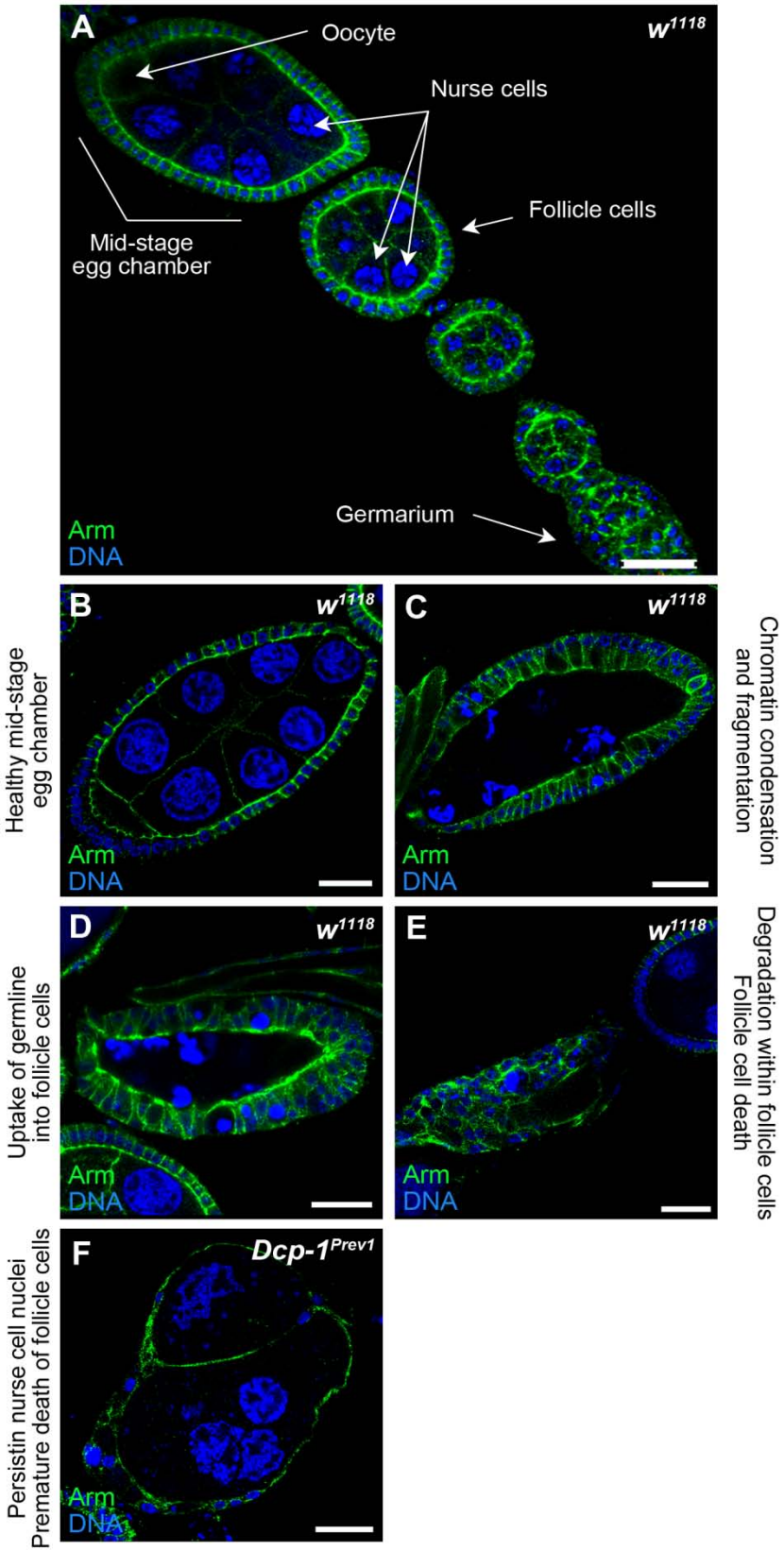
A
Oocyte
w1118
Nurse cells
Follicle cells
Mid-stage
egg chamber
Germarium
Arm
DNA
B
w1118
Arm
DNA
Healthy mid-stage
egg chamber
C
w1118
Arm
DNA
Chromatin condensation
and fragmentation
D
w1118
Arm
DNA
Uptake of germline
into follicle cells
E
w1118
Arm
DNA
Degradation within follicle cells
Follicle cell death
F
Dcp-1Prev1
Arm
DNA
Persistin nurse cell nuclei
Premature death of follicle cells

length Dcp-1 in the developing eye showed only weak protease activity and had little effect on cell death, whereas expression of a truncated (activated) form of Dcp-1 resulted in a small and rough eye phenotype due to increased cell death (Song et al., 2000). This phenotype was suppressed by overexpression of the caspase inhibitor p35, and enhanced by overexpression of rpr and grim (Song et al., 2000) suggesting that active Dcp-1 is sensitive to IAP inhibition by p35 and that Dcp-1 acts downstream of rpr and grim in the developing eye. Notably, expression of Atg5 in the developing eye rescued the small and rough eye phenotype caused by Dcp-1 expression, whereas expression of Dcp-1 in eye imaginal discs induced autophagy, indicating that autophagy functions to suppress Dcp-1 induced cell death and that Dcp-1 regulates autophagy, perhaps by a feedback mechanism (Kim et al., 2010).

Both Drice and Dcp-1 have partially redundant roles during apoptosis, and genetic studies have revealed that some cells require only Drice for apoptosis, while other cells require either Drice or Dcp-1 (Xu et al., 2006). Flies carrying mutations in Drice are pupal lethal and show reduced developmental cell death during embryogenesis (Xu et al., 2006), whereas null mutations of Dcp-1 ($Dcp\text{-}1^{Prev1}$) are viable (Laundrie et al., 2003). $Dcp\text{-}1^{Prev1}$ flies have only weak effects on embryonic cell death patterning, however flies mutant for both Dcp-1 and Drice (a hypomorphic allele) show a significant reduction in embryonic apoptosis compared to single Drice mutants (Xu et al., 2006) indicating that Drice and Dcp-1 have partially overlapping functions in the apoptosis pathway. However, Dcp-1 can induce apoptosis independently of Drice, as loss of Drice function failed to rescue the small and rough eye phenotype following Dcp-1 overexpression in the developing eye (Xu et al., 2006).

Another cell death phenotype that has been characterized for Dcp-1 is the defective cell death observed during mid-oogenesis in response to starvation (Laundrie et al., 2003). Dcp-1 is required for the proper localization and activation of Drice during oogenesis, as degenerating mid-stage egg chambers from *Dcp-1*^{Prev1} flies show reduced active Drice that localizes around nurse cell nuclei rather than in a cytosolic distribution as in wild-type files (Laundrie et al., 2003). In addition to the role that Dcp-1 plays in cell death during mid-oogenesis (Laundrie et al., 2003), Dcp-1 is also required to promote starvation induced autophagy in mid-stage egg chambers undergoing degeneration (Hou et al., 2008). *Dcp-1*^{Prev1} flies contained reduced LTR staining and diffuse GFP-LC3 in degenerating mid-stage egg chambers following starvation, and overexpression of Dcp-1 in the germline resulted in numerous degenerating mid-stage egg chambers that had high levels of GFP-LC3 puncta, indicating autophagy occurs in a Dcp-1 dependent manner during oogenesis. An *in vitro* RNAi screen using LysoTracker Green and GFP-LC3 puncta quantification revealed that Dcp-1 is also required for starvation-induced autophagy in *Drosophila l(2)mbn* cells (Hou et al., 2008).

1.7. Crosstalk between autophagy and apoptosis and its implications for human disease

Advances in understanding the molecular nature and functions of autophagy have provided insight into the relationship between autophagy and apoptosis. In many cases the survival function of autophagy negatively regulates apoptosis, whereas the cell death function of apoptosis functions to block autophagy. There are several points of intersection between these two pathways, including “dual-function” proteins that regulate both autophagy and apoptosis. Cleavage of Atg proteins by cell death proteases and degradation of apoptosis-related proteins by autophagy are additional mechanisms of

crosstalk. For example, interaction of Beclin 1 with Bcl-2 family members via its BH3 only domain prevents the formation of the Beclin 1/Vsp34 PI3K complex and blocks autophagy (Pattingre et al., 2005). Following autophagy induction, Beclin 1 dissociates from Bcl-2 leading to Vps34 activation and autophagy (Pattingre et al., 2005). In addition to its role in autophagy, Atg12 is also a mediator of apoptosis. Atg12 conjugated to Atg3, rather than its well known conjugation partner Atg5, mediates mitochondrial homeostasis and cell death with no effect on autophagy (Radoshevich et al., 2010). In addition, non-conjugated Atg12 antagonizes the anti-apoptotic activity of Bcl-2 and Mcl-1 via its BH3-like domain to induce apoptosis (Rubinstein et al., 2011), and mutation in the BH3-like domain inhibited apoptosis rather than autophagy. Interaction of Atg5 with the death domain of FADD following interferon-γ (IFN-γ) treatment induced cell death rather than autophagy (Pyo et al., 2005). Moreover, Calpain mediated cleavage of Atg5 generates a novel Atg5 cleavage product that translocates to the mitochondria and enhances cell death (Yousefi et al., 2006) further revealing the dual regulatory role that Atg5 plays in autophagy and apoptosis. Autophagy can also lead to the degradation of apoptosis-related proteins. For example, autophagic degradation of Caspase 8 in TRAIL resistant tumour cells protects cells from apoptosis (Hou et al., 2010), whereas caspase inhibition leads to the autophagic degradation of the ROS scavenger Catalase to promote cell death (Yu et al., 2006).

Studies in several tissues in *Drosophila* have also helped to uncover the complex relationship between autophagy and apoptosis. Elimination of tissues including the salivary gland and amnioserosa during *Drosophila* development requires the concerted actions of both autophagy and apoptosis for their efficient removal (Berry and Baehrecke, 2007; Mohseni et al., 2009), whereas efficient removal of the larval midgut

relies solely on autophagy (Denton et al., 2009). Overexpression of *Atg1* in the larval fat body, a nutrient storage organ responsible for storing lipids and glycogen, induces caspase-dependent apoptosis (Scott et al., 2007). Moreover, during late oogenesis, the autophagic degradation of the IAP protein Bruce controls nurse cell DNA fragmentation and nurse cell death (Nezis et al., 2010)

The mechanisms underlying the complex relationship between autophagy and apoptosis are incompletely understood. It is ultimately the interplay between autophagy and apoptosis proteins or pathways that will help determine the fate of the cell in death or survival, and this decision is a key determinant in the outcome of many human diseases including cancer and neurodegeneration (reviewed in Levine and Kroemer, 2008). Specifically in cancer, autophagy can act as a tumour suppressor or tumour promoter depending on the cancer type, stage and context (Roy and Debnath, 2010). Autophagy can protect from malignant transformation by acting as a quality control mechanism to remove sources of metabolic and genotoxic stress. In this regard, deregulated autophagy may increase the susceptibility to metabolic stress and lead to an accumulation of genomic damage that may ultimately promote tumour formation (Degenhardt et al., 2006; Mathew et al., 2007). For example, Beclin 1 is a haploinsufficient tumour suppressor that is monoallelically deleted in 40-75% of ovarian, breast and prostate cancers (Qu et al., 2003). *Beclin 1* heterozygosity increased the frequency of spontaneous tumours in mice (Qu et al., 2003), and Ras-induced down-regulation of Beclin 1 promoted the detachment of epithelial cells from the extracellular matrix, a hallmark of malignant transformation (Yoo et al., 2010). Moreover, frameshift mutations in Atg genes including Atg2b, Atg5, Atg9b and Atg12 were found in gastric and colorectal cancers with microsatellite instability suggesting that deregulated

autophagy may contribute to cancer development (Rosenfeldt and Ryan, 2009). In contrast, autophagy can promote cancer cell survival and cancer progression by providing nutrients and energy to cancer cells within a hypoxic and nutrient-depleted environment (Spowart et al., 2012; White and DiPaola, 2009). In this regard, autophagy inhibition is an attractive therapeutic target to promote the death of cancer cells. Clinical trials are now underway to examine the effects of combined autophagy inhibition and chemotherapy treatment in several cancers including prostate, pancreatic, breast, and lung cancer (reviewed in Amaravadi et al., 2011). However, as some autophagy proteins have been shown to have a pro-death function, inhibition of autophagy in some disease contexts could potentially be detrimental rather than beneficial. Therefore, it is essential to better understand the crosstalk between autophagy and apoptosis in normal development to fully appreciate the impact of autophagy and apoptosis modulation for treatment in human diseases.

1.8. Rationale

It is clear that an intricate relationship between autophagy and apoptosis exists. Understanding this crosstalk is important as it plays critical roles in both normal development and in human diseases including cancer. Using *Drosophila melanogaster* oogenesis as a model system for the crosstalk between autophagy and apoptosis, it was previously determined that the effector caspase Dcp-1 is required for starvation-induced autophagy in mid-stage egg chambers. However, it was undetermined whether autophagic flux occurs in response to starvation in non-degenerating and degenerating mid-stage egg chambers, and whether this occurred in a Dcp-1 dependent manner. To examine the mechanism of Dcp-1 mediated autophagy, an immunoprecipitation and

mass spectrometry assay was undertaken previously (Hou YC, Moradian A, Morin GB, Gorski SM, unpublished) to identify candidate interactors and substrates of Dcp-1 (Table 1.2). The results from that assay identified several candidate substrates/interactors of Dcp-1 to be mitochondrial proteins, heat shock proteins, transcriptional and translational regulators, and components of the ubiquitin and proteasome systems (Table 1.2). These results provided a foundation for some of the experiments formed in this thesis, aimed at elucidating the mechanisms underlying Dcp-1-mediated autophagy.

1.9. Hypothesis and specific aims

I hypothesize that Dcp-1 is a positive regulator of autophagic flux during mid-oogenesis and functions in this capacity via a mechanism involving the mitochondria. To test this hypothesis, my thesis addresses 3 specific aims:

Specific Aim 1: Examine the role of Dcp-1 in starvation-induced autophagic flux.

Analyses of mCherry-GFP-Atg8 distribution and Ref(2)P levels were performed to determine if autophagic flux occurs in response to starvation in wild-type mid-stage egg chambers of the ovary. In addition, these methods were employed to determine if Dcp-1 is required for starvation-induced autophagic flux during mid-oogenesis (Chapter 3).

Specific Aim 2: Characterize and validate the role of candidate Dcp-1 interactors/substrates in autophagic flux.

An RNAi based screen using LTG was employed to determine if candidate Dcp-1 interactors/substrates modify autophagy-associated lysosomal activity following

Table 1.2 Candidate Dcp-1 interactors and substrates identified by mass spectrometry

Flybase Symbol	CG Number	Molecular function	Predicted cleavage site[a]	UniProt human gene name
14-3-3ε	CG31196	Protein binding; protein heterodimerization activity	-	14-3-3ε
14-3-3δ	CG17870	Protein binding, protein heterodimerization activity, protein homodimerization activity	-	14-3-3δ
ATPsyn-β	CG11154	Hydrogen exporting ATPase activity; phosphorylative mechanism	LEVDN	ATP5B
Blw	CG3612	Hydrogen exporting ATPase activity; phosphorylative mechanism	-	ATP5A1
CG7033	CG7033	Unfolded protein binding; ATP binding	-	Tcp-1 beta
Clic	CG10997	Calcium ion binding; chloride channel activity; lipid binding	-	CLIC2
Ef1α48D	CG8280	Translation elongation factor activity	DALDA	EEF1A1
Ef1-γ	CG11901	Translation elongation factor activity	EELD	EEF1G
Ef1-β	CG6341	Translation elongation factor activity	DDVDL	EEF1B2
EIF-4a	CG9075	Translation initiation factor activity; RNA helicase activity	-	EIF4A1/EIF4A2
Hsc70-4	CG4264	Chaperone binding	IEIDS	HSPA8
Hsc70Cb	CG6603	Chaperon binding	-	HSPA4L
Hsp60	CG12101	Unfolded protein binding	-	HSPD1
Hsp70Aa	CG31366	ATP binding, response to hypoxia	-	HSPA1A/1B
Hsp83	CG1242	ATPase activity, coupled	DEADD	HSP90AA1
Jafrac1	CG1633	Thioredoxin peroxidise activity		PRDX1
Mi-2	CG8103	Protein binding; nucleosome-dependent ATPase activity; chromatin binding	NDSDA	CHD4
Rack1	CG7111	Protein kinase c binding	DLNDG	GNB2L1
REG	CG1591	Endopeptidase inhibitor activity; endopeptidase activator activity	-	PSME3
SesB	CG16944	ATP:ADP antiporter activity	-	ANT2
Sta	CG14792	Structural constituent of ribosome	TNTDS	RPSA
Ter94	CG2331	ATPase activity; golgi & ER organization	DEIDA	VCP
Uba1	CG1782	Ubiquitin activating enzyme activity	-	UBA1
Sgl	CG10072	UDP-glucose 6-dehydrogenase activity	-	UGDH

[a]Predicted caspase cleavage sites were determined by CasPredictor (Garay-Malpartida et al., 2005).

starvation. Validated hits were prioritized and top candidates were then chosen for *in vivo* autophagy analyses (Chapter 3).

Specific Aim 3: Examine the mechanism by which Dcp-1 promotes autophagic flux.

Several candidate interactors and substrates of Dcp-1 identified previously (Hou YC, Moradian A, Morin GB, Gorski SM, unpublished) were mitochondrial-associated proteins. I therefore examined if Dcp-1 mediates autophagy via a mitochondrial-associated mechanism. Immunofluorescence studies and cell fractionation assays were performed to determine the localization of Dcp-1. Moreover, RNAi knockdown of Dcp-1 *in vitro*, and analysis of Dcp-1 loss-of-function flies were undertaken to examine the mechanism of Dcp-1-mediated autophagy. Finally, genetic interaction studies were performed to examine the mechanism of Dcp-1-mediated autophagic flux (Chapter 4).

1.10. Co-authorship statement

DeVorkin L, Go NE, Hou YC, Moradian A, Morin GB and Gorski SM. The Drosophila effector caspase Dcp-1 localizes within mitochondria and regulates mitochondrial dynamics and autophagic flux via SesB. *In review, Journal of Cell Biology*

I performed 80% of the experiments presented in this paper. NE Go assisted in the mitochondrial fractionation, proteinase K treatment, ATP assays and *in vitro* cleavage assays. SesB identification was done by Drs YC. Hou, A. Moradian and GB. Morin. I conducted all other experiments and prepared the manuscript in collaboration with Dr. SM. Gorski.

DeVorkin L, Go NE, Hou YC, Chung D, Moradian A, Morin GB and Gorski SM. Identification of Dcp-1-associated novel regulators of starvation induced autophagy. *Manuscript in preparation*

The immunoprecipitation and mass spectrometry analysis was performed by Drs YC. Hou. A. Moradian and GB. Morin. Creation of the stable RFP-GFP-Atg8 cell line and the *in vitro* cleavage assay were performed by NE Go. D Chung helped to optimize the *in vitro* autophagic flux assays. I conducted all other experiments and prepared the manuscript in collaboration with Dr. SM. Gorski.

DeVorkin L and Gorski SM. Monitoring autophagy in Drosophila. *Submitted, Cold Spring Harbor Laboratory Manual*

I conducted all experiments except for Figure 4A from T. Neufeld. I prepared the manuscript in collaboration with Dr. S. Gorski.

DeVorkin L, Choutka C and Gorski SM. The interplay between autophagy and apoptosis. *Submitted, Elsevier Publishing Company*

C. Choutka wrote the section on “Cleavage of Atg proteins by caspases and calpain”. I wrote all other sections and prepared the manuscript in collaboration with Dr. SM. Gorski.

2. Materials and Methods

2.1. Fly Strains

w^{1118} was used as the control "wild type" *Drosophila melanogaster* strain. Other fly strains used included: *NGT;nosGAL4::VP16* and *UASp-mitoGFP* (Cox and Spradling, 2003), *Dcp-1*^{Prev1} and *UASp-FL-Dcp-1*(Laundrie et al., 2003), *Atg7*^{d77} and *Atg7*^{d14} (Juhász et al., 2007), *UASp-GFP-mCherry-DrAtg8a* (Nezis et al., 2010) and *Hsp83*^{582} and *Hsp83*^{13F3} (Andersen et al., 2012). *SesB*^{Org} and *UAS-Drc-2;nosGAL4* flies were obtained from the Bloomington Stock Center. *Hsc70-4* (transformant ID 101734), *eIF-4a* (transformant ID 42202), *Ter94* (transformant ID 24354), *Sta* (transformant ID 101495), *Hsp83* (transformant ID 7716) and *Clic* (transformant ID 105975) RNAi lines were obtained from Vienna Drosophila Resource Center.

2.2. Cell culture conditions

Drosophila l(2)mbn cells were grown in Schneider's medium (Invitrogen) supplemented with 10% FBS in 25cm^2 suspension cell flasks (Sarstedt) at 25°C. All experiments were carried out 3-4 days after passage of cells.

2.3. Immunofluorescence studies

For immunofluorescence studies of fly tissues, flies were conditioned on wet yeast paste for 2 days (well fed) and then transferred to a vial containing 10% sucrose

for amino acid starvation for 4 days, unless otherwise noted. Ovaries were dissected in PBS and immediately fixed with 4% paraformaldehyde diluted in PBS for 20 minutes at room temperature. Ovaries were washed two times with PBS-T (PBS+0.3% Triton X-100), 5 minutes each, permeabilized with 0.5% Triton X-100, 5 minutes, and blocked with 2% BSA in PBS-T for 1 hour at room temperature (Hou et al., 2008).

For *in vitro* studies, 200μl of *l(2)mbn* cells were plated into an 8 well CC2 coated chamber slide and incubated for at least 30 minutes to let the cells adhere. For starvation treatments, media was replaced with 2mg/ml glucose/PBS. For MitoTracker experiments, 500nm of MitoTracker Red CMXRos (Invitrogen) was added to each well and incubated for 30 minutes in the dark at 25°C. Media was removed and cells were fixed with 4% paraformaldehyde for 20 minutes at room temperature. Cells were washed twice with PBS-T, 5 minutes each, permeabilized with 0.5% Triton X-100, 5 minutes, and blocked with 2% BSA in PBS-T for 1 hour at room temperature.

Primary antibodies were diluted in 0.5% BSA+PBS-T and incubated overnight at 4°C. Primary antibodies included Ref(2)P (1:5000, Tor Erik Rusten), Armadillo (1:100, N2 7A1 Developmental Studies Hybridoma Bank) ATPsynthase-α (1:500, MitoSciences), Dcp-1 (1:500,(Tenev et al., 2005)), PDI (1:100, Abcam) and GM130 (1:100, Abcam). Following primary antibody incubation, cells were washed 3 times with PBS-T, and incubated with the appropriate Alexa-488 and/or Alexa-546 conjugated secondary antibodies (2μg/ml, Invitrogen). Secondary antibodies , diluted 1:1000 in 0.5% BSA+PBS-T, were incubated for 2 hours at room temperature in the dark followed by 3 washes with PBS-T for 5 minutes each. For Draq5 DNA stain (Biostatus), Draq5 was diluted in PBS (1:500) with 100μg/mL RNase A for 10 minutes at room temperature. Samples were mounted with Slowfade Gold Antifade Reagent (Invitrogen) and viewed

with a Nikon Confocal C1 microscope equipped with a Plan APO 60X/1.45 oil immersion objective (Nikon). Images were acquired at room temperature using EZ-C1 Ver 3.00 software (Nikon). All images were scanned using the same pinhole and laser brightness settings. Brightness and contrast were adjusted using Photoshop (CS4, Adobe) and were applied to the whole image.

2.4. Primer design and dsRNA synthesis

Each dsRNA PCR primer for RT-PCR was designed to contain a 5' T7 RNA polymerase-binding site (5'-TAATACGACTCACTATAGG-3') followed by sequences specific for the target gene. The ampicillin resistance gene from bacteria was used as a control dsRNA. The PCR products were generated by RT-PCR using Superscript one-step RT-PCR with platinum taq (Invitrogen) according the the manufacturer's instructions. RT-PCR products were ethanol precipitated and used as a template for *in vitro* transcription reactions using T7 RiboMax Express RNAi systems (Promega). Quality of the RNA was analyzed by gel electrophoresis. dsRNA was quantitated using PicoGreen and adjusted to 200ng/μl-400ng/μl with nuclease free water. Sequences of primers for dsRNA synthesis can be found in Table 2.1.

Table 2.1 Sequences of primers used for dsRNA synthesis

1st set		
Gene Name	**Forward Primer Sequence (5'-3')**	**Reverse Primer Sequence (5'-3')**
14-3-3ε	TAATACGACTCACTATAGGGACAGGTGGAGAAGGAGCTG	TAATACGACTCACTATAGGTCAGTGTATCCAACTCGGCA
14-3-3ζ	TAATACGACTCACTATAGGGTCACAGAGACTGGCGTTGA	TAATACGACTCACTATAGGCGTAGCAGATTTCCCTCAGC
ATPsyn-β	TAATACGACTCACTATAGGCGTCGATGTCCAGTTTGATG	TAATACGACTCACTATAGGTGATGCGTCCTAGTGTTTCG
Blw	TAATACGACTCACTATAGGTGTGTTCTACCTGCATTCGC	TAATACGACTCACTATAGGCACGTACTGACCCTGCTTGA
CG7033	TAATACGACTCACTATAGGGTGGACAACATCATCCGTTG	TAATACGACTCACTATAGGCAGCACTCATCCTCGAATCA
Clic	TAATACGACTCACTATAGGTTCCGTACCAATTTTGAGGC	TAATACGACTCACTATAGGATCAGCTCACAGTCGAAGCA
Ef1α48D	TAATACGACTCACTATAGGGTGACTCCAAGGCTAACCCC	TAATACGACTCACTATAGGTTAGAGGGCACCAGGTTGAC
Ef1-β	TAATACGACTCACTATAGGGAAGTCTAAGAAACCCGCCC	TAATACGACTCACTATAGGTGCTTAGTTCGCTTTGCTCA
Ef1-γ	TAATACGACTCACTATAGGGGTGTTCATGTCGTGCAATC	TAATACGACTCACTATAGGGAAGATCTTGCCCTGGTTGA
eIF-4a	TAATACGACTCACTATAGGTTACGTCAACGTGAAGCAGG	TAATACGACTCACTATAGGAATGTAGTTCTCGCGGTTCG
Hsp60	TAATACGACTCACTATAGGCACCCTCACCGATATGGC	TAATACGACTCACTATAGGGGGTGTCGTCCTTGGTGA
Hsc70-4	TAATACGACTCACTATAGGATCTGACCACCAACAAGCGT	TAATACGACTCACTATAGGATGACCGACTTGTCCAGCTT
Hsp70Aa	TAATACGACTCACTATAGGGGGAGGATTTGGAGGCTACT	TAATACGACTCACTATAGGTCGATCGAAACATTCTTATCAGTC
Hsc70Cb	TAATACGACTCACTATAGGGAAAAACACAGTTGGCGGAT	TAATACGACTCACTATAGGGGTCTTGGCGTTGATCTTGT
Hsp83	TAATACGACTCACTATAGGGAGCTGAACAAGACCAAGCC	TAATACGACTCACTATAGGTTGCGGATCACCTTTAGGAC
Jafrac1	TAATACGACTCACTATAGGATGGAGTGCTCGATGAGGAG	TAATACGACTCACTATAGGTACTCCTTGGACTTGGTGGG
Mi-2	TAATACGACTCACTATAGGCGCAAGTACGACATGGAAGA	TAATACGACTCACTATAGGTCGACCTTGAGCTTGGACTT
Rack1	TAATACGACTCACTATAGGACCTCAATGACGGCAAGAAC	TAATACGACTCACTATAGGATTTGACGCCCGTTACAAAG
REG	TAATACGACTCACTATAGGCCATTCAAGAGGACACGCTT	TAATACGACTCACTATAGGACAAGAATTGCTGACCGTCC
SesB	TAATACGACTCACTATAGGCTGATACTGGCAAGGGTGGT	TAATACGACTCACTATAGGCCCAGCTGATGTAGATGGGT
Sgl	TAATACGACTCACTATAGGAATCTCCAGCATCAATTCGC	TAATACGACTCACTATAGGAACAAACTCATCCCACTCCG
Sta	TAATACGACTCACTATAGGAGTTCGCCAAGTACACCGAC	TAATACGACTCACTATAGGGGATCGCGGTAGAAGAACAG
Ter94	TAATACGACTCACTATAGGCATGGGAGCCAAGAAGAATG	TAATACGACTCACTATAGGGTCACCTTGGCGATGTAGGT
Uba1	TAATACGACTCACTATAGGGATTTCGCAAAGCTGGACTC	TAATACGACTCACTATAGGTAGGCTTCTGCACATCATGC

2nd set		
ATPsyn-β	TAATACGACTCACTATAGGCTCCTGGCTCCATACGC	TAATACGACTCACTATAGGATATGGCCTGAACAGAAGTAAT
Blw	TAATACGACTCACTATAGGGTACTGCATCTACGTCGCCA	TAATACGACTCACTATAGG ACGTTGGTTGGAATGTAGGC
Clic	TAATACGACTCACTATAGGATCAGCCTGAAGGTGACGAC	TAATACGACTCACTATAGGACAGGTTCTCGATCAGGGTG
eIF4A	TAATACGACTCACTATAGGTCGATTGCTATCCTTCAGCA	TAATACGACTCACTATAGGGATCTGATCCTTGAAACCGC
Hsp60	TAATACGACTCACTATAGGGGGAGGGAGATGTGATGAGA	TAATACGACTCACTATAGGGCGAAGCAAAACAAAGTTCC
Hsc70-4	TAATACGACTCACTATAGGGGCTGACAAGGAGGAGTACG	TAATACGACTCACTATAGGTGTCGTTTGACCCGTTTGTA
Hsp70Aa	TAATACGACTCACTATAGGCCCACTTTCATTGGGAATTG	TAATACGACTCACTATAGGAATGCATTGTTGTCCTTCGTC
Hsp83	TAATACGACTCACTATAGGATTGCTCAGCTGATGTCCCT	TAATACGACTCACTATAGGGGAGTAGAAACCCACACCGA
Mi-2	TAATACGACTCACTATAGGATTTGCGTGGTAAATCGGAG	TAATACGACTCACTATAGGGTTCTTGCTTCACCTCGCTC
REG	TAATACGACTCACTATAGGGTTGATCCTCAAGGCAGAGC	TAATACGACTCACTATAGGTCCTCCACAAGCTTCCTGAT
SesB	TAATACGACTCACTATAGGGCAAGAACCCTTCCTTCCTC	TAATACGACTCACTATAGGTTCGGAGGCGAAAGAATCTA
Sta	TAATACGACTCACTATAGGTTTCCACGTTAACATGTCGG	TAATACGACTCACTATAGGCCCAGGTTGAGGATGTTGAC
Ter94	TAATACGACTCACTATAGGGCATGATGATGTTGACCTGG	TAATACGACTCACTATAGGCTGCATGCCAAACTTCAAGA

2.5. RNAi

For *in vitro* RNAi experiments, I used a protocol similar to what was previously described (Hou et al., 2008). Cells were washed two times with ESF921 medium (Expression Systems) and cell pellets were resuspended in ESF921 medium to a concentration of $2x10^6$ cells/ml. 333ul of adjusted cells were plated in each well of a 24 well plate. 5-10μg of dsRNA was added per well and incubated at 25°C for 1 hour. Following incubation, 667μl of Schneider's + 10% FBS was added back to each well and was incubated for an additional 72 hours at 25°C. For LTG (Invitrogen) experiments for flow cytometry, 66μl of $2X10^6$ cells/ml were plated in triplicates into a 96 well plate. 10μg of dsRNA was added per well and incubated for 1 hour at room temperature. 134μl of Schneider's + 10% FBS was added back to each well and incubated for 72 hours at 25°C.

2.6. LysoTracker analysis by flow cytometry

For LysoTracker and flow cytometry experiemtns, I used a protocol similar to what was previously described (Hou et al., 2008). RNAi treated cells were transferred to a U–bottom 96 well plate and were centrifuged at 850 rpm for 5 minutes at room temperature. For starvation experiments, cell pellets were resuspended in 2mg/ml glucose in 1XPBS with 2ug of dsRNA and incubated for 2 hours at 25°C. Cells were collected by centrifugation and resuspended in 50nm LTG (Invitrogen) to detect acidic compartments and 2μg/mL propidium iodide (PI, Invitrogen) to detect dead cells. Cells were incubated for 20 minutes in the dark, and following centrifugation, cell pellets were washed with ice cold 1XPBS, resuspended in ice cold 1XPBS and aliquoted into flow cytometry tubes on ice. Cells were then analyzed by flow cytometry (FACSCalibur,

Becton Dickinson). A minimum of 10,000 cells per sample was acquired in triplicate for each experiment. Fluorescence intensities were obtained using the FL1 channel to measure LTG, and the FL3 channel to measure PI. PI positive cells were excluded and LTG fluorescence was analyzed using FlowJo Software version 5.7.2.

2.7. Protein extraction and western blot analysis

For ovary lysates, ovaries were dissected and placed immediately on dry ice. Cell and ovary lysates were extracted using lysis buffer (20mM Tris pH 7.5, 150mM NaCl, 1mM EDTA, 1% NP-40) supplemented with a complete protease inhibitor cocktail (Roche). Alternatively, RIPA lysis buffer (Santa-Cruz) plus complete protease inhibitors (Roche) was used. Protein was quantitated using the BCA Protein assay (Thermo Scientific). Proteins were separated on a 4-12% NuPAGE bis-tris gel (Invitrogen) and transferred to PVDF membranes. Membranes were blocked in milk or odyssey blocking buffer and incubated in primary antibodies overnight at 4°C. Primary antibodies included Ref(2)P (1:10000), Actin (1:500, JLA20 Developmental Studies Hybridoma Bank), Tubulin (1:1000, E7 Developmental Studies Hybridoma Bank) ATPsynthase-α (1:1000, MitoSciences), Porin (1:1000, MitoSciences), ANT (1:500, MitoSciences) and Dcp-1 (Laundrie et al., 2003) (1:500). Membranes were incubated with HRP conjugated secondary antibodies or IR-labelled secondary antibodies and were detected using the Amersham ECL^{TM} Enhanced Western Blotting System or the Odyssey System (LI-COR Biosciences). Densitometry was performed using Image Quant-5.1 software.

2.8. Isolation of crude mitochondrial and cytosolic fractions

Approximately $5x10^7$ cells were collected by centrifugation at 800 rpm for 10 minutes, resuspended in cold SEM-P (10 mM MOPS pH 7.5, 320 mM sucrose, 1 mM EDTA with complete protease inhibitor cocktail (Roche) and ground using a dounce homogenizer. Lysates were centrifuged twice at 3000 rpm to remove cell debris and supernatants were collected. The membrane fraction (pellet) was separated from the cytosolic fraction (supernatant) by centrifugation at 12,000 rpm. The pellets were washed once with 500μl SEM-P and finally resuspended in 50μl SEM-P. Protein concentrations were determined using the BCA Protein Assay (Thermo Scientific). Aliquots of 50μg protein were either spun down (membrane fraction) or TCA precipitated (cytosolic fraction) and analyzed by western blot.

For TCA precipitation, 50μg of protein was adjusted to 500μL with water, to which 110μL of 72% trichloroacetic acid (Sigma) was added. The tubes were incubated on ice for 1 hour and centrifuged at 4°C, 15,000 rpm for 30 minutes. The pellets were then washed with 1mL of acetone and spun at 4°C, 15,000 rpm for 15 minutes and allowed to dry for 30 minutes in a 37°C incubator.

2.9. Proteinase K protection assay

For mitochondrial lysis, mitochondria were resuspended in the appropriate amount of swelling buffer (50mM Tris, pH 7.5) for 30 minutes on ice with vigorous vortexing. Intact and lysed mitochondria were incubated with 20μg/ml Proteinase K (Roche) on ice for 15 minutes. Proteinase K was inactivated by adding PMSF (Fluka) to

a final concentration of 1mM. Intact mitochondria were spun down at 4°C, 12,000 rpm for 20 minutes while lysed samples were TCA precipitated.

2.10. Mitochondrial mass and mitochondrial membrane potential analysis

RNAi treated cells were transferred from Schneider+10% FBS to 2mg/ml glucose/PBS starvation media plus 10μg of dsRNA for 1-24 hours. For mitochondrial mass measurements, following starvation cells were incubated with 10μM 10-nonyl acridine orange (NAO) for 10 minutes at 25°C in the dark. Cells were spun down at 850 rpm for 5 minutes at 4°C, and cell pellets were resuspended in ice cold PBS and put on ice to be analyzed by flow cytometry (FACSCalibur, Becton Dickinson). Fluorescence was detected in the FL1 channel, and a minimum of 30,000 cells were acquired for triplicate samples per experiment. Mean fluorescence was analyzed using FlowJo Software version 5.7.2. For mitochondrial membrane potential analysis, following starvation treatments, cells were incubated with 1X JC-1 (Invitrogen) for 20 minutes in the dark at 25°C according to the manufacturer's instructions. Cells were spun down at 850 rpm for 5 minutes at 4°C,washed once with ice cold 1XPBS, and then resuspended in ice cold PBS and put on ice to be analyzed by flow cytometry (FACSCalibur, Becton Dickinson). A minimum of 30,000 cells were acquired for triplicate samples per experiment. Green fluorescence was measured in the FL1 channel, and red fluorescence was measured in the FL2 channel, and appropriate compensation was applied. Mean red and green fluorescence was analyzed using FlowJo Software version 5.7.2.

2.11. Determination of ATP levels

For ATP measurements in fed and nutrient deprived *l(2)mbn* cells, cells were transferred into 15mL tubes and spun at 800 rpm for 10 min. Cell pellets were resuspended in fresh Schneiders + 10% FBS (fed) or PBS + 2mg/ml glucose (starved). Following treatments, cells were centrifuged at 800 rpm for 10 minutes at 4^{o}C. Cell pellets were resuspended in 400μl of hot ATP Reaction Buffer (ATP Determination Kit, Invitrogen) and incubated in a 100^{o}C heating block for 5 minutes. Cell debris was removed by centrifugation at 14,000 rpm for 15 minutes at 4^{o}C.

For ATP measurements in ovaries, ovaries were collected from 7-10 flies and frozen immediately on dry ice. Ovaries were ground in 200μl of ATP Extraction Buffer (ATP Reaction Buffer, Invitrogen), Complete protease inhibitor cocktail (Roche), Phosphatase Inhibitor Cocktail (Santa Cruz) and 20mM sodium fluoride (NaF). Samples were centrifuged twice at 3000 rpm for 5 minutes, 4^{o}C, to remove the tissue debris. The supernatants were aliquoted equally into 2 tubes – one tube was used directly for protein quantitation. The second tube was used for ATP determination and was incubated in a 100^{o}C heating block for 5 minutes. Samples were centrifuged at 14,000 rpm for 15 minutes at 4^{o}C to remove insoluble materials.

ATP levels were measured using a bioluminescence ATP Determination Kit (Invitrogen). 10μl of standard and test samples were aliquoted in triplicates into 96-well plates, and 125μl of ATP Standard Reaction Buffer was added to each well. The plates were incubated at room temperature for 30 minutes and luminescence was measured using Wallac1420 Victor plate reader (Perkin Elmer).

2.12. Oligomycin A treatment

3-5 day old flies were transferred to a vial containing wet yeast paste supplemented with 200μl of 25μg/mL Oligomycin A or DMSO added directly to the top of the yeast paste. Following two days of treatment, flies were transferred to a vial containing a Kimwipe soaked with 10% sucrose supplemented with 25μg/mL Oligomycin A (Bahadorani et al., 2010) or DMSO for 4 days.

2.13. Generation of constructs for *in vitro* synthesis

Drice (Tenev et al., 2005) was PCR amplified using primers containing flanking *Att*B1 and *Att*B2 sequences. SesB and Hsp83 were amplified from a full length cDNA construct (*Drosophila* Genomics Resource Center) using primers containing flanking *Att*B1 and *Att*B2 sequences. Primer sequences are shown in Table 2.2. PCR products were cloned into the pDONR221 Gateway Entry Vector and were sequenced verified. The entry clones were then shuttled into pEXP2-DEST or pEXP1-DEST expression vectors, respectively, for *in vitro* translation experiments. SesB, Hsp83 and Drice were synthesized using the Expressway™ Mini Expression Module (Invitrogen). 1μg of template DNA was used for every 100μL reaction according to the manufacturer's instructions and was incubated for 6 hours at 37°C in a shaking incubator. Proteins were precipitated with acetone, centrifuged at room temperature at 12,000 rpm, and supernatant removed. Pellets were resuspended in 1X NuPAGE LDS sample buffer (Invitrogen) and loaded onto a 10% NuPAGE bis-tris gel (Invitrogen) and analyzed by western blot.

Table 2.2 Gene-*Att*B primer sequences for *in vitro* synthesis

Primer Name	Sequence
Drice *Att*B1	5'-GGGGACAAGTTTGTACAAAAAAGCAGGCTTCACCATGGACGCCACTAACAATGGAGAAT-3'
Drice *Att*B2	5'-GGG GAC CAC TTT GTA CAA GAA AGC TGG GTCTCAAACCCGTCCGGCTGGT-3'
SesB *Att*B1	5'-GGGGACAAGTTTGTACAAAAAAGCAGGCTTCACCATGGGCAAGGATTTCGATGCTGTT-3'
SesB *Att*B2	5'- GGGGACCACTTTGTACAAGAAAGCTGGGTCCAAGACCTTCTTGATCTCAT-3'
Hsp83 *Att*B1 (N-terminal tag)	5'- GGGGACAAGTTTGTACAAAAAAGCAGGCTTCCCAGAAGAAGCAGAGACCTTT-3'
Hsp83 *Att*B2 (N-terminal tag)	5'-GGGGACCACTTTGTACAAGAAAGCTGGGTCTTAATCGACCTCCTCCATGTG-3'
Hsp83 *Att*B1 (C-terminal tag)	5'-GGGGACAAGTTTGTACAAAAAAGCAGGCTTCACCATGCCAGAAGAAGCAGAGACCTTT-3'
Hsp83 *Att*B2 (C-terminal tag)	5'-GGGGACCACTTTGTACAAGAAAGCTGGGTCATCGACCTCCTCCATGTGGGAA-3'

2.14. Transfection and purification of Dcp-1

For transfection experiments, 5μg of His-V5-Dcp-1^{FL} or His-V5-Dcp-$1^{C<A}$ plasmid DNA (Tenev et al., 2005) was added to 1ml of Grace medium (Invitrogen) and vortexed to mix. 100μl of Cellfectin (Invitrogen) was added to the DNA/Grace mixture and was incubated for at least 30 minutes. 3.75 x 10^6 cells in 4mL of Grace media were incubated with DNA/Grace/Cellfectintransfection medium overnight. 10mL of Schneider's medium + 10% FBS was added back to the cells and the cells were incubated for an additional 3 days before Ni-NTA purification. Purification of His-V5-Dcp-1^{FL} or His-V5-Dcp-$1^{C<A}$ was carried out using HisPur^{TM} Ni-NTA Spin Columns (Thermo Scientific). Cells were resuspended in 400μL of Equilibration Buffer (PBS, 10mM imidazole, pH 7.4) with 1% Triton X-100, incubated on a rotary shaker at 4^{o}C for 10 minutes and centrifuged at 15,0000 rpm at 4^{o}C for 15 minutes to remove insoluble material. Supernatants were added to the Ni-NTA beads and mixed at 4^{o}C for 30 minutes. The column was centrifuged at 15,000 rpm at 4^{o}C for 2 minutes to remove the flow-through. The columns were then washed three times with 400μl of wash buffer (PBS, 25mM imidazole), and

His-tagged Dcp-1 was eluted three times with 200μl of elution buffer (PBS, 250 mM imidazole). The elutions were assayed for caspase activity using the Caspase-Glo 3/7 Kit (Promega). 10μl of eluate was added to 100μl of Caspase-Glo 3/7 Reagent and incubated at 25°C for 30 minutes. Luminescence was detected using the Wallac1420 Victor plate reader (Perkin Elmer). The elutions were immediately used for *in vitro* cleavage assays. The caspase reaction buffer used in this experiment was as previously described (Tenev et al., 2005). A 100μL reaction consisting of increasing volumes of Ni-NTA purified Dcp-1^{FL} or Dcp-$1^{C<A}$ (10, 20, 40μL) and 5μL of *in vitro* translated SesB or Drice incubated in caspase reaction buffer (10mM Tris, pH 7.5, 150mM NaCl, 2mM DTT, 0.1% Triton X-100 (Tenev et al., 2005)). The reaction mixture was incubated at 25°C overnight and precipitated with 400μL of acetone for western blot analysis.

2.15. LysoTracker Red and TUNEL analysis

For LTR staining, ovaries from well fed and amino acid starved flies were dissected in PBS and incubated in 50μm LTR DND-99 (Invitrogen) for 3 minutes, washed 3 times with PBS and fixed with 4% paraformaldehyde for 20 minutes. Ovaries were washed 3 times with PBS-T (PBS+0.1% Triton X-100), incubated in 1:500 Draq5 + 100μg/mL RNase A for 10 minutes at room temperature and mounted in SlowFade Gold Reagent (Hou et al., 2008). For TUNEL (terminal deoxynucleotidyl transferase dUTP nick end labelling, Promega) analysis, ovaries were dissected in PBS and fixed with 4% paraformaldehyde. Ovaries were washed two times with PBS, permeabilized with 0.2% Triton X-100 for 5 minutes and washed two additional times with PBS. Cells were incubated with equilibration buffer for 5 minutes at room temperature, followed by

incubation in rTdT incubation buffer for 60 minutes at 37°C protected from light. Reaction was terminated by the addition of 2X SSC. Ovaries were washed two times with PBS+0.1% Triton X-100 and incubated with 1:500 Draq5 + 100μg/mL RNase A for 10 minutes at room temperature. Ovaries were mounted in SlowFade Gold reagent and viewed by confocal microscopy (Hou et al., 2008).

2.16. Generation of *UASp-Dcp-1$^{C<A}$* transgenic flies

Dcp-1$^{C<A}$ plasmid (Tenev et al., 2005) was PCR amplified with the primers 5'-GGGGACAAGTTTGTACAAAAAAGCAGGCTTCACCATGACCGACGAGTGCGTAACCAGAAACT-3' and 5'-GGGGACCACTTTGTACAAGAAAGCTGGGTCGCCAGCCTTATTGCCGTTC-3' and cloned into the pDONR221 Gateway Entry vector. Clones were sequence verified and shuttled into the pUASP expression vector (DGRC). Plasmids generated by HiPure plasmid purification kit (Invitrogen) were sent to Genetic Services, (Massachusetts, USA) for injection into fly embryos for germline transformation. Transgenic flies with red eyes were established as stocks by crossing with white eyed *w^{1118};Dp(1;Y)y^{+};CyO/nub^{1}b^{1}sna^{Sco}lt^{1}stw^{3};MKRS/TM6B,Tb^{1}* flies (Stock 3703, Bloomington). Chromosome insertion was mapped by crossing red eyed transgenic flies with white eyed 3703 flies, and resulting red-eyed progeny was crossed with *w^{1118}* flies. 10 strains of *UASp-Dcp-1$^{C<A}$* were generated, of which *UASp-Dcp-1$^{C<A}$-1* showed the highest protein expression by western blot.

2.17. Transfection and Immunoprecipitation

15μg of plasmid DNA was added to 3mL of Grace Medium (Invitrogen) and was vortexed to mix. 300μl of Cellfectin (Invitrogen) was added to the Grace/DNA mixture

and was incubated for 45 minutes to 1 hour. *Drosophila l(2)mbn* cells growing in Schneiders + 10% FBS were washed twice with Grace media and resuspended at a concentration of $3.75x10^6$ cells/mL. 12mL of these cells were then combined with the Grace/DNA/Cellfectin mixture in a T75 flask and incubated overnight at 25°C. The following day, 30mL of Schneiders + 10% FBS were added back to the transfection and incubated for an additional 48-72 hours. For immunoprecipitation experiments, transfected cells were spun down at 850 rpm for 10 minutes and the cell pellet was resuspended in lysis buffer (20mM Tris pH 7.5, 150mM NaCl, 1mM EDTA, 1% NP-40 supplemented with a protease inhibitor cocktail (Roche)). Cells were disrupted by passing through a 21G syringe five times and lysate was incubated at 4°C on a nutator for 30 minutes. Lysates were centrifuged at 4°C for 15 minutes at 15,000 rpm and supernatants were clarified by passing through a 0.45μm nylon syringe filter. Supernatants were then incubated with 50μl of a 50% slurry of Sepharose 4B (Sigma) on a nutator for 1 hour at 4°C. Sepharose was removed by centrifugation and supernatants were incubated with anti-FLAG M2 agarose or anti-V5 agarose resin (Sigma) overnight at 4°C on a nutator. Anti-FLAG resin was recovered by centrifugation and washed 5 times with ice cold lysis buffer. Bound proteins were eluted by boiling at 70°C for 15 minutes in LDS sample buffer, and eluates were separated on a 4-12% NuPAGE bis-tris gel (Invitrogen) with 1XMOPS buffer (Invitrogen) and were transferred to PVDF membranes. Membrane was blocked for 1 hour in odyssey blocking buffer and was incubated with 1:500 anti-Dcp-1 antibody and 1: 1000 anti-FLAG or 1:1000 anti-V5 antibodies. Anti-rabbit HRP antibodies (Santa-Cruz) were diluted in 5% non-fat milk in 0.1% PBST, and anti-mouse IR800 antibody (Rockland Immunochemicals) was diluted in Odyssey blocking buffer and detected using the Amersham ECL™ Enhanced Western Blotting System or the Odyssey System (LI-COR Biosciences) respectively.

2.18. Statistics

Statistical significance was calculated by ANOVA plus a Dunnett or Bonferroni post test, or a two-tailed Student t-test. P values <0.05 were considered significant. In each graph shown, error bars represent ± s.e.m. or s.d. of (n) independent experiments.

3. Identification of Dcp-1-associated, novel regulators of starvation induced autophagy

Portions of this chapter were submitted in DeVorkin L, Go NE, Hou YC, Moradian A, Morin GB and Gorski SM "The Drosophila effector caspase Dcp-1 localizes within mitochondria and regulates mitochondrial dynamics and autophagic flux via SesB".

3.1. Introduction

The relationship between autophagy and apoptosis is complex, with core machinery components and signalling molecules of each pathway interconnected (Eisenberg-Lerner et al., 2009). However, the molecular mechanisms governing these interactions are largely unknown. Several studies have begun to examine the multifunctional signalling molecules that take part in each pathway. For example, anti-apoptotic Bcl-2 and Bcl-xL bind Beclin1, a core autophagy component of the Class III PI3K/Vps34 complex, and inhibit autophagy (Pattingre et al., 2005; Maiuri et al., 2007a). Furthermore, the core autophagy protein Atg12 enhances mitochondrial apoptosis by binding to and inactivating anti-apoptotic family members including Bcl-2 and Mcl-1 to promote apoptosis (Rubinstein et al., 2011). Several investigations have further revealed that core autophagy proteins undergo proteolytic processing, and in some cases the newly generated fragment gains a novel pro-apoptotic role (Wirawan et al., 2010; Yousefi et al., 2006; Cho et al., 2009; Zhu et al., 2010).

Studies using *Drosophila melanogaster* have also examined the complex relationship between autophagy and apoptosis. Overexpression of the autophagy gene *Atg1* in the larval fat body, a nutrient storage organ analogous to the mammalian liver, induces apoptosis in a caspase-dependent manner (Scott et al., 2007), whereas overexpression of Atg1 in the salivary gland induces premature cell death in a caspase-independent manner (Berry and Baehrecke, 2007). Moreover, degradation of larval tissues, including the salivary gland (Berry and Baehrecke, 2007) and the midgut (Denton et al., 2009), during development requires autophagy, and although *Atg7* mutant flies are homozygous viable, they show reduced DNA fragmentation in the larval midgut (Juhász et al., 2007) and the ovary (Hou et al., 2008). Although these studies show autophagy can lead to the induction of death as well as contribute to death-related processes, autophagy functions primarily as a cell survival mechanism in *Drosophila* in response to cellular stress. JNK signaling in the intestinal epithelium and fat body stimulates autophagy gene transcription to promote cell survival during oxidative stress (Wu et al., 2009). Furthermore, autophagy is induced to high levels in the larval fat body (Scott et al., 2004) and the midgut (Wu et al., 2009) to remobilize nutrients and promote cell survival following starvation.

Nutrient status checkpoints exist in the germarium and mid-stage egg chambers of the *Drosophila* ovary to remove defective egg chambers prior to the energy demanding process of vitellogenesis (Drummond-Barbosa and Spradling, 2001). Cell death at these checkpoints occurs spontaneously, although at a low level, and is upregulated in response to starvation (Drummond-Barbosa and Spradling, 2001). This cell death is accompanied by increased LysoTracker Red (LTR) staining and GFP-LC3 puncta indicating that autophagy also occurs at these checkpoints (Barth et al., 2011;

Hou et al., 2008). The effector caspase Dcp-1 functions non-redundantly at these checkpoints, as Dcp-1 loss-of-function flies (*Dcp-1*^{Prev1}) contain degenerating mid-stage egg chambers with persisting nurse cell nuclei, reduced TUNEL staining, and follicle cells that undergo a premature cell death (Hou et al., 2008; Laundrie et al., 2003). Degenerating mid-stage egg chambers from *Dcp-1*^{Prev1} flies also contain diffuse GFP-LC3 staining even in the presence of starvation indicating that Dcp-1 is required for cell death and autophagy at these checkpoints (Hou et al., 2008). Moreover, overexpression of Dcp-1 in the germline resulted in numerous degenerating mid-stage egg chambers that contained GFP-LC3 puncta suggesting that Dcp-1 is necessary and sufficient for starvation-induced autophagy during mid-oogenesis (Hou et al., 2008). However, the role of Dcp-1 in autophagic flux in mid-stage egg chambers and the mechanism by which Dcp-1 regulates autophagy remains to be determined.

In this chapter, we confirm that Dcp-1 functions as a positive regulator of starvation-induced autophagic flux in degenerating mid-stage egg chambers, and does so in a catalytically dependent manner. An immunoprecipitation (IP) and mass spectrometry (MS) assay previously undertaken in the laboratory (Hou YC, Moradian A, Morin G and Gorski SM, unpublished) identified several candidate substrates and interactors of Dcp-1 (Table 1.2). We utilized the IP-MS data to identify candidate Dcp-1-associated novel regulators of starvation-induced autophagy *in vitro* using LysoTracker Green analyses coupled with flow cytometry. Thirteen candidate interactors and/or substrates of Dcp-1 were identified as novel regulators of starvation-induced autophagy and included heat shock proteins, proteins involved in the ubiquitin-proteasome pathway, proteins involved in transcription and translation, and mitochondrial proteins. We further examined the *in vivo* function of two candidates, Clic and Hsp83, in

starvation-induced autophagy in the ovary. Loss of *Clic* or *Hsp83* function in the germline increased the percentage of degenerating mid-stage egg chambers undergoing autophagic flux following starvation compared to starved control flies. Further characterization of Hsp83 revealed that although Dcp-1 interacts with Hsp83, it does not cleave Hsp83 as assessed by *in vitro* cleavage assays, suggesting that Hsp83 is a binding partner of Dcp-1 rather than a substrate. This study identifies novel regulators of starvation-induced autophagy *in vitro* and *in vivo* during *Drosophila* oogenesis, and provides a foundation for further studies to better understand the mechanism of Dcp-1-mediated autophagic flux.

3.2. Autophagic flux occurs during *Drosophila* oogenesis in a Dcp-1 dependent manner

To investigate autophagic flux during *Drosophila* mid-oogenesis, we examined transgenic flies expressing a UASp-GFP-mCherry-Atg8a transgene specifically in the germline using the nosGAL4 driver. Under non-autophagy inducing conditions, the dual tagged Atg8a protein is diffuse throughout the cytoplasm and appears yellow (overlap of green and red). When autophagy is induced, Atg8a becomes lipidated and associates with the autophagosomal membrane where it fluoresces as yellow puncta. Once autophagosomes fuse with lysosomes, GFP fluorescence is quenched by acidic hydrolases and the resulting autolysosomes will fluoresce red (Nezis et al., 2010). Healthy egg chambers from flies conditioned on yeast paste (well fed) showed diffuse yellow GFP-mCherry-Atg8a staining throughout the nurse cells (Figure 3.1 A). Following amino acid deprivation (starvation conditions), an increase in yellow autophagosomes and red autolysosomes in healthy non-degenerating mid-stage egg chambers was observed (Figure 3.1 B), indicating that autophagic flux occurs in otherwise healthy egg

Figure 3.1 Dcp-1 is necessary for autophagic flux during mid-oogenesis

GFP-mCherry-DrAtg8a was expressed in the germline using the nosGAL4 driver. Staining shows DNA (blue), GFP (green) and mCherry (red). **(A)** *UASp-GFP-mCherry-DrAtg8a/+; nosGAL4/+* flies conditioned on yeast paste had diffuse GFP-mCherry-DrAtg8a staining in mid-stage egg chambers. **(B)** Non-degenerating mid-stage egg chambers from nutrient deprived flies contained autophagosomes (yellow) and autolysosomes (red). **(C)** Egg chambers early in the degeneration process showed follicle cells that take up portions of the nurse cell cytoplasm, followed by **(D)** condensation of the nurse cell nuclei and further uptake of the nurse cell cytoplasm into follicle cells. **(E)** Late stage degenerating egg chambers lose all GFP staining and fluoresce red. **(F)** Well fed *Dcp-1^{Prev1}/Dcp-1^{Prev1}; UASp-GFP-mCherry-DrAtg8a/nosGAL4* flies showed diffuse GFP-mCherry-DrAtg8a staining in the germline. **(G)** Starved *Dcp-1^{Prev1}/Dcp-1^{Prev1}; UASp-GFP-mCherry-DrAtg8a/nosGAL4* flies showed an accumulation of autophagosomes in degenerating mid-stage egg chambers. **(H)** Well fed flies over-expressing an activated form of Dcp-1 (tDcp-1) in the germline showed an increase in autophagosomes and autolysosomes in non-degenerating mid-stage egg chambers. **(I)** Well fed flies overexpressing tDcp-1 in the germline also contained degenerating mid-stage egg chambers that lose all GFP fluorescence and fluoresce red. Scale bars, 25μm.

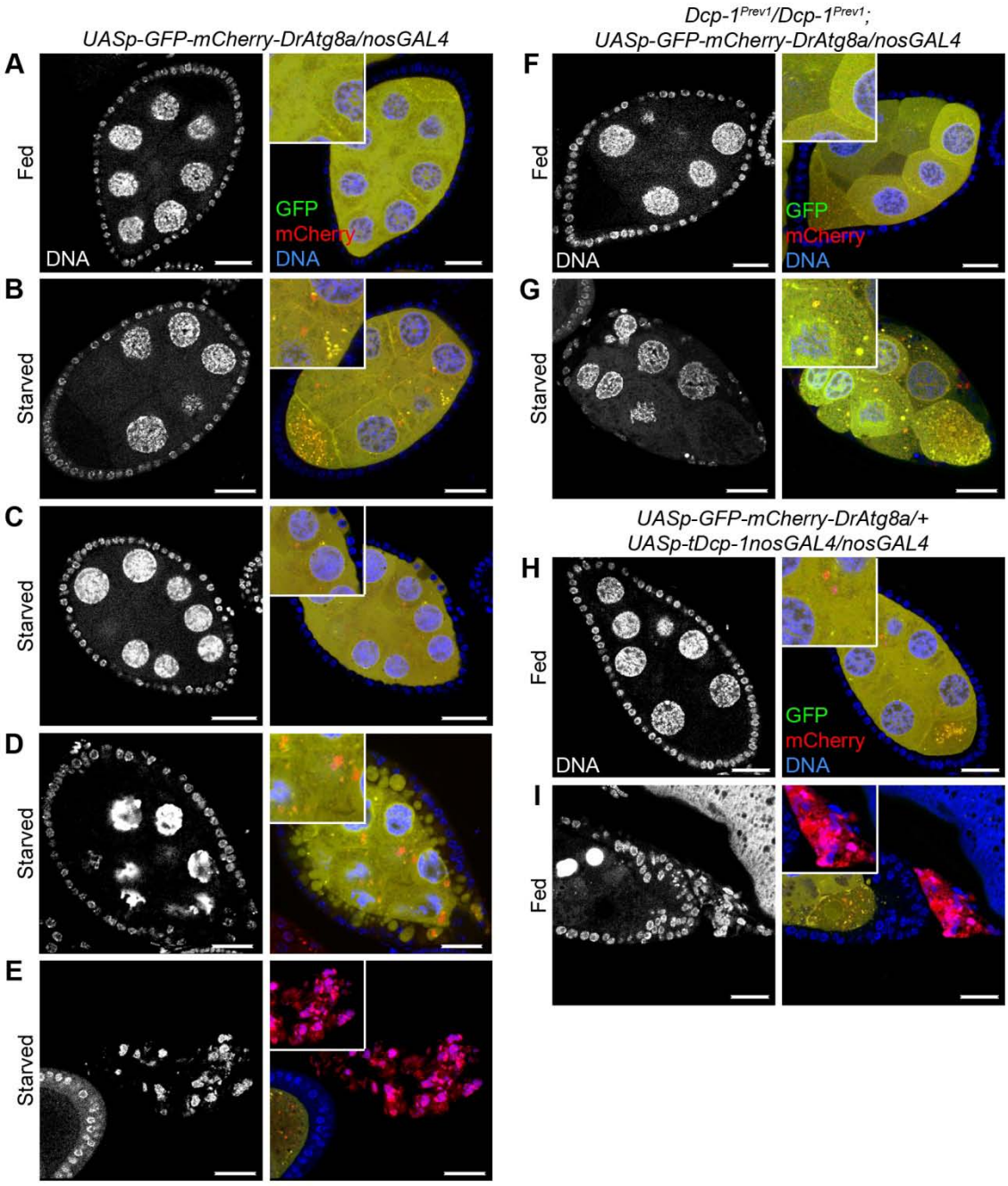
UASp-GFP-mCherry-DrAtg8a/nosGAL4
Dcp-1Prev1/Dcp-1Prev1;
UASp-GFP-mCherry-DrAtg8a/nosGAL4
A
Fed
DNA
GFP
mCherry
DNA
F
Fed
DNA
GFP
mCherry
DNA
B
Starved
G
Starved
C
Starved
UASp-GFP-mCherry-DrAtg8a/+
UASp-tDcp-1nosGAL4/nosGAL4
H
Fed
DNA
GFP
mCherry
DNA
D
Starved
I
Fed
E
Starved

chambers. In response to a cell death signal, nurse cell nuclei condense and fragment, follicle cells take up portions of the nurse cell cytoplasm, and this is followed by follicle cell death (Giorgi and Deri, 1976). In addition to the cell death phenotype, degenerating mid-stage egg chambers taking up nurse cell cytoplasm (Figure 3.1 C) and those later in the degeneration process (Figure 3.1 D) contained both autophagosomes and autolysosomes. Follicle cells phagocytose the degenerating germline in a process referred to as macropinocytosis (Etchegaray et al., 2012). Single membrane phagosomes can also fuse with lysosomes, forming phagolysosomes, and therefore it may be hard to distinguish between phagosomes and phagolysosomes in follicle cells using fluorescence base methods. In late degenerating mid-stage egg chambers the GFP signal was lost and the remaining follicle cells fluoresced red (Figure 3.1 E) indicating that there may be a late stage acidification of the dying follicle cells. All together, these data show that autophagic flux occurs in the germline in response to starvation.

We next examined if Dcp-1 regulates autophagic flux in the germline. Well-fed *Dcp-1* loss-of-function flies (*Dcp-1*^{Prev}) expressing GFP-mCherry-Atg8a in the germline had diffuse yellow staining (Figure 3.1 F). Following starvation, degenerating mid-stage egg chambers from *Dcp-1*^{Prev1} flies, which are characterized by a premature loss of follicle cells and persisting nurse cell nuclei (Laundrie et al., 2003), contained an accumulation of autophagosomes (Figure 3.1 G, compare to Figure 3.1 D) suggesting that Dcp-1 is required for autophagic flux in degenerating mid-stage egg chambers. To determine if Dcp-1 is sufficient to induce autophagic flux, we over-expressed an active form of Dcp-1 lacking its pro-domain (tDcp-1) and GFP-mCherry-Atg8a in the germline. We observed an increase in autophagosomes and autolysosomes in both non-

degenerating (Figure 3.1 H, compare to Figure 3.1 A) and degenerating (Figure 3.1 I) mid-stage egg chambers even in the absence of starvation. These results show that Dcp-1 is a positive regulator of autophagic flux during mid-oogenesis in both healthy and degenerating mid-stage egg chambers.

3.3. Dcp-1 is required for the degradation of Ref(2)P following starvation

Ref(2)P, the *Drosophila* homolog of p62 (Nezis et al., 2008), is a substrate of autophagy and was shown to be a marker of autophagic activity (Bartlett et al., 2011; Nezis et al., 2010), and therefore we used Ref(2)P analyses to confirm that Dcp-1 is a positive regulator of autophagic flux. Compared to well fed wild-type flies (Figure 3.2 A), nutrient deprived flies had reduced Ref(2)P in follicle cells and nurse cells (Figure 3.2 B), and western blot analysis of wild-type ovaries revealed that the level of Ref(2)P was reduced following starvation (Figure 3.2 C). In addition, ovaries from nutrient deprived flies carrying a mutation in the autophagy gene *Atg7* showed an accumulation of Ref(2)P in follicle cells and nurse cells (Figure 3.2 D), and this accumulation was also confirmed by western blot (Figure 3.2 C) demonstrating that both an increase and block in autophagic flux can be detected. Degenerating mid-stage egg chambers from nutrient deprived *Dcp-1*^{Prev1} flies contained increased levels of Ref(2)P (Figure 3.2 E), and western blot analyses on whole ovaries confirmed that Ref(2)P failed to be completely degraded following starvation compared to ovaries from nutrient deprived wild-type flies (Figure 3.2 F). As autophagic flux appeared to be blocked only in degenerating mid-stage egg chambers of nutrient deprived *Dcp-1*^{Prev1} flies, the slight decrease in Ref(2)P levels observed by western blot following starvation is due to autophagic flux occuring in

Figure 3.2 Ref(2)P analyses confirm that Dcp-1 is required for autophagic flux during mid-oogenesis.

Staining shows DNA (blue), Ref(2)P (red) and Armadillo (green). Zoomed insets show Ref(2)P staining. **(A)** Non-degenerating mid-stage egg chambers from well fed w^{1118} flies showed Ref(2)P staining in somatic follicle cells and germline nurse cells. **(B)** Starved w^{1118} flies contained degenerating mid-stage egg chambers with reduced Ref(2)P staining in nurse cells and follicle cells. **(C)** A representative western blot of ovaries from w^{1118} and $Atg7^{d77/d14}$ flies subjected to well fed or starvation conditions for four days. Samples were subjected to immunoblotting using Ref(2)P. Actin served as a loading control. Densitometry was performed to quantitate Ref(2)P protein levels relative to actin. Graph represents ± SD from five independent experiments (n=5). Statistical significance was determined using a two-tailed Student's t-test. p=0.004 for fed samples, and p=0.008 for starved samples. **(D)** Starved *Atg7* flies showed an accumulation of Ref(2)P in the follicle cells and nurse cells of degenerating mid-stage egg chambers. **(E)** Starved $Dcp\text{-}1^{Prev1}$ flies contained increased levels of Ref(2)P in degenerating mid-stage egg chambers**. (F)** A representative western blot of ovaries from w^{1118} and $Dcp\text{-}1^{Prev1}$ flies that were subjected to well fed or starvation conditions for four days. Samples were subjected to immunoblotting using Ref(2)P. Actin served as a loading control. Densitometry was performed to quantitate Ref(2)P protein levels relative to actin. Graph represents ± SD from five independent experiments (n=5). Statistical significance was determined using a two-tailed Student's t-test. p=0.04. Scale bars, 25μm, zoomed images, 10μm.

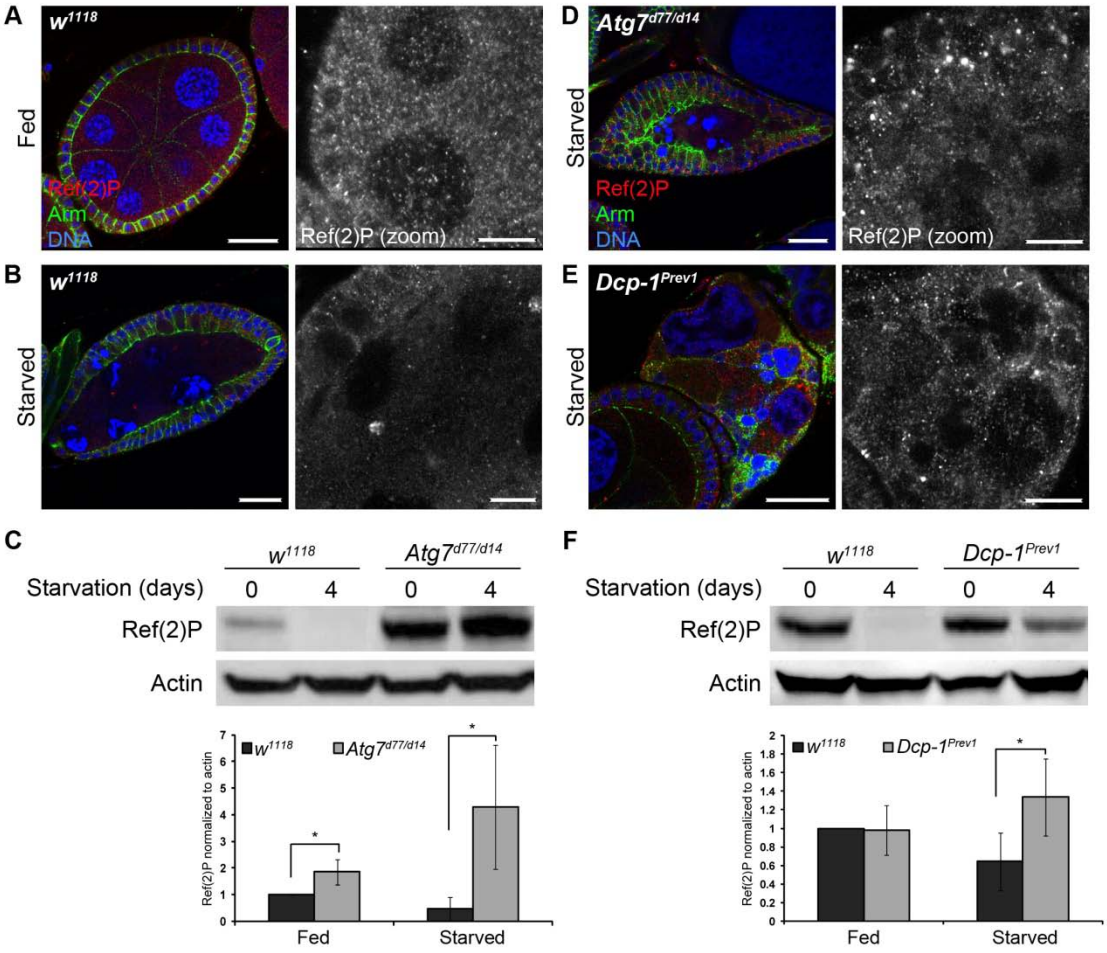
A
w1118
Fed
Ref(2)P
Arm
DNA
Ref(2)P (zoom)
B
w1118
Starved
D
Atg7d77/d14
Starved
Ref(2)P
Arm
DNA
Ref(2)P (zoom)
E
Dcp-1Prev1
Starved
C
w1118
Atg7d77/d14
Starvation (days)
0
4
0
4
Ref(2)P
Actin
w1118
Atg7d77/d14
Ref(2)P normalized to actin
Fed
Starved
F
w1118
Dcp-1Prev1
Starvation (days)
0
4
0
4
Ref(2)P
Actin
w1118
Dcp-1Prev1
Ref(2)P normalized to actin
Fed
Starved

all other egg chambers. These data demonstrate that autophagic flux occurs in response to starvation during *Drosophila* mid-oogenesis in a Dcp-1 dependent manner.

3.4. The catalytic activity of Dcp-1 is required for starvation induced autophagy in the germline

We next investigated whether the catalytic activity of Dcp-1 is required for autophagic flux in the germline. To examine this, a catalytically inactive construct of Dcp-1 harbouring a cysteine to alanine mutation in the catalytic active site (Dcp-$1^{C<A}$) (Tenev et al., 2005), or a catalytically active construct of Dcp-1 (Dcp-1^{FL}) (Hou et al., 2008) was overexpressed in the germline of *Dcp-1^{Prev1}* flies. Degenerating mid-stage egg chambers from *Dcp-1^{Prev1}* flies contained persisting nurse cell nuclei and increased levels of Ref(2)P compared to nutrient deprived *w^{1118}* flies (Figure 3.3 A-B). Overexpression of catalytically inactive Dcp-1 in the germline of *Dcp-1^{Prev1}* flies using the nosGAL4 driver failed to rescue the persisting nurse cell nuclei phenotype (Table 3.1), nor did it result in a reduction of Ref(2)P levels following starvation in degenerating mid-stage egg chambers (Figure 3.3 C). In contrast, overexpression of catalytically active Dcp-1 in the germline of *Dcp-1^{Prev1}* flies resulted in nurse cell nuclei condensation and fragmentation, and a reduction in Ref(2)P levels even under fed conditions (Figure 3.3 D, Table 3.1), confirming that the catalytic activity of Dcp-1 is required for cell death and autophagic flux in degenerating midstage egg chambers.

Figure 3.3 The catalytic activity of Dcp-1 is required for starvation induced autophagy.

Staining shows DNA (blue), Ref(2)P (red), and Armadillo (green). Zoomed insets show Ref(2)P. **(A)** Degenerating mid-stage egg chambers from nutrient deprived w^{1118} files have reduced Ref(2)P, whereas **(B)** nutrient deprived $Dcp\text{-}1^{Prev1}$ flies show increased Ref(2)P levels in degenerating mid-stage egg chambers. **(C)** Overexpression of catalytically inactive Dcp-1 ($Dcp\text{-}1^{C<A}$) in the germline of $Dcp\text{-}1^{Prev1}$ flies does not rescue the apoptotic or autophagic defect in $Dcp\text{-}1^{Prev1}$ flies following starvation. **(D)** Overexpression of catalytically active Dcp-1 ($Dcp\text{-}1^{FL}$) in the germline of $Dcp\text{-}1^{Prev1}$ flies results in normally condensed and fragmented nurse cell nuclei and reduced Ref(2)P levels even without a starvation signal. Scale bars, 25μm, zoomed images, 10μm.

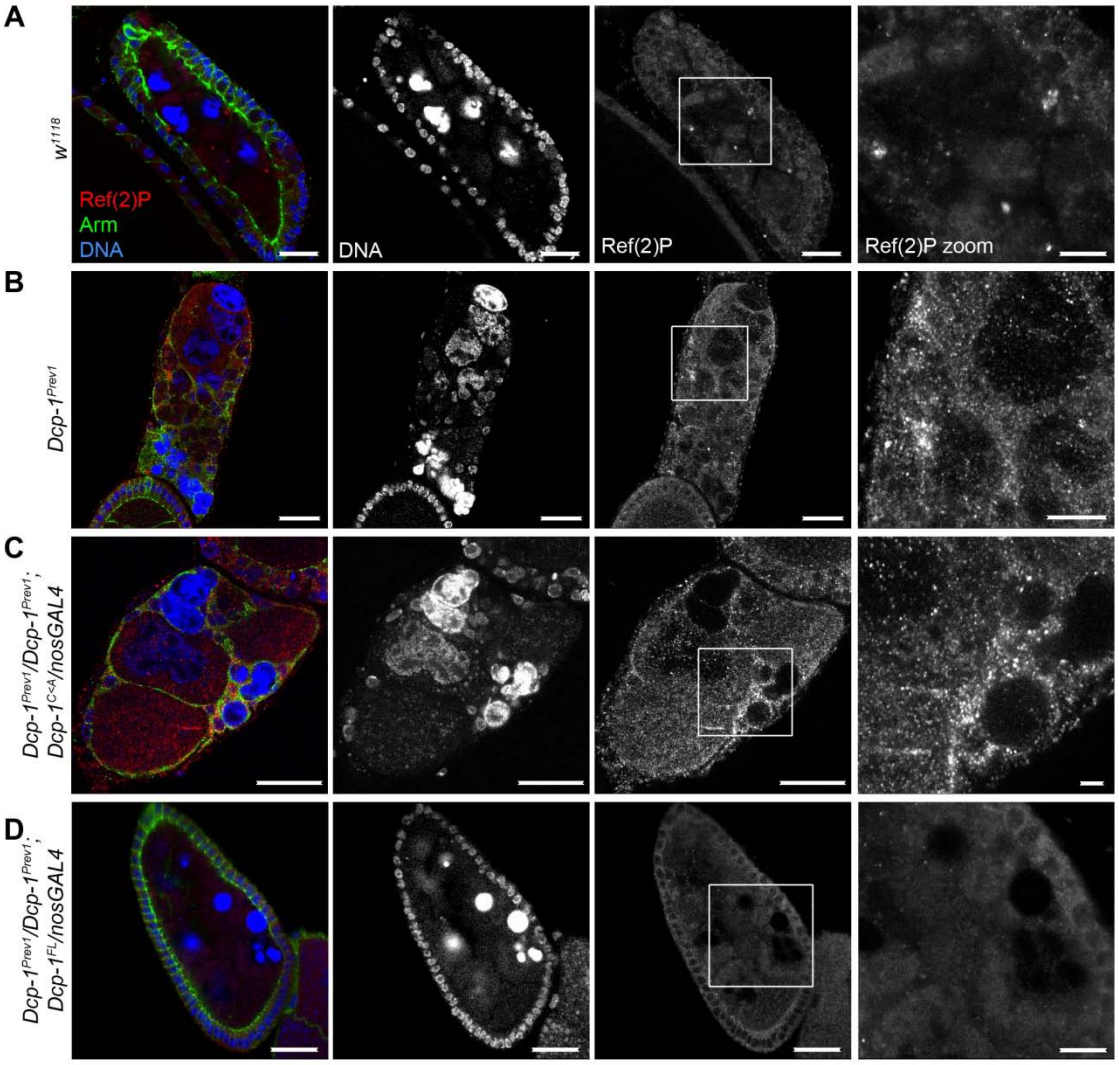
A
w1118
Ref(2)P
Arm
DNA
DNA
Ref(2)P
Ref(2)P zoom
B
Dcp-1Prev1
C
Dcp-1Prev1/Dcp-1Prev1 ;
Dcp-1C<A/nosGAL4
D
Dcp-1Prev1/Dcp-1Prev1 ;
Dcp-1FL/nosGAL4

Table 3.1 Quantification of normally degenerating and persisting mid-stage egg chambers in *Dcp-1^{Prev1}* rescue experiments

Genotype	Treatment	# of ovarioles	% normal degenerating	% persisting
w^{1118}	Starved	184	66	0
Dcp-1^{Prev1}	Starved	173	0	97
Dcp-1$^{Prev1/}$Dcp-1^{Prev1}; UASp-Dcp-1$^{C<A}$/nosGAL4	Starved	95	0	94
Dcp-1$^{Prev1/}$Dcp-1^{Prev1}; UASp-Dcp-1^{FL}/nosGAL4	Starved	122	60	12

3.1. Candidate Dcp-1 interacting partners modify LTG levels following starvation

To better understand the mechanism of Dcp-1 mediated autophagic flux, results from an immuno-affinity purification (IP) and tandem mass spectrometry (MS/MS) assay (IP-MS) undertaken previously in the laboratory (Hou YC, Moradian A, Morin GB, Gorski SM, unpublished) were used to identify candidate substrates and interactors of Dcp-1 that regulate starvation-induced autophagy. To prevent the proteolytic cleavage of Dcp-1's candidate substrates and allow for their identification (Kamada et al., 1998), a catalytically inactive, V5-tagged construct of Dcp-1 (Dcp-$1^{C<A}$) was overexpressed in the *Drosophila* tumourous larval hemocyte cell line *l(2)mbn*. A subset of high confidence candidate proteins were identified by removing proteins that were identified in the vector-only negative control and by removing abundant proteins including actin and tubulin (Gingras et al., 2007). In addition, proteins that were found in only one experimental sample and those without an X! Tandem average log(E) score of ≤ -3 were also removed (Lisacek, 2006). A set of 24 candidate interacting partners and/or substrates of Dcp-1 were identified that met our selection threshold (Table 1.2). CasPredictor, a web-based tool for caspase substrate predictions, was used to assess which candidates contain a predicted caspase cleavage site (Garay-Malpartida et al., 2005). It was found that 10 of the 24 candidates have predicted caspase cleavage sites (Table 1.2). As several caspase substrates have non-canonical cleavage sites (Crawford and Wells, 2011), and Dcp-1 may also regulate autophagy in a non-direct manner through one or more of the identified interacting partners, we selected all candidates for further autophagy analyses to enrich the list of autophagy modulators involved in Dcp-1 mediated autophagic flux.

Drosophila l(2)mbn cells were previously shown to undergo autophagy (Hou et al., 2008) and therefore we utilized this cell line in all subsequent assays. In addition, we used LysoTracker Green coupled with flow cytometry to identify positive and negative regulators of autophagy. Lysotracker accumulates in both lysosomes and autolysosomes (Klionsky et al., 2012; Scott et al., 2004), and therefore is not specific for autophagy but is a good indicator of autophagy-associated lysosomal activity. LTG coupled with flow cytometry was previously used in the laboratory to identify known as well as novel regulators of starvation induced autophagy (Hou et al., 2008). Double-stranded RNAs (dsRNAs) were designed for each candidate interactor of Dcp-1, and following RNAi, *l(2)mbn* cells were transferred from nutrient full (fed) media to amino acid and serum deprived (starvation) media for 2 hours, and LTG was analyzed by flow cytometry. Compared to control RNAi treated cells, RNAi of *RheB*, a negative regulator of autophagy, significantly increased LTG fluorescence following starvation whereas RNAi of *S6K*, a positive regulator of autophagy, significantly reduced LTG fluorescence (Figure 3.4 A-B). This confirms that the LTG assay is sensitive enough to identify both positive and negative regulators of starvation induced autophagy. dsRNAs were designed against all 24 candidate substrates and interactors of Dcp-1, and of these, 13 showed a statistically significant increase in LTG fluorescence following RNAi and starvation treatment, indicating that these candidates act as potential negative regulators of autophagy (Figure 3.4 A). These candidates included the heat shock proteins Hsc70-4, Hsp70Aa, Hsp60 and Hsp83, translation initiation factor eIF-4a, the chromatin remodeler Mi-2, the ribosomal constituent Sta, the AAA^+ ATPase Ter94, the chloride intracellular channel protein Clic, the proteasome activator REG, and the mitochondrial proteins ATPsynthase-β, Blw and SesB. A second set of non-overlapping dsRNAs were designed and used to validate these LTG findings (Figure 3.4 B).

Figure 3.4 Candidate Dcp-1 interactors/substrates modify LTG following starvation *in vitro.*

(A) RNAi treated cells were subjected to starvation conditions and stained with LysoTracker Green (LTG) to measure autophagy-associated activity. Fluorescence was measured by flow cytometry. Error bars represent the SEM of at least 3 independent experiments (n=3). Statistical significance was determined using one-way ANOVA with a Dunnet post-test. Knockdown of genes that significantly increased LTG levels are indicated in red ($p<0.05$), and knockdown of genes that significantly decreased LTG levels are indicated in blue ($p<0.05$). dsRNA designed against the Ampicillin resistance gene from bacteria was used as a negative control dsRNA and is shown in black. **(B)** A second set of non-overlapping dsRNAs were designed to confirm the findings in Figure 3.4 A.

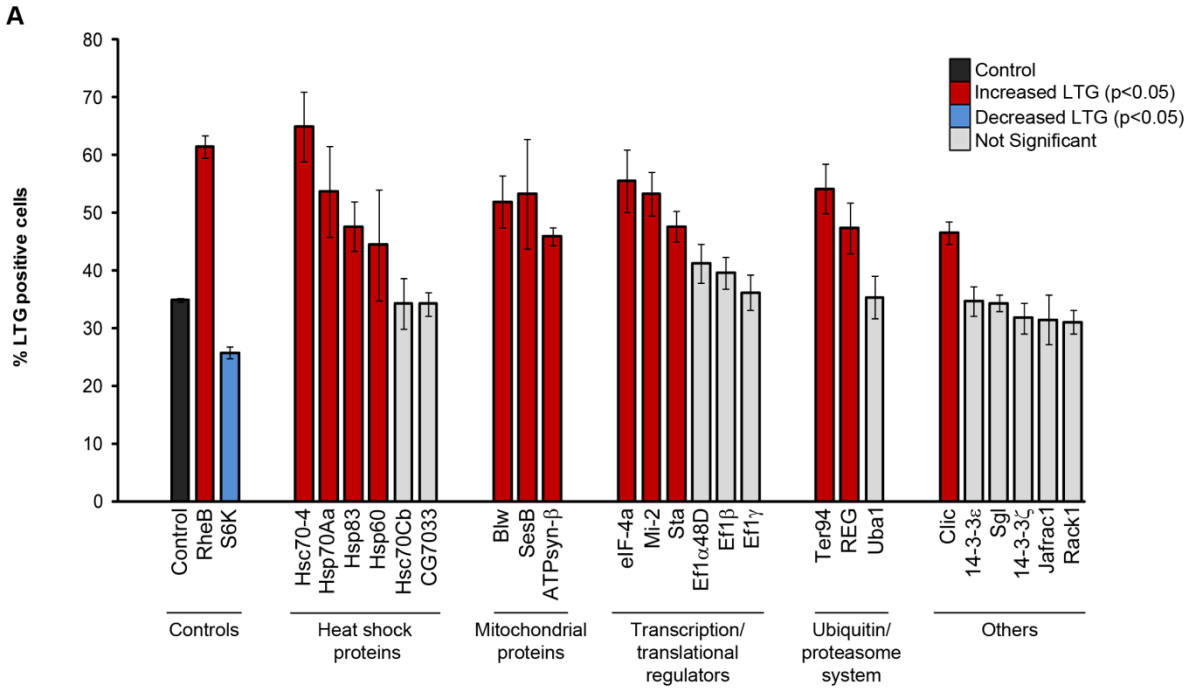
A
% LTG positive cells
80
70
60
50
40
30
20
10
0
Control
Increased LTG (p<0.05)
Decreased LTG (p<0.05)
Not Significant
Control
RheB
S6K
Hsc70-4
Hsp70Aa
Hsp83
Hsp60
Hsc70Cb
CG7033
Blw
SesB
ATPsyn-β
eIF-4a
Mi-2
Sta
Ef1α48D
Ef1β
Ef1γ
Ter94
REG
Uba1
Clic
14-3-3ε
Sgl
14-3-3ζ
Jafrac1
Rack1
Controls
Heat shock proteins
Mitochondrial proteins
Transcription/ translational regulators
Ubiquitin/ proteasome system
Others

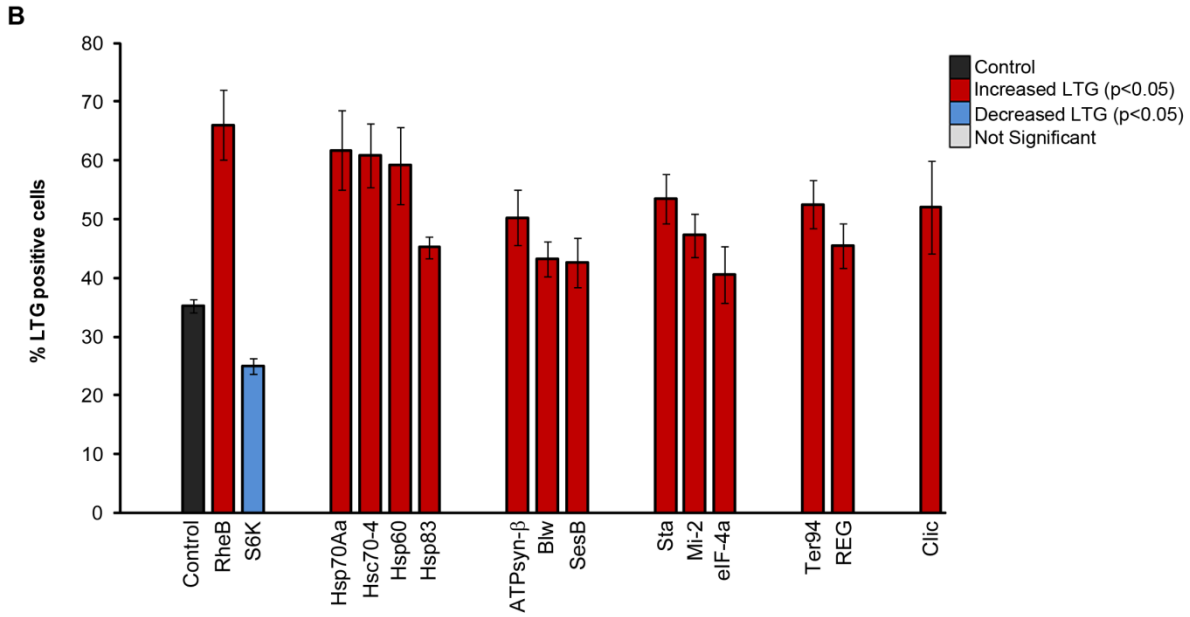
B
% LTG positive cells
80
70
60
50
40
30
20
10
0
Control
Increased LTG (p<0.05)
Decreased LTG (p<0.05)
Not Significant
Control
RheB
S6K
Hsp70Aa
Hsc70-4
Hsp60
Hsp83
ATPsyn-β
Blw
SesB
Sta
Mi-2
eIF-4a
Ter94
REG
Clic

3.2. Loss of Clic or Hsp83 enhances the percentage of degenerating mid-stage egg chambers undergoing autophagic flux

To determine whether candidate substrates/interactors of Dcp-1 also regulate starvation-induced autophagy *in vivo* during *Drosophila* oogenesis, we utilized an *in vivo* RNAi approach. Since Dcp-1 plays a non-redundant role in cell death and autophagy in the ovary, we wanted to determine if its candidate interactors/substrates also function in this tissue. We began by overexpressing Dicer in the germline, in combination with long double-stranded hairpin constructs using the nos-GAL4 driver, to induce efficient target gene knockdown in the ovary (Handler et al., 2011; Wang and Elgin, 2011). 6 available RNAi lines targeting candidate Dcp-1 interactors and substrates, including *Hsc70-4, Ter94, Sta, eIF-4a*, *Hsp83* and *Clic,* were obtained for *in vivo* autophagy analyses. We found that RNAi-mediated knockdown of 5 candidates, *Hsc70-4, Ter94, Sta, eIF-4a* and *Hsp83* in the germline resulted in agametic, rudimentary ovaries characterized by a lack of germ cells (Figure 3.5 A-E). Loss of germ cells during development, or the failure to form germ cells, can lead to agametic ovaries (Rongo and Lehmann, 1996; Staab and Steinmann-Zwicky, 1996; Tavosanis and Gonzalez, 2003). These observations indicate that *Ter94, Sta, Hsc70-4, eIF-4a* and *Hsp83* are required for germ cells to form, or are required for germ cell survival during development, and therefore, their effects on autophagic flux in the germline could not be assessed using this method.

Clic proteins were first identified based on their intracellular chloride channel activity (Landry et al., 1993, 1989), but the functional roles of Clic proteins are poorly understood. As the *Drosophila* genome encodes only one *Clic* gene, it makes *Drosophila* an attractive model to study the function of Clic and its possible role in autophagy. Clic was knocked down in the germline using *Dcr-2;nosGAL4* and flies were

Figure 3.5 Candidate Dcp-1 interactors/substrates are required for germ cell development and/or survival.

RNAi mediated knockdown of **(A)** Ter94, **(B)** Sta, **(C)** eIF-4a, **(D)** Hsc70-4 and **(E)** Hsp83 in the germline using *Dicer-2;nosGAL4* led to agametic ovaries. Ovaries were stained with anti-Armadillo (green) to visualize cell-cell junctions and Draq5 (blue) to visualize nuclei. The posterior (P) and anterior (A) of the ovary is indicated in (A). n=15 pairs of ovaries were examined for each genotype. Scale bars, 50μm.

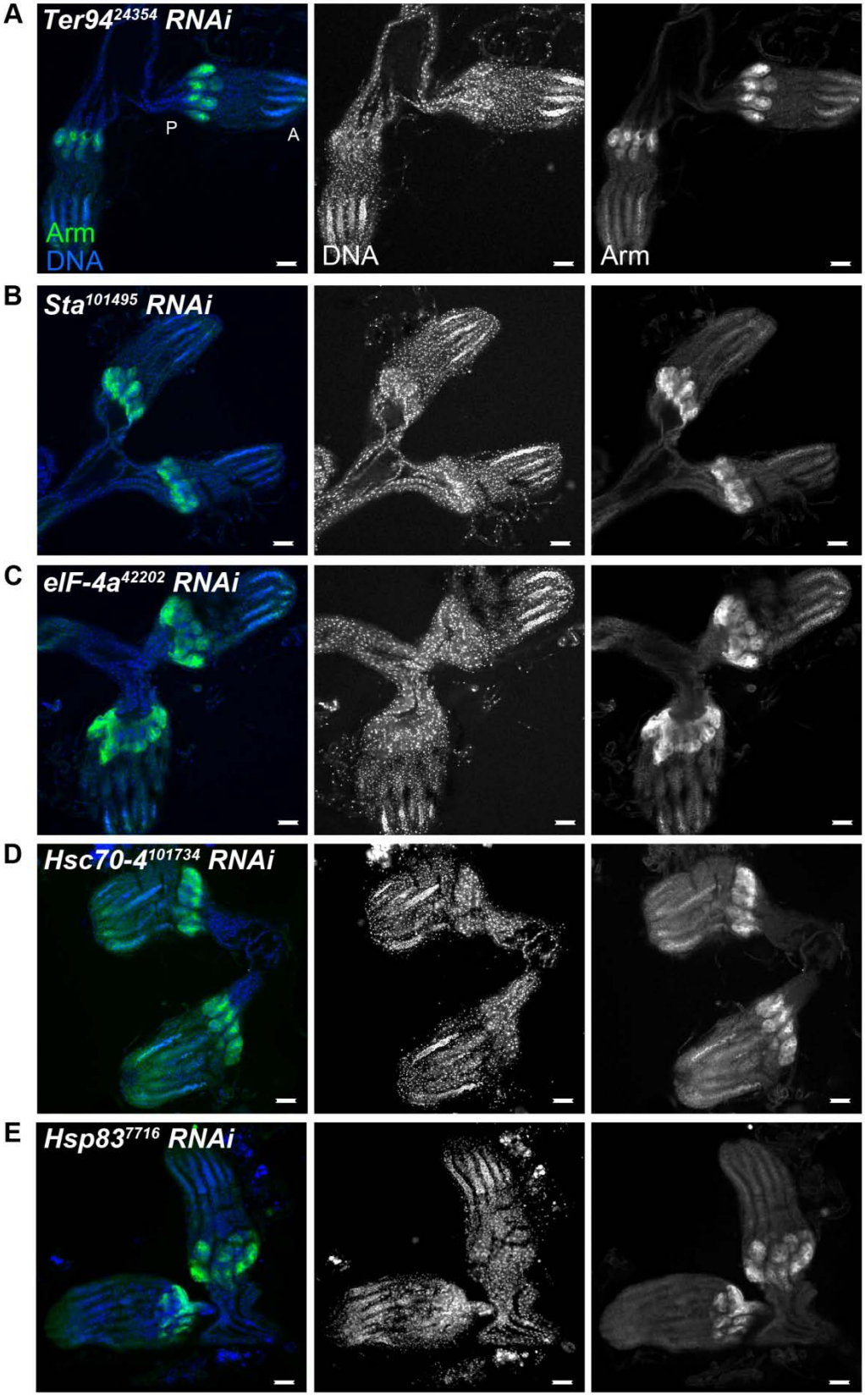
A
Ter94^24354 RNAi
P
A
Arm
DNA
DNA
Arm
B
Sta^101495 RNAi
C
elF-4a^42202 RNAi
D
Hsc70-4^101734 RNAi
E
Hsp83^7716 RNAi

conditioned on yeast paste for 3 days followed by starvation conditions for 4 days. Although we observed no significant differences in LTR staining between well fed *Clic-RNAi* and control flies (Figure 3.6 A-C), starved *Clic-RNAi* flies contained an increase in the percentage of degenerating mid-stage egg chambers that stained positively for LTR compared to starved control flies (Figure 3.6 C). To examine if the increased LTR was associated with increased autophagic flux, we performed Ref(2)P analyses on ovaries from nutrient deprived control and *Clic-RNAi* flies (Figure 3.6 E-F). As expected, nutrient deprived control flies contained reduced Ref(2)P in degenerating mid-stage egg chambers compared to well fed control flies (Figure 3.6 D-E). Similarly, nutrient deprived *Clic-RNAi* flies contained low levels of Ref(2)P in degenerating mid-stage egg chambers (Figure 3.6 F). This data indicates that loss of Clic enhances the percentage of degenerating mid-stage egg chambers undergoing autophagic flux.

RNAi mediated knockdown of Hsp83 in the germline resulted in agametic ovaries (Figure 3.5 E), and although Hsp83 homozygous mutant flies are lethal (Yue et al., 1999), some trans-heterozygous combinations of Hsp83 are viable (Andersen et al., 2012; van der Straten et al., 1997). Therefore, we examined the role of a trans-heterozygous hypomorphic combination of Hsp83 alleles, $Hsp83^{582}/Hsp83^{13F3}$, for its role in starvation induced autophagy during *Drosophila* oogenesis. Ovaries from nutrient-deprived $Hsp83^{582}/Hsp83^{13F3}$ flies contained an increase in the percentage of degenerating mid-stage egg chambers that stained positive for LTR relative to nutrient deprived control flies (Figure 3.6 G-I). Moreover, these degenerating mid-stage egg chambers had reduced levels of Ref(2)P, similar to nutrient deprived wild-type flies (Figure 3.6 J-L). These observations indicate that, like Clic, Hsp83 acts as a negative

Figure 3.6 Loss of Clic or Hsp83 in the germline increases degenerating mid-stage egg chambers undergoing autophagic flux.

Ovaries from nutrient deprived **(A)** control flies (genotype *Dcr-2/+;nosGAL4/+)* or **(B)** Clic RNAi flies (genotype *Clic-RNAi/Dcr-2;nosGAL4/+*) had increased LTR (Red) in degenerating midstage egg chambers (arrow). **(C)** Knockdown of Clic in the germline resulted in an increase in the percentage of degenerating mid-stage egg chambers that stained positively for LTR following starvation compared to the control. At least 100 ovarioles from 8 animals of each genotype were scored. **(D)** Well fed *control RNAi* flies contained Ref(2)P distributed throughout the follicle cells and nurse cells. **(E)** Following starvation, degenerating midstage egg chambers from control RNAi flies contained reduced Ref(2)P (red) levels. **(F)** Degenerating mid-stage egg chambers from *Clic-RNAi* flies have reduced levels of Ref(2)P (red), similar to nutrient deprived control flies. **(G)** Nutrient deprived w^{1118} or **(H)** $Hsp83^{582}/Hsp83^{13F3}$ flies had high levels of LTR staining (red) in degenerating midstage egg chambers (arrow). **(I)** $Hsp83^{582}/Hsp83^{13F3}$ flies had an increase in the percentage of degenerating mid-stage egg chambers that stained positively for LTR. At least 100 ovaries from 8 different flies of each genotype were quantified. **(J)** Well fed w^{1118} flies contained Ref(2)P distributed throughout the germline and follicle cells, whereas **(K)** nutrient deprived w^{1118} flies contained degenerating mid-stage egg chambers with reduced Ref(2)P staining. **(L)** Nutrient deprived $Hsp83^{582}/Hsp83^{13F3}$ flies contained reduced levels of Ref(2)P staining in degenerating mid-stage egg chambers, similar to what was observed in nutrient deprived w^{1118} flies. Scale bars 25μm.

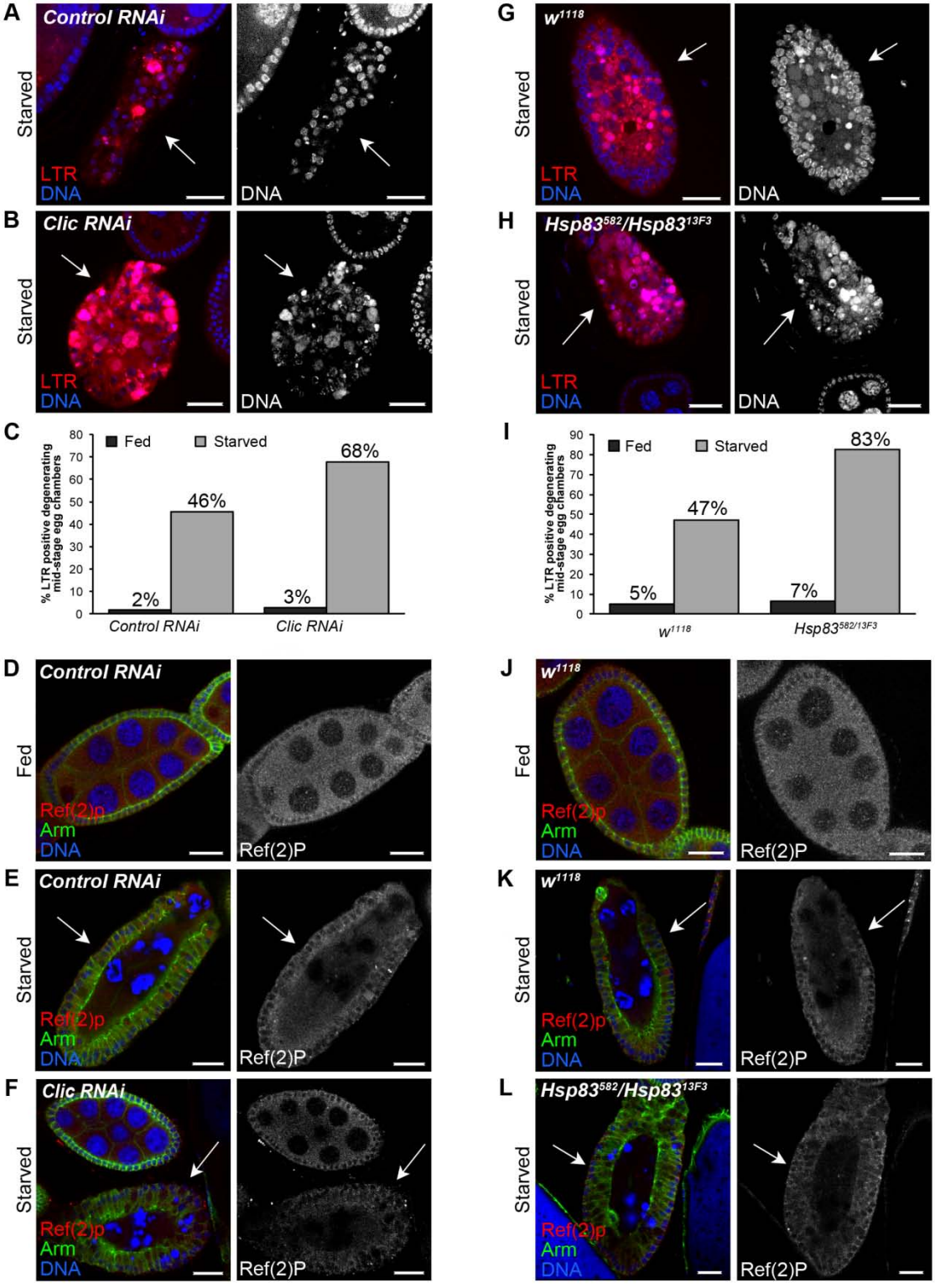
A
Control RNAi
Starved
LTR
DNA
DNA
B
Clic RNAi
Starved
LTR
DNA
DNA
C
% LTR positive degenerating mid-stage egg chambers
Fed
Starved
2%
46%
3%
68%
Control RNAi
Clic RNAi
G
w1118
Starved
LTR
DNA
DNA
H
Hsp83582/Hsp8313F3
Starved
LTR
DNA
DNA
I
% LTR positive degenerating mid-stage egg chambers
Fed
Starved
5%
47%
7%
83%
w1118
Hsp83582/13F3
D
Control RNAi
Fed
Ref(2)p
Arm
DNA
Ref(2)P
E
Control RNAi
Starved
Ref(2)p
Arm
DNA
Ref(2)P
F
Clic RNAi
Starved
Ref(2)p
Arm
DNA
Ref(2)P
J
w1118
Fed
Ref(2)p
Arm
DNA
Ref(2)P
K
w1118
Starved
Ref(2)p
Arm
DNA
Ref(2)P
L
Hsp83582/Hsp8313F3
Starved
Ref(2)p
Arm
DNA
Ref(2)P

regulator of starvation-induced mid-stage egg chamber degeneration and autophagic flux during *Drosophila* oogenesis.

3.3. Dcp-1 and Hsp83 interact but Hsp83 is not a target of Dcp-1's proteolytic activity

As Hsp83 acts as a negative regulator of autophagic flux following starvation during mid-oogenesis, and has a predicted caspase cleavage site, we next examined whether Hsp83 is a proteolytic target of Dcp-1 by performing *in vitro* cleavage assays. Purified catalytically active Dcp-1 (Dcp-1^{FL}) and catalytically inactive Dcp-1 (Dcp-$1^{C<A}$) were expressed in *l(2)mbn* cells and Dcp-1 was purified by Ni^{2+}-NTA columns. Whereas Dcp-1^{FL} was able to cleave *in vitro* translated Drice, a known target of Dcp-1's proteolytic activity (Song et al., 2000b), there were no detectable Hsp83 cleavage products suggesting that Hsp83 is not a Dcp-1 substrate (Figure 3.7 A). To confirm the interaction between Dcp-1 and Hsp83, we performed immunoprecipitation experiments. V5-tagged Dcp-$1^{C<A}$ was expressed in *l(2)mbn* cells and cell lysates were immunoprecipitated with anti-V5 antibody (Figure 3.7 B). V5-Dcp-$1^{C<A}$ immunoprecipitated endogenous Hsp83 confirming previous IP-MS results (Hou YC, Moradian A, Morin GB and Gorski SM, unpublished). In addition, when N- and C-terminal FLAG-tagged Hsp83 constructs were overexpressed in *l(2)mbn* cells, both FLAG-Hsp83 constructs immunoprecipitated endogenous pro-Dcp-1 further confirming that Hsp83 and Dcp-1 interact (Figure 3.7 C). Notably, only pro-Dcp-1 and not processed Dcp-1 was pulled down by FLAG-Hsp83 constructs further suggesting that Hsp83 is not a substrate of Dcp-1 but rather a binding partner. All together, this data shows that Dcp-1 binds Hsp83 in a non-proteolytic manner, however future studies are required to determine the precise relationship between Dcp-1 and Hsp83.

Figure 3.7 Dcp-1 interacts with Hsp83 but Hsp83 is not a target of Dcp-1's proteolytic activity.

(A) Purified catalytically active Dcp-1 (Dcp-1^{FL}) and catalytically inactive Dcp-1 (Dcp-$1^{C<A}$) were incubated with *in vitro* translated Drice or Hsp83. Dcp-1^{FL} cleaved Drice but not Hsp83. **(B)** V5-Dcp-$1^{C<A}$ was expressed in *l(2)mbn* cells and immunoprecipitated with V5 agarose. A representative western blot shows that V5-Dcp-$1^{C<A}$ immunoprecipitated endogenous Hsp83. **(C)** N and C terminal FLAG tagged constructs of Hsp83 were expressed in *l(2)mbn* cells and immunoprecipitated with FLAG agarose. A representative western blot shows that both N and C FLAG tagged constructs immunoprecipitated endogenous pro-Dcp-1. No processed Dcp-1 was detected following immunoprecipitation.

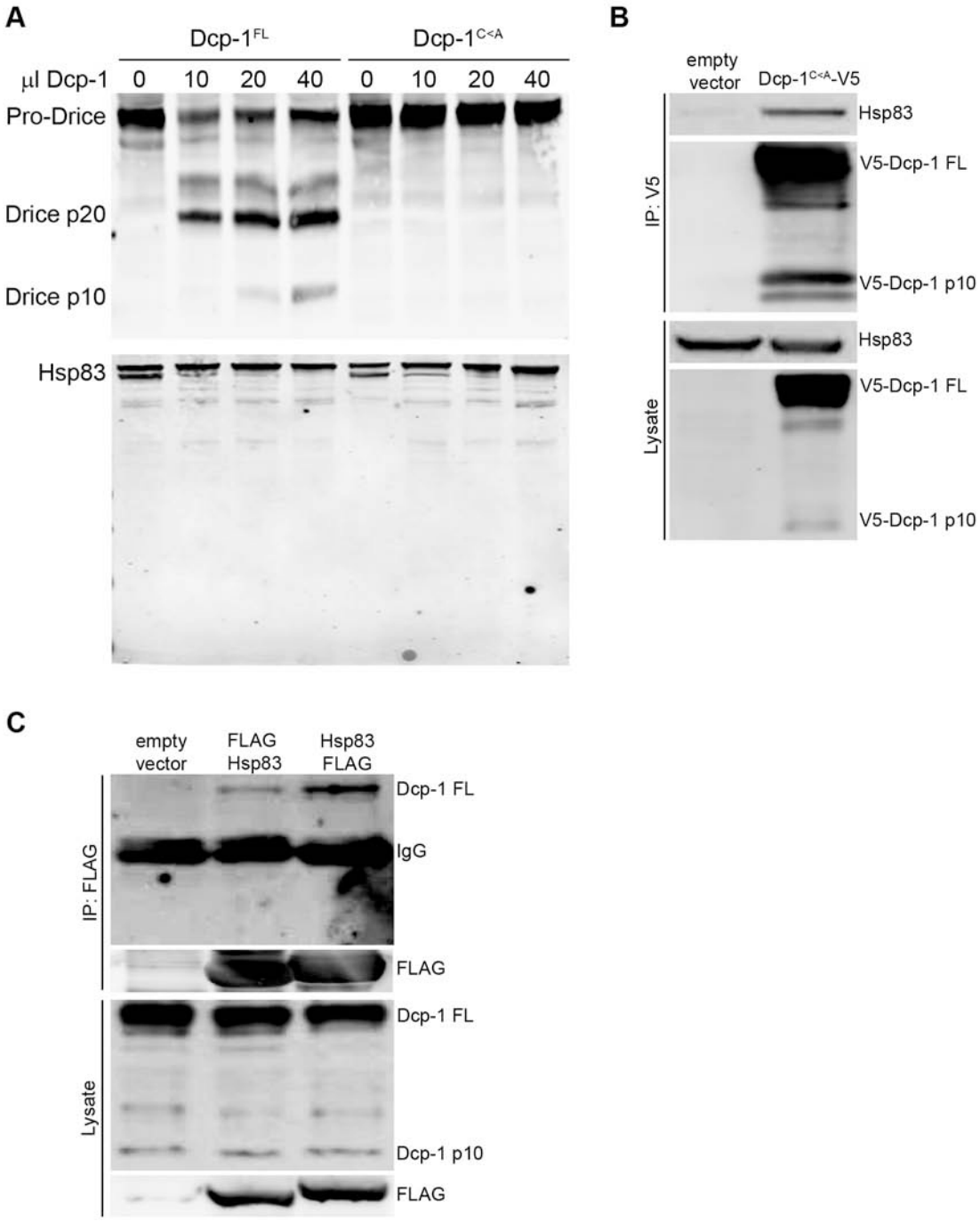
A
Dcp-1FL
Dcp-1C<A
µl Dcp-1
0
10
20
40
0
10
20
40
Pro-Drice
Drice p20
Drice p10
Hsp83
B
empty vector
Dcp-1C<A-V5
IP: V5
Hsp83
V5-Dcp-1 FL
V5-Dcp-1 p10
Lysate
Hsp83
V5-Dcp-1 FL
V5-Dcp-1 p10
C
empty vector
FLAG Hsp83
Hsp83 FLAG
IP: FLAG
Dcp-1 FL
IgG
FLAG
Lysate
Dcp-1 FL
Dcp-1 p10
FLAG

3.4. Discussion

The data presented in this chapter demonstrate that autophagic flux occurs during *Drosophila* mid-oogenesis in response to starvation. Mid-stage egg chambers undergoing degeneration require Dcp-1 for both autophagy and cell death in a catalytically dependent manner. It has been previously shown that low activity levels of Dcp-1 induce autophagy, whereas high activity levels of Dcp-1 induce apoptosis (Kim et al., 2010). Perhaps low levels of Dcp-1 mediate autophagy in a catalytically-dependent manner as a first response to starvation in mid-stage egg chambers, and once cellular stress reaches a certain apoptotic threshold, Dcp-1 becomes fully activated to induce apoptosis.

Using an *in vitro* RNAi approach, we identified 13 novel Dcp-1-associated regulators of starvation-induced autophagy including the heat shock proteins Hsc70-4, Hsp70Aa, Hsp60 and Hsp83, translation initiation factor eIF-4a, the chromatin remodeler Mi-2, the ribosomal constituent Sta, the AAA^+ ATPase Ter94, the chloride intracellular protein Clic, the proteasome activator REG, and the mitochondrial proteins ATPsynthase-β, Blw and SesB. It is possible that additional genes identified in the IP-MS study may positively or negatively regulate autophagy, but due to incomplete RNAi knockdown or functional redundancy, they were not detected. Consistent with our *in vitro* data, Hsc70-4 was previously identified as a potential regulator of autophagy in *Drosophila*. Hsc70-4, a clathrin-uncoating ATPase, was shown to regulate the TOR signalling pathway, and loss of Hsc70-4 function in larvae showed decreased TOR activity (Hennig et al., 2006). As Hsc70-4 has a predicted caspase cleavage site (Table 1.2), perhaps Dcp-1 mediated cleavage of Hsc70-4 leads to decreased TOR activity and induction of autophagy, however, further studies are required to determine if Hsc70-4 is

a proteolytic target of Dcp-1. In addition, regulators identified in the RNAi screen including Hsp83 and Ter94 have mammalian homologues that have been implicated in autophagy. For example, the mammalian homolog of Ter94, Valosin Containing Protein (VCP), is required for autophagic degradation of ubiquitinated proteins (Tresse et al., 2010). RNAi mediated knockdown of VCP led to an accumulation of partially acidified autophagosomes containing ubiquitin positive contents (Tresse et al., 2010). Consistently, RNAi of *Ter94* in *Drosophila* S2 cells led to an accumulation of polyubiquitinated proteins (Wójcik et al., 2004). This finding is consistent with our data, and although knockdown of Ter94 by RNAi led to increased LTG levels, further *in vitro* autophagic flux assays are required to confirm the role of Ter94 in autophagy. Validating the remaining genes identified in the RNAi screen for their autophagy-regulatory role *in vivo* during *Drosophila* oogenesis or in other tissues will be valuable. In summary, our *in vitro* RNAi screen used in this study identified several novel regulators of starvation-induced autophagy and provides a foundation for further *in vivo* analyses to identify the role of these genes in starvation induced autophagy.

Clic proteins represent a unique class of channel proteins as they exist as both a membrane bound channel and as a soluble protein within the cytoplasm. It has been hypothesized that the transition of Clic proteins between a membrane bound and soluble form is influenced by redox status (Littler et al., 2005, Singh et al., 2006). Mammalian Clic proteins contain a conserved C-terminal Clic module that has weak sequence homology to the glutathione S-transferase (GST) superfamily (Harrop et al., 2001; Littler et al., 2008). In addition, Clic proteins are highly conserved among vertebrates and non-vertebrates (Littler et al., 2008). *Drosophila* Clic contains a glutathione S-transferase (GST) fold and is more closely related to human Clic1 and Clic4 than to other GST-fold

family members (Littler et al., 2008). Purified recombinant *Drosophila* Clic can bind artificial lipid bilayers and can form ion channels in artificial bilayers at low pH (Littler et al., 2008). However, little is known about the function of *Drosophila* Clic. We have shown that loss of Clic in the germline by RNAi enhanced the percentage of degenerating mid-stage egg chambers undergoing autophagic flux. Our data is consistent with the recent finding that knockdown of mammalian Clic4 by RNAi enhanced autophagy and cell death following starvation in U251 glioma cancer cells (Zhong et al., 2012). Following starvation, Clic4 is upregulated and translocates from the cytoplasm to the nucleus where it functions to mediate autophagy (Zhong et al., 2012). Clic4 RNAi blocked the interaction of Clic4 with 14-3-3ε, leading to Beclin 1 over activation and a further increase in autophagy and cell death following starvation (Zhong et al., 2012). Our results reveal a novel role for *Drosophila* Clic in starvation-induced autophagy during *Drosophila* oogenesis, providing the first *in vivo* evidence that Clic proteins modulate autophagy. Although Clic does not have a favourable cleavage site, Dcp-1 may still regulate Clic in a proteolytic dependent manner, or alternatively, in a non-proteolytic manner, perhaps by altering its localization or function. Further studies including *in vitro* cleavage assays and immunoprecipitation assays are required to confirm the interaction between Clic and Dcp-1.

Drosophila Hsp83 is part of the evolutionary conserved heat shock protein-90 family and is involved in cellular homeostasis. Inhibition of Hsp90, the mammalian homolog of *Drosophila* Hsp83, specifically in the mitochondria activates AMPK leading to inhibition of mTOR complex 1 and induction of autophagy in several different cancer cell lines (Chae et al., 2012a). Moreover, the Hsp90-Cdc37 chaperone complex is required for Ulk1 and Atg13 mediated mitophagy (selective removal of mitochondria by

autophagy) (Joo et al., 2011). Hsp83 was a promising candidate for Dcp-1 mediated cleavage as it negatively regulates LTG levels following starvation *in vitro*, contains a potential caspase cleavage site, and its mammalian homolog, Hsp90, was shown to be cleaved following ionizing radiation in breast cancer cells (Prasad et al., 1998). Although Dcp-1 interacts with Hsp83, *in vitro* cleavage assays revealed that Hsp83 is not cleaved by Dcp-1. This does not rule out the possibility that Drice may cleave Hsp83. Given the fact that only pro-Dcp-1 and not processed Dcp-1 interacts with Hsp83 suggests that Hsp83 is a binding partner of Dcp-1 rather than its substrate. Perhaps Hsp83 acts as an upstream regulator of Dcp-1, as it was shown that specific inhibition of mammalian Hsp90 by 17-AAG led to increased caspase activation and induction of cell death (Karkoulis et al., 2010; Nimmanapalli et al., 2003). We postulate that endogenous Dcp-1 requires a starvation signal to induce autophagy. Therefore, following starvation Dcp-1 activity is enhanced in the absence of Hsp83, leading to increased degenerating mid-stage egg chambers undergoing autophagic flux. Further studies are required to determine the exact relationship between Hsp83 and Dcp-1.

In summary, we have identified Dcp-1 as a positive regulator of starvation induced autophagic flux in degenerating mid-stage egg chambers. Our *in vitro* LTG assay coupled with flow cytometry identified 13 novel negative regulators of starvation induced autophagy, indicating that Dcp-1 may act through a wide range of substrates or interactors to execute autophagy. Further *in vivo* analysis of two candidates, Clic and Hsp83, revealed that they are normally required to suppress degeneration of mid-stage egg chambers undergoing autophagic flux following starvation. This is the first report to our knowledge identifying *Drosophila* Clic and Hsp83 in the regulation of autophagy. Further *in vivo* examination into the role of additional regulators of starvation induced

autophagy will be valuable to not only understand how they contribute to the autophagy process, but to also better understand the mechanism of Dcp-1 mediated autophagy.

4. The *Drosophila* effector caspase Dcp-1 localizes within mitochondria and regulates mitochondrial dynamics and autophagic flux via SesB

Portions of this chapter were submitted for publication as DeVorkin L, Go NE, Hou YC, Moradian A, Morin GB and Gorski SM "The Drosophila effector caspase Dcp-1 localizes within mitochondria and regulates mitochondrial dynamics and autophagic flux via SesB".

4.1. Introduction

Caspases are a group of cysteine proteases that function to execute the apoptotic cell death pathway. Caspases are synthesized as inactive zymogens (also called pro-caspases) and become proteolytically activated by dimerization or a cleavage event. In general, initiator caspases are activated by dimerization that is facilitated by a multiprotein complex such as the apoptosome, and once activated they cleave and activate downstream effector caspases (Boatright et al., 2003). Effector caspases are present as inactive zymogen dimers and require a cleavage event between their interdomain linker for activation (Chai et al., 2001; Boatright et al., 2003; Riedl and Shi, 2004). Once activated, they cleave a variety of cellular substrates to induce cell death. In *Drosophila*, there are 3 initiator caspases including Dronc, Dredd and Strica, and 4 effector caspases including Dcp-1, Drice, Decay and Damm (Hay and Guo, 2006). Although caspases are well known for their role in apoptosis, it is becoming increasingly evident that caspases have non-apoptotic functions in diverse processes such as immunity, differentiation, compensatory proliferation and autophagy (Wirawan et al.,

2010; Kuranaga and Miura, 2007; Hou et al., 2008). For example, Soti, an E3 ubiquitin ligase complex inhibitor required for caspase activation, and the Inhibitor of Apoptosis Protein (IAP) Bruce, are expressed in a gradient in developing spermatids. This results in an inverse gradient of caspase activity thereby promoting caspase-dependent differentiation while preventing apoptosis (Kaplan et al., 2010). In *Drosophila* neural stem cells (neuroblasts), Numb protein asymmetrically localizes to the differentiating daughter cell to restrict self-renewal and differentiation, and phosphomimetic numb leads to ectopic neuroblast formation (Ouyang et al., 2011). Dronc was shown to bind Numb in a non-apoptotic, and possibly non-catalytic manner to attenuate ectopic neuroblast formation (Ouyang et al., 2011) implicating Dronc in a novel role of neural stem cell homeostasis. Dronc is also involved in compensatory proliferation in the wing imaginal disc in response to cell death (Huh et al., 2004), and Dronc and several other cell death regulators including Ark, Hid, Drice and Bruce are involved in spermatid individualization, a non-apoptotic process (Arama et al., 2003; Huh et al., 2003; Muro et al., 2004) In addition, border cell migration in the *Drosophila* ovary is inhibited by dominant-negative Rac, and overexpression of DIAP1 suppressed the migration defect, whereas loss-of-function mutations in DIAP1 lead to migration defects in the absence of apoptosis implicating DIAP1 as a mediator of apoptosis-independent cell migration (Geisbrecht and Montell, 2004). Moreover, overexpression of Dcp-1 in motor neurons induced motor neuron degeneration in the absence of TUNEL staining (Keller et al., 2011), and Dcp-1 was also shown to be required for starvation induced autophagic flux in degenerating mid-stage egg chambers in response to starvation (Hou et al., 2008) (Figure 3.1 G).

A caspase activity threshold must be met in order for apoptosis to occur, and the levels of pro-caspases are proportional to the sensitivity of the cell to apoptosis

(Florentin and Arama, 2012). Drice was proposed to act as the major effector caspase in *Drosophila* while Dcp-1 was proposed to finely tune the rate of apoptosis (Florentin and Arama, 2012). To prevent excess caspase activation, caspase activity may be low or caspases may be temporally or subcellularly restricted (Florentin and Arama, 2012). In mammalian cells, effector Caspase 3 and initiator Caspase 9 localize to the mitochondria during apoptosis (Chandra and Tang, 2003), and S-nitrosylation of mitochondrial pro-Caspase 3 and pro-Caspase 9 in their catalytic active site prevents their activation (Mannick et al., 2001). In *Drosophila*, both Dronc and Drice have been shown to localize to mitochondria (Dorstyn et al., 2002), however their role at the mitochondria remains unknown.

Mitochondria are highly dynamic, double membrane organelles that take part in a number of cellular processes including oxidative phosphorylation, calcium signaling and apoptosis. In *Drosophila*, the role of mitochondria in apoptosis is still not completely understood, however in addition to Dronc and Drice localizing to mitochondria (Dorstyn et al., 2002), other cell death regulators including Reaper (Olson et al., 2003), Hid (Haining et al., 1999), Grim (Clavería et al., 2002) and the Bcl-2 family members Buffy and Debcl (Doumanis et al., 2007; Quinn et al., 2003) also localize to the mitochondria. It was recently shown that both Buffy and Debcl regulate mitochondrial morphology in degenerating mid-stage egg chambers (Tanner et al., 2011), and overexpression of Reaper resulted in mitochondrial fragmentation and inhibition of mitochondrial fusion (Thomenius et al., 2011), thus implicating the cell death machinery in mitochondrial dynamics. The dynamic nature and morphology of mitochondria vary among cell types and may be a function of different energetic demands of the cell or different motility requirements (Youle and van der Bliek, 2012). For example, fibroblasts contain

mitochondria that are usually long filaments, whereas hepatocytes contain mitochondria that are ovoids or spheres (Youle and van der Bliek, 2012). In addition to the upregulation of nuclear encoded mitochondrial chaperones and proteases that ensure the efficient removal of mis-folded or aggregated proteins (Baker et al., 2011; Nargund et al., 2012; Youle and van der Bliek, 2012), mitochondria also undergo fusion and fission as a quality control mechanism (Sheng and Cai, 2012). Mitochondrial fission is mediated by the Dynamin-like GTPase Drp-1, whereas mitochondrial fusion is mediated by Opa-1 and the mitofusins, *Drosophila* Marf and Fuzzy Onions, or mammalian Mfn1 and Mfn2. Mitochondria undergo fusion to exchange proteins and lipids to reduce damage (Chen and Chan, 2009; Legros et al., 2002), and fusion is thought to also maximize oxidative phosphorylation in response to cellular stress (Gomes et al., 2011). Moreover, mitochondria with mutant DNA may fuse with other mitochondria to allow wild-type DNA to compensate for mutant DNA (Yoneda et al., 1994; Youle and van der Bliek, 2012). Mitochondrial dynamics are thought to play a role in cell death, as inhibition of Drp-1 blocks caspase activation and cell death (Goyal et al., 2000), and both Drp-1 and Opa1-like were shown to be required for cell death in mid-stage egg chambers during oogenesis (Tanner et al., 2011). Mitochondria that are damaged beyond repair are sequestered and degraded by autophagy, also known as mitophagy. Mitochondrial fission is required for mitophagy as its been shown that overexpression of dominant negative Drp1 or Fis1 RNAi inhibited mitophagy (Twig et al., 2008).

We previously showed that Dcp-1 is required for autophagic flux in degenerating mid-stage egg chambers during oogenesis (Chapter 3; Figure 3 E-G). One potential mechanism of Dcp-1 mediated autophagy is through cleavage of its downstream substrates; however, it is possible that Dcp-1 acts in a non-apoptotic, non-proteolytic

manner to regulate autophagy by affecting the stability or activity of its interacting partners. Previous immunoprecipitation and mass spectrometry assays revealed that candidate interacting partners/substrates of Dcp-1 are mitochondrial proteins, including ATPsynthase-β and Blw, the catalytic components of the mitochondrial ATP synthase, as well as SesB, the mitochondrial adenine nucleotide translocase (Table 1.2). Therefore, we investigated the possible mitochondrial-related role of Dcp-1 in the regulation of autophagy. In this chapter, we show that Dcp-1 localizes to the mitochondria where it functions to regulate the mitochondrial network morphology and ATP levels. Dcp-1 controls the levels of the adenine nucleotide translocase SesB, a mitochondrial protein that functions to regulate ATP levels, in a non-catalytic manner. *SesB* mutant analysis reveals a new role for SesB as a negative regulator of autophagic flux in *Drosophila* mid-stage egg chambers. Depletion of ATP or *SesB* loss-of-function flies can rescue the autophagy defect in *Dcp-1* loss-of-function flies, demonstrating that SesB acts downstream of Dcp-1 in the regulation of autophagy. This data uncovers a novel mechanism of caspase mediated regulation of autophagy *in vivo*.

4.2. Dcp-1 localizes to mitochondria and its levels increase following starvation

To elucidate the mechanism by which Dcp-1 mediates autophagic flux, we first determined the subcellular location of Dcp-1 in *Drosophila l(2)mbn* cells by immunostaining with an antibody to Dcp-1 (Tenev et al., 2005). We observed co-localization between Dcp-1 and the mitochondrial markers ATPsynthase-α (Figure 4.1 A) and MitoTracker Red (MTR; Figure 4.1 B), but did not observe co-localization between Dcp-1 and markers for the endoplasmic reticulum or cis-golgi (Figure 4.1 C-D). To

Figure 4.1 Dcp-1 partially localizes to the mitochondria.

Drosophila l(2)mbn cells were labelled with antibodies to Dcp-1 (green) and **(A)** ATPsynthase-α (red), **(B)** MitoTracker Red (MTR, red), **(C)** endoplasmic reticulum (red), and **(D)** cis-golgi (red). Merged images show co-localization between Dcp-1 and the mitochondria. Scale bars, 5μm.

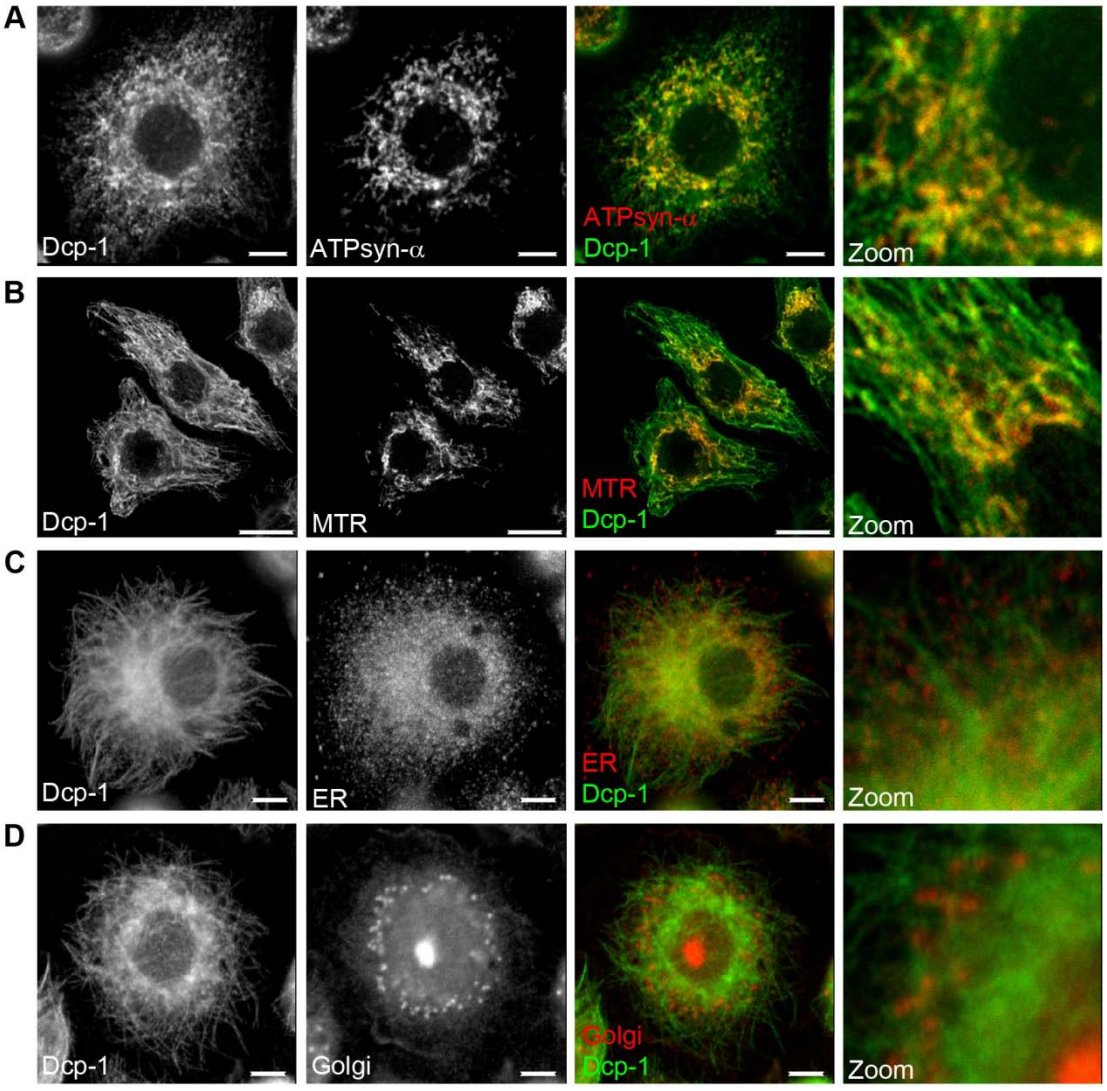
A
Dcp-1
ATPsyn-α
ATPsyn-α
Dcp-1
Zoom
B
Dcp-1
MTR
MTR
Dcp-1
Zoom
C
Dcp-1
ER
ER
Dcp-1
Zoom
D
Dcp-1
Golgi
Golgi
Dcp-1
Zoom

further confirm that Dcp-1 is located at the mitochondria, a subcellular fractionation assay was performed on *l(2)mbn* cells subjected to nutrient rich medium or 6 hours of starvation (Figure 4.2 A). Purity of the fractions was determined using tubulin as a cytosolic (C) marker and ATPsynthase-α, VDAC and Cytochrome-c as mitochondrial (M) markers. The pro-form (zymogen) of Dcp-1 was located only in the mitochondrial fraction in nutrient rich and starvation conditions, whereas the processed p10 subunit of Dcp-1 was found in both the membrane and cytosolic fractions (Figure 4.2 A). To determine if Dcp-1 is located inside the mitochondria or is associated with the surface of the outer mitochondrial membrane, a proteinase K protection assay was performed with or without hypotonic disruption of the mitochondria (Figure 4.2 B). Mitochondrial proteins within the mitochondria are resistant to proteinase K treatment, whereas proteins located on the surface of the outer mitochondrial membrane, but not embedded within the lipid bi-layer of mitochondria, are sensitive to proteinase K. VDAC, an embedded outer mitochondrial membrane protein, and ATPsynthase-α, an inner mitochondrial membrane protein, remained intact upon proteinase K treatment, as expected, but were digested by proteinase K following hypotonic disruption of the mitochondria. Similarly, Dcp-1 was digested only following hypotonic disruption of the mitochondria, indicating that Dcp-1 is internalized within the mitochondria (Figure 4.2 B). These observations suggest that the pro-form of Dcp-1 translocates into the mitochondria where a fraction of it is processed into its active form, and this active form either remains in the mitochondria or translocates back into the cytosol.

The fractionation results revealed that Dcp-1 is in its processed form even under nutrient rich conditions (Figure 4.2 C), and starvation up to 6 hours resulted in increased

Figure 4.2 Dcp-1 localizes within mitochondria and its levels are increased following starvation.

(A) Western blot from *l(2)mbn* cells subjected to nutrient rich or starvation conditions for 6 hours. Cells were separated into cytosolic "C" and mitochondrial "M" fractions. An antibody to the C-terminus of Dcp-1 was used to assess the localization of Dcp-1 (Laundrie et al., 2003) **(B)** Intact and lysed mitochondria isolated from *l(2)mbn* cells were treated with proteinase K. The effects of proteinase K treatment were assessed by antibodies to VDAC, ATPsyn-α and Dcp-1. **(C)** A representative western blot from *l(2)mbn* cells subjected to nutrient rich or starvation conditions as indicated. Dcp-1 was detected by immunoblot and actin served as a loading control. **(D)** Cell viability was assessed by trypan blue exclusion assay on *l(2)mbn* cells subjected to nutrient rich or starvation conditions. Graph represents ± SD of 4 independent experiments (n=4). Statistical significance was determined using one-way ANOVA with a Dunnett post test (***$p<0.001$). **(E)** Control and *Dcp-1* RNAi treated cells were subjected to nutrient rich or starvation conditions and stained with the mitochondrial mass marker 10-nonyl acridine orange (NAO). Mean fluorescence was measured by flow cytometry. Graph represents ± SEM of 3 independent experiments (n=3). **(F)** Control and *Dcp-1* RNAi treated cells were subjected to nutrient rich or starvation conditions and stained with the mitochondrial membrane potential marker JC-1. Mean fluorescence was measured by flow cytometry. Graph represents ± SEM of 3 independent experiments (n=3).

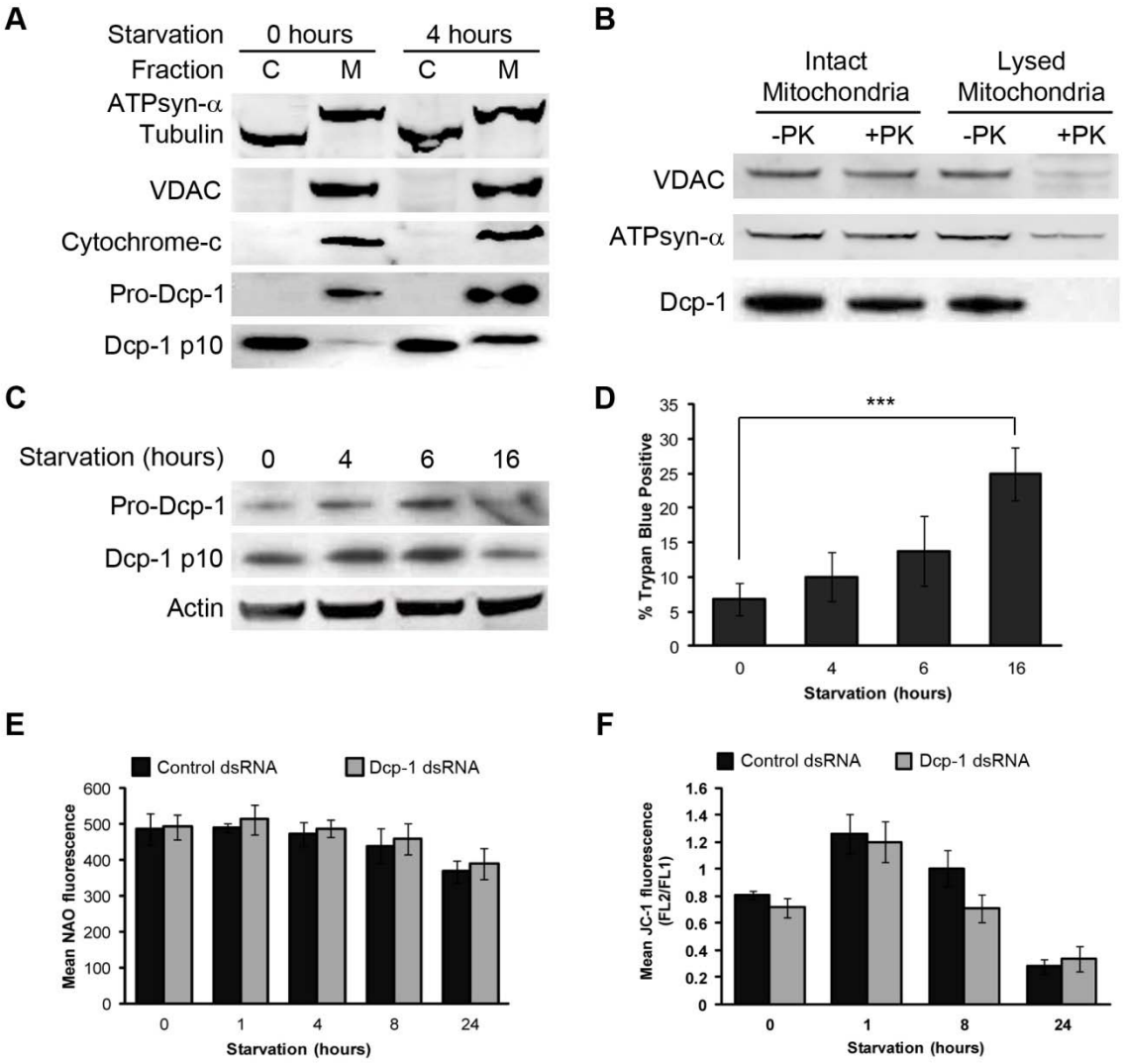
A
Starvation
0 hours
4 hours
Fraction
C
M
C
M
ATPsyn-α
Tubulin
VDAC
Cytochrome-c
Pro-Dcp-1
Dcp-1 p10
B
Intact Mitochondria
Lysed Mitochondria
-PK
+PK
-PK
+PK
VDAC
ATPsyn-α
Dcp-1
C
Starvation (hours)
0
4
6
16
Pro-Dcp-1
Dcp-1 p10
Actin
D
***
% Trypan Blue Positive
35
30
25
20
15
10
5
0
0
4
6
16
Starvation (hours)
E
Control dsRNA
Dcp-1 dsRNA
Mean NAO fluorescence
600
500
400
300
200
100
0
0
1
4
8
24
Starvation (hours)
F
Control dsRNA
Dcp-1 dsRNA
Mean JC-1 fluorescence (FL2/FL1)
1.6
1.4
1.2
1
0.8
0.6
0.4
0.2
0
0
1
8
24
Starvation (hours)

levels of full length and processed Dcp-1 (Figure 4.2 C) with no significant change in cell viability (Figure 4.2 D). Following 16 hours of starvation however, a decrease in cell viability was observed (Figure 4.2 D), and counterintuitively, Dcp-1 levels were also decreased (Figure 4.2 C) suggesting that high levels of Dcp-1 are not required for cell death following prolonged starvation. To determine if the observed increase in Dcp-1 was due to an increase in overall mitochondrial biomass or block in mitophagy (the selective removal of mitochondria by autophagy) following starvation, we measured mitochondrial mass using 10-nonyl acridine orange (NAO) (Figure 4.2 E). NAO binds to mitochondrial cardiolipin independently of mitochondrial membrane potential and is therefore a useful indicator of mitochondrial mass. Dcp-1 RNAi did not significantly alter mitochondrial mass following 0-24 hours of starvation compared to the control RNAi treated cells (Figure 4.2 E). Additionally, we tested whether Dcp-1 altered mitochondrial membrane potential as a mechanism to induce autophagy or apoptosis (Figure 4.2 F). Mitochondrial membrane potential was measured using JC-1 (5,5',6,6'-tetrachloro-1,1',3,3'- tetraethylbenzimidazolylcarbocyanine iodide). In healthy cells, JC-1 accumulates in the mitochondrial matrix when the mitochondrial membrane potential is intact. When a critical concentration is exceeded, JC-1 forms J-aggregates and fluoresces bright red. When the mitochondrial membrane potential collapses, JC-1 no longer accumulates in the mitochondrial matrix and remains in the cytoplasm where it fluoresces green. Treatment of *l(2)mbn* cells with Dcp-1 RNAi did not alter mitochondrial membrane potential compared to control treated cells under any of the starvation conditions tested (Figure 4.2 F). Together, these data demonstrate that Dcp-1 localizes to the mitochondria but does not regulate mitophagy or mitochondrial membrane potential. Instead, Dcp-1 is present in its pro-form and processed form even under nutrient rich conditions and its levels are increased following starvation with no

associated changes in cell viability. This indicates that Dcp-1 is required for the initial stages of autophagy and does not induce cell death at the time points tested.

4.3. Loss of Dcp-1 alters the morphology of the mitochondrial network

To examine a potential role of Dcp-1 at the mitochondria, we analyzed whether loss of Dcp-1 alters mitochondrial morphology. Mitochondria were labelled with the mitochondrial antibody ATPsynthase-α and were scored as having a fragmented, a normal (containing both short and elongated mitochondria), or an elongated morphology(Figure 4.3 A). The majority of control RNAi treated cells in nutrient rich media contained mitochondria with a normal morphology, and following starvation, there was an increase in the percentage of cells with elongated mitochondria (Figure 4.3 B). Treatment with Dcp-1 RNAi resulted in a significant increase in cells that contained elongated mitochondria in both nutrient rich and starvation media (Figure 4.3 B) suggesting that Dcp-1 may play a role in maintaining the mitochondrial network under well fed and starvation conditions.

To determine if Dcp-1 alters mitochondrial morphology *in vivo*, we expressed a mitochondrial-targeted-GFP (mito-GFP) specifically in the germline using the nosGAL4 driver. All well fed control flies contained short, tubular mitochondria that were dispersed throughout the entire nurse cell (Figure 4.3 C) and were scored as “healthy (“H”, Figure 4.3 D). Starvation induces a series of mitochondrial events in degenerating mid-stage egg chambers including mitochondrial re-modeling and clustering, uptake by the follicle cells and finally degradation within the follicle cells (Tanner et al., 2011). Well fed *Dcp-1^{Prev1}* flies expressing mito-GFP in the germline contained mitochondria with an altered

Figure 4.3 Loss of Dcp-1 promotes mitochondrial elongation.

(A) *Drosophila l(2)mbn* cells were labelled with the mitochondrial marker ATPsynthase-α. Mitochondrial morphology was scored as fragmented, normal or elongated. Scale bars, 5μm. **(B)** Cells were treated with control or *Dcp-1* dsRNA and subjected to nutrient rich media or 1 hour of starvation. Quantifications represent the percentage of cells with elongated mitochondria divided by the total number of cells examined. At least 100 cells were examined in 3 independent experiments (n=3). Error bars represent the average ± SD. Statistical significance was determined using one-way ANOVA with a Bonferroni post test (*p<0.05, **p<0.01). **(C)** Mitochondrial targeted GFP (mito-GFP) was expressed in the germline using the nosGAL4 driver. Staining shows mito-GFP (green), Armadillo (red) and DNA (blue). **(D)** Mitochondria were scored as healthy "H", clustered "C", or elongated and overly connected "E". All of mitochondria from well fed *UASpmitoGFP/+;;nosGAL4/+* flies were scored as healthy. n=15 egg chambers examined**. (E)** mito-GFP was expressed in well fed *Dcp-1*^{Prev1} flies using the nosGAL4 driver. **(F)** 54% of egg chambers from *UASpmitoGFP/+;Dcp-1*^{Prev1}*/Dcp-1*^{Prev1}*;nosGAL4/+* flies contained mitochondria that were elongated and overly connected, 39% contained mitochondria that were scored as healthy, and 7% contained fragmented mitochondria. n=28 egg chambers examined. Scale bars, 25μm, zoomed images, 10μm.

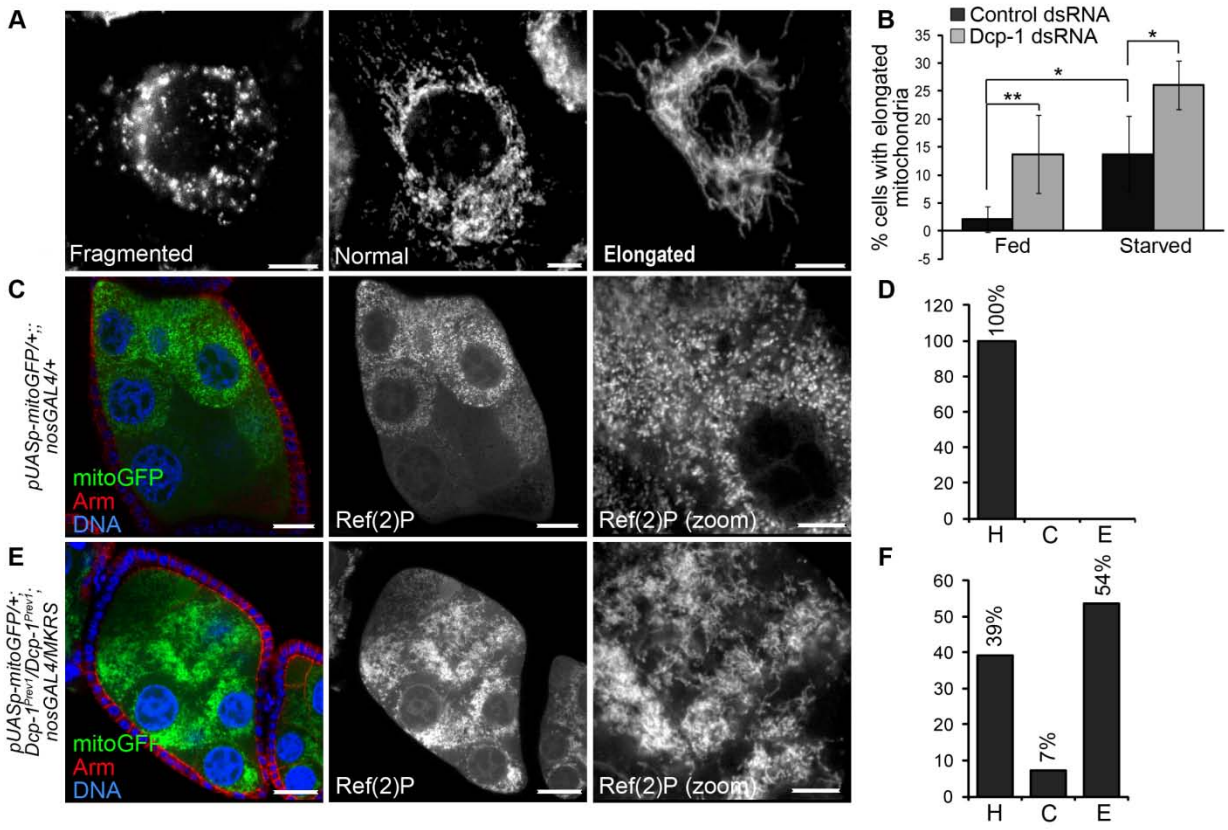
A
Fragmented
Normal
Elongated
B
Control dsRNA
Dcp-1 dsRNA
% cells with elongated mitochondria
Fed
Starved
C
pUASp-mitoGFP/+;;
nosGAL4/+
mitoGFP
Arm
DNA
Ref(2)P
Ref(2)P (zoom)
D
100%
H
C
E
E
pUASp-mitoGFP/+;
Dcp-1Prev1/Dcp-1Prev1;
nosGAL4/MKRS
mitoGFP
Arm
DNA
Ref(2)P
Ref(2)P (zoom)
F
39%
7%
54%
H
C
E

morphology even in the absence of starvation. 54% of mid-stage egg chambers from *Dcp-1*^{Prev1} flies contained mitochondria that were elongated and overly connected ("E", Figure 4.3 E-F), whereas only 39% of mid-stage egg chambers contained mitochondria that were healthy ("H", Figure 4.3 F). These data demonstrate that Dcp-1 plays a role in the regulation of mitochondrial network morphology even in the absence of a starvation signal, underscoring a novel non-apoptotic role of an effector caspase in regulating mitochondrial dynamics under both well fed and starvation conditions.

4.4. High ATP levels in *Dcp-1*^{Prev1} flies suppress autophagic flux

Loss of Dcp-1 promotes elongation of the mitochondrial network, and mitochondrial elongation has been shown to sustain ATP levels following starvation to promote cell survival (Gomes et al., 2011). In addition, the cellular energy sensor AMP activated protein kinase (AMPK) is activated when the ratio of ATP/AMP falls, for example during periods of starvation (Gleason et al., 2007; Salt et al., 1998), thus stimulating energy producing pathways such as autophagy (Hubbard et al., 2010; Kim et al., 2011). Therefore, we wanted to determine if Dcp-1 also alters ATP levels as a mechanism to induce autophagic flux. Cells treated with Dcp-1 RNAi showed a significant increase in ATP levels within 4 hours of starvation (Figure 4.4 A) suggesting that at least under starvation *in vitro*, the elongated mitochondrial phenotype in Dcp-1 RNAi treated cells is associated with increased ATP levels. *In vivo* analyses of ovaries from wild-type and *Dcp-1*^{Prev1} flies subjected to well fed or starvation conditions showed ATP levels to be significantly increased in *Dcp-1*^{Prev1} flies under both conditions tested (Figure 4.4 B). We reasoned that the increased ATP levels in *Dcp-1*^{Prev1} flies may inhibit autophagic flux following starvation. Reduction of ATP with oligomycin A, an inhibitor of

Figure 4.4 Dcp-1 alters ATP levels that in turn regulate autophagy.

(A) Total cellular ATP levels were measured in *l(2)mbn* cells treated with control or *Dcp-1* dsRNA. Data represents ± SEM of 3 independent experiments (n=3). Statistical significance was determined using a two-tailed Students t-test (*p=0.02). **(B)** Total cellular ATP levels were measured in ovaries extracted from well fed or nutrient deprived w^{1118} and $Dcp\text{-}1^{Prev1}$ flies. Data represents ± SEM of 5 independent experiments (n=5). Statistical significance was determined using a two-tailed students t-test (*p=0.014, ***p<0.001). **(C)** Well fed or nutrient deprived w^{1118} and $Dcp\text{-}1^{Prev1}$ flies were treated with DMSO or 25ug/mL oligomycin A and Ref(2)P levels were assessed by immunoblot analysis. Actin served as a loading control. Densitometry was performed to quantitate protein levels relative to actin. Graph represents ± SD from three independent experiments (n=3). Statistical significance was determined using a two-tailed Student's t-test (*p=0.02). **(D)** Control *UASp-GFPmCherry-DrAtg8a/+;nosGAL4/+* flies and **(E)** $Dcp\text{-}1^{Prev1}/Dcp\text{-}1^{Prev1}$; *UASp-GFPmCherry-DrAtg8a/nosGAL4* flies were subjected to starvation conditions supplemented with DMSO or 25ug/mL oligomycin A. Arrows denote degenerating mid-stage egg chambers. Scale bars, 25μm.

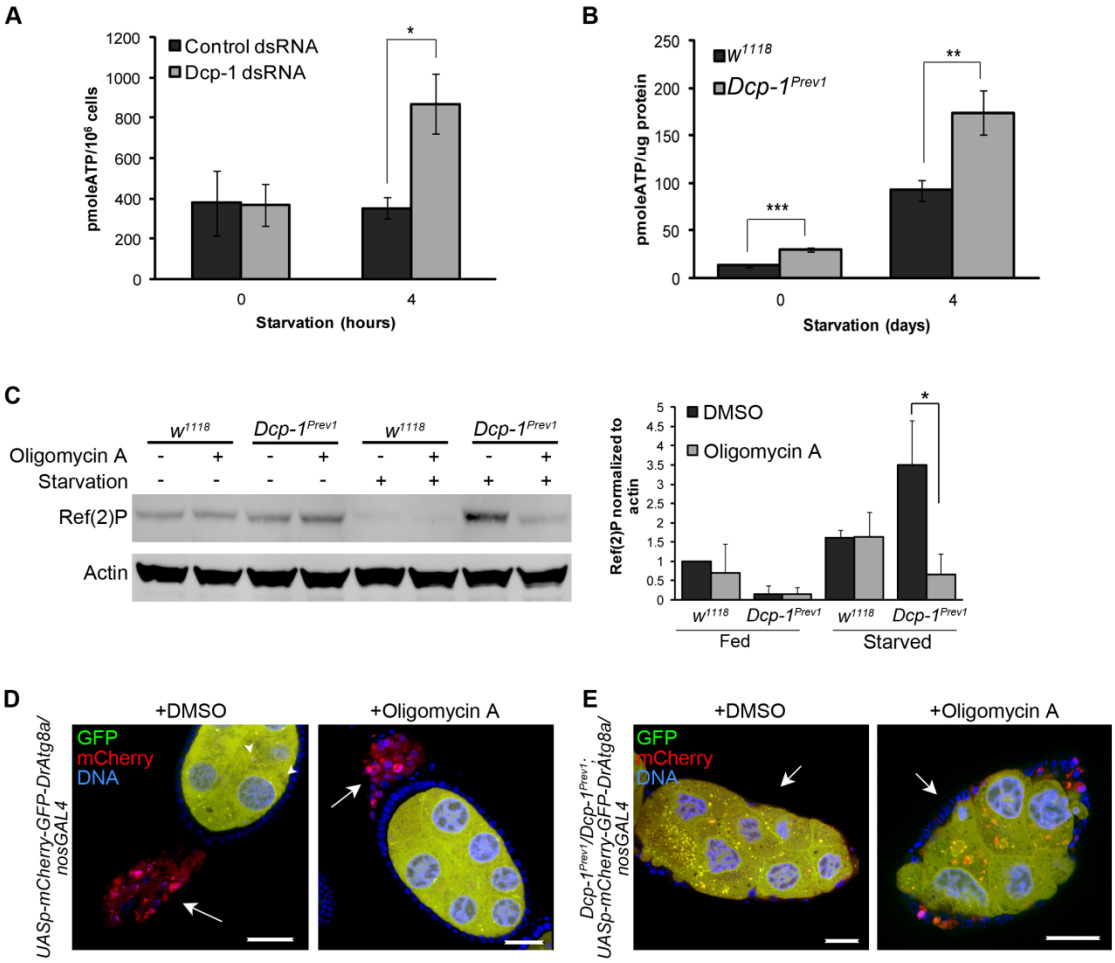
A
Control dsRNA
Dcp-1 dsRNA
pmoleATP/10^6 cells
Starvation (hours)
B
w1118
Dcp-1Prev1
pmoleATP/ug protein
Starvation (days)
C
Oligomycin A
Starvation
Ref(2)P
Actin
DMSO
Oligomycin A
Ref(2)P normalized to actin
Fed
Starved
D
+DMSO
+Oligomycin A
GFP
mCherry
DNA
UASp-mCherry-GFP-DrAtg8a/ nosGAL4
E
Dcp-1Prev1/Dcp-1Prev1; UASp-mCherry-GFP-DrAtg8a/ nosGAL4

the mitochondrial ATP synthase, induces autophagy in the IPLB-LdFB insect cell line (Tettamanti et al., 2006), and so we tested whether oligomycin A would induce autophagy in *Drosophila* ovaries. Although oligomycin A did not alter Ref(2)P levels under well fed conditions, ovaries from starved *Dcp-1*^{Prev1} flies treated with oligomycin A showed a significant reduction in Ref(2)P protein compared to those treated with DMSO (Figure 4.4 C). In addition, starved oligomycin A treated *Dcp-1*^{Prev1} flies expressing GFP-mCherry-DrAtg8a in the germline showed an increase in autolysosomes compared to those treated with DMSO (red puncta; Figure 4.4 E), whereas we observed no additional increase in autolysosomes in starved control flies treated with oligomycin A (Figure 4.4 D). This suggests that high ATP levels are sufficient to block autophagic flux in *Dcp-1*^{Prev1} flies following starvation. Collectively, these data demonstrate that Dcp-1 controls autophagic flux by a mechanism involving the regulation of the mitochondrial network and maintenance of ATP levels.

4.1. Dcp-1 negatively regulates the levels of the adenine nucleotide translocase SesB

We next determined the molecular mechanism by which Dcp-1 could regulate ATP levels to induce autophagy. *Drosophila SesB* (stress-sensitiveB) encodes an adenine nucleotide translocase that localizes to the inner mitochondrial membrane and function's to exchange ATP for ADP across the mitochondrial inner membrane (Terhzaz et al., 2010). RNAi of *SesB* in malpighian (renal) tubules significantly decreased ATP levels and altered mitochondrial morphology from a threadlike appearance to a short and globular morphology (Terhzaz et al., 2010). Moreover, SesB was identified in the IP-MS study as a candidate substrate or interactor of Dcp-1 (Hou et al., unpublished, Table 1.2). We began by examining whether Dcp-1 altered the levels of SesB following

Figure 4.5 Dcp-1 regulates levels of SesB but SesB is not a direct target of Dcp-1's proteolytic activity.

(A) Well fed or nutrient deprived *l(2)mbn* cells were treated with *control* or *Dcp-1* RNAi. SesB and ATPsyn-α levels were assessed by immunoblot analysis. Actin served as a loading control. Results are representative of three independent experiments (n=3). **(B)** A representative western blot of ovaries dissected from well fed or nutrient deprived w^{1118} or $Dcp\text{-}1^{Prev1}$ flies. SesB and ATPsyn-α were detected by immunoblot. Actin served as a loading control. Densitometry was performed to quantitate SesB protein levels relative to actin. Graph represents ± SD from three independent experiments (n=3). Statistical significance was determined using a two-tailed Student's t-test (*$p<0.05$). **(C)** Purified catalytically active Dcp-1^{FL}, but not catalytically inactive Dcp-$1^{C<A}$, cleaved *in vitro* translated Drice into its p20 and p10 subunits, whereas cleavage of *in vitro* translated SesB was not detected. **(D)** Flag-SesB or a vector only control were expressed in *Drosophila l(2)mbn* cells and were immunoprecipitated with FLAG-agarose. Immunoblots show association of FLAG-SesB with endogenous pro-Dcp-1**.**

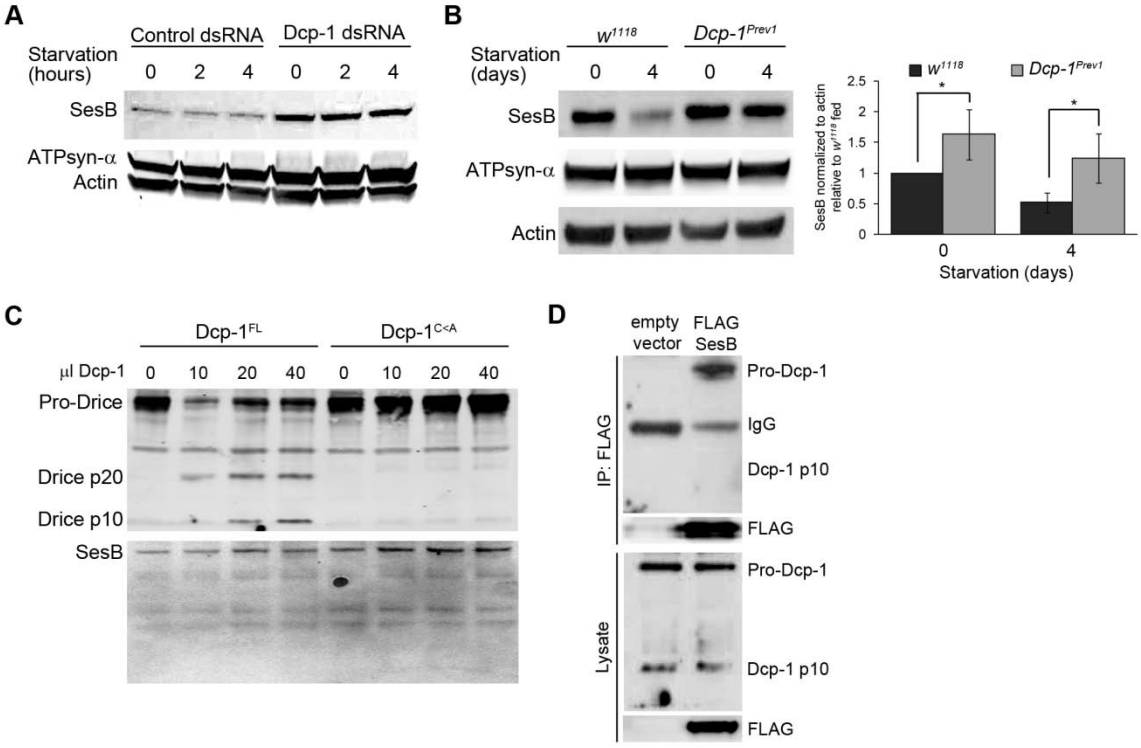
A
Control dsRNA
Dcp-1 dsRNA
Starvation (hours)
0 2 4 0 2 4
SesB
ATPsyn-α
Actin
B
w1118
Dcp-1Prev1
Starvation (days)
0 4 0 4
SesB
ATPsyn-α
Actin
w1118
Dcp-1Prev1
SesB normalized to actin relative to w1118 fed
2.5
2
1.5
1
0.5
0
*
*
0
4
Starvation (days)
C
Dcp-1FL
Dcp-1C<A
µl Dcp-1
0 10 20 40 0 10 20 40
Pro-Drice
Drice p20
Drice p10
SesB
D
empty vector
FLAG SesB
IP: FLAG
Pro-Dcp-1
IgG
Dcp-1 p10
FLAG
Lysate
Pro-Dcp-1
Dcp-1 p10
FLAG

starvation. Treatment of *l(2)mbn* cells with Dcp-1 RNAi resulted in increased levels of SesB whereas ATPsyn-α levels remained unaltered (Figure 4.5 A). To test this *in vivo*, we examined ovaries from well fed and nutrient deprived wild-type and *Dcp-1*^{Prev1} flies. We observed decreased SesB levels following starvation in wild-type flies (Figure 4.5 B), whereas ovaries from well fed or nutrient deprived *Dcp-1*^{Prev1} flies contained increased SesB levels indicating that Dcp-1 may be required to negatively regulate the levels of SesB, and thus ATP. To determine if SesB is a direct target of Dcp-1's proteolytic activity, *in vitro* cleavage assays were performed. Catalytically active Dcp-1 (Dcp-1^{FL}) and inactive Dcp-1 (Dcp-1$^{C<A}$) were expressed in *l(2)mbn* cells and purified by Ni^{2+}-NTA columns. Only Dcp-1^{FL} was able to cleave *in vitro* translated Drice (Figure 4.5 C), another *Drosophila* effector caspase and known substrate of Dcp-1 (Song et al., 2000b). Treatment of *in vitro* translated SesB with Dcp-1^{FL} or Dcp-1$^{C<A}$ failed to induce cleavage of SesB (Figure 4.5 C) suggesting that Dcp-1 does not directly cleave SesB but rather affects its stability. We next tested if Dcp-1 interacts with SesB as a mechanism to regulate its stability. Previous immunoprecipitation and mass spectrometry assays revealed that V5-Dcp-1$^{C<A}$ interacts with SesB (Hou YC, Moradian A, Morin GB, Gorski SM, unpublished and Table 1.2). To confirm this, we expressed FLAG-SesB in *Drosophila l(2)mbn* cells and found that FLAG-SesB immunoprecipitated endogenous pro-Dcp-1 (Figure 4.5 D). Notably, no processed Dcp-1 was detected (Figure 4.5 D) further suggesting that the interaction between Dcp-1 and SesB occurs in a non-proteolytic manner. All together, these data show that pro-Dcp-1 interacts with SesB and affects its stability in a non-proteolytic manner.

4.2. SesB is a negative regulator of autophagic flux and interacts genetically with Dcp-1

The reduction in SesB levels following starvation suggests that SesB may negatively regulate autophagy. Moreover, RNAi of SesB *in vitro* increased LTG levels (Figure 3.5 A-B) following starvation indicating that SesB acts as a potential negative regulator of autophagy *in vitro*. We next examined the role of SesB in autophagy *in vivo*. Null alleles of SesB are lethal, whereas hypomorphic alleles of SesB are viable and display a range of phenotypes including reduced flight ability and hypoactivity (Zhang et al., 1999). Therefore, we examined ovaries from SesB hypomorphic flies ($SesB^{Org}$) that were shown to have reduced adenine nucleotide translocase activity (Rikhy et al., 2003). Whereas well fed wild-type flies rarely contain degenerating mid-stage egg chambers (Table 4.1), well fed $SesB^{Org}$ flies contained an increase in degenerating mid-stage egg chambers (Table 4.1) that stained positively for LTR (Figure 4.6 C) compared to egg chambers from well fed control flies (Figure 4.6 A-C). LTR staining in degenerating mid-stage egg chambers from well fed $SesB^{Org}$ flies was similar to LTR staining from degenerating mid-stage egg chambers from nutrient deprived wild-type flies (Figure 4.6 B-C). In addition, degenerating mid-stage egg chambers from $SesB^{Org}$ flies had reduced Ref(2)P levels, and this reduction was confirmed by western blot analysis indicating that SesB negatively regulates autophagic flux during *Drosophila* oogenesis (Figure 4.6 D). To confirm that SesB is a negative regulator of autophagic flux, GFP-mCherry-DrAtg8a was overexpressed in the germline of $SesB^{Org}$ flies using the nosGAL4 driver. Whereas well fed control flies contain diffuse mCherry-GFP-Atg8a staining throughout the germline (Figure 4.6 E, left), $SesB^{Org}$ flies contained an increase in autolysosomes in both non-degenerating (Figure 4.6 E, middle) and degenerating (Figure 4.6 E, right) mid-stage egg chambers, confirming that there is increased autophagic flux in $SesB^{Org}$ flies.

Figure 4.6 SesB hypomorphic flies have increased autophagic flux in midstage egg chambers.

(A) Well fed w^{1118} flies contain low levels of LTR staining in mid-stage egg chambers. **(B)** Nutrient deprived w^{1118} flies contain increased degenerating mid-stage egg chambers that stain positively for LTR. **(C)** Well fed $SesB^{Org}$ flies contain increased degenerating mid-stage egg chambers that stain positively for LTR. **(D)** Ovaries from well fed $SesB^{Org}$ flies showed reduced Ref(2)P staining in degenerating mid-stage egg chamber (arrow), and Ref(2)P levels of ovaries from well fed w^{1118} and $SesB^{Org}$ were analyzed by western blot. Actin served as a loading control. Results are representative of three independent experiments. **(E)** Well fed control flies expressing GFP-mCherry-DrAtg8a in the germline (genotype: *GFP-mCherry-Atg8a/+;nosGAL4/+*) contain diffuse GFP-mCherry-Atg8a staining, whereas overexpression of GFP-mCherry-Atg8a in the germline of $SesB^{Org}$ flies (genotype: $SesB^{Org}/SesB^{Org}$*;GFP-mCherry-Atg8a/+;nosGAL4/+*) showed an increase in autophagosomes and autolysosomes in non-degenerating (middle) and degenerating (right) mid-stage egg chambers. **(F)** Degenerating mid-stage egg chambers from $SesB^{Org}$ flies are TUNEL positive. Scale bars, 25μm.

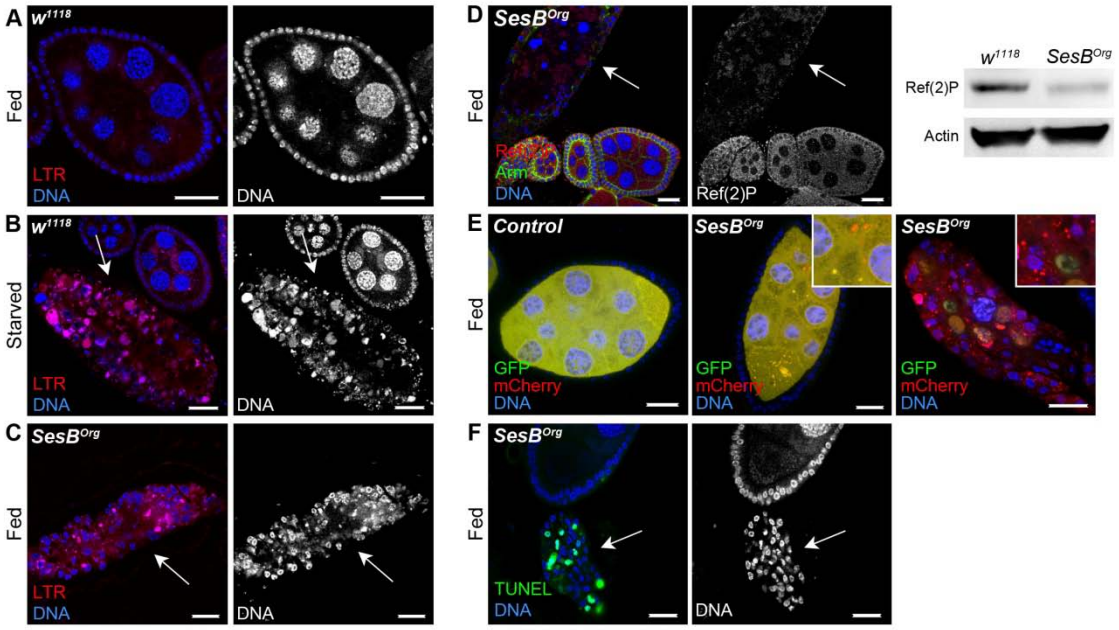
A
w1118
Fed
LTR
DNA
DNA
B
w1118
Starved
LTR
DNA
DNA
C
SesBOrg
Fed
LTR
DNA
DNA
D
SesBOrg
Fed
Ref(2)P
Arm
DNA
Ref(2)P
w1118
SesBOrg
Ref(2)P
Actin
E
Control
Fed
GFP
mCherry
DNA
SesBOrg
GFP
mCherry
DNA
SesBOrg
GFP
mCherry
DNA
F
SesBOrg
Fed
TUNEL
DNA
DNA

Table 4.1 Quantification of TUNEL positive germaria and mid-stage egg chambers.

	# of ovarioles examined	% degenerating mid-stage egg chambers	% TUNEL (+) mid-stage egg chambers	% TUNEL (+) germaria
w^{1118}	71	4	3	6
$SesB^{Org}$	156	30	24	33

Degenerating mid-stage egg chambers from *SesB*^{Org} flies also stained positively for TUNEL (Figure 4.6 F) suggesting that SesB is normally required to suppress autophagic flux and cell death during *Drosophila* oogenesis. All together, this data suggests that the Dcp-1 dependent downregulation of SesB is required for the induction of autophagic flux.

To confirm the epistatic relationship between Dcp-1 and SesB, we examined *SesB*^{Org}*;Dcp-1*^{Prev1} double mutant flies. Due to the increased levels of SesB in *Dcp-1*^{Prev1}flies, we reasoned that by reducing SesB in the *Dcp-1*^{Prev1} background a *SesB*^{Org} phenotype will result. Degenerating mid-stage egg chambers from nutrient deprived control *SesB*^{Org}*/FM7a;Dcp-1*^{Prev1}*/Dcp-1*^{Prev1} flies contained persisting nurse cell nuclei and an accumulation of Ref(2)P (Figure 4.7 A). In contrast, ovarioles from well fed *SesB*^{Org}*/SesB*^{Org}*;Dcp-1*^{Prev1}*/Dcp-1*^{Prev1} flies arrested during mid-oogenesis and these mid-stage egg chambers contained condensed and fragmented nurse cell nuclei and reduced Ref(2)P levels (Figure 4.7 B), similar to the *SesB*^{Org} phenotype. These data place Dcp-1 upstream of SesB, suggesting that Dcp-1 may promote autophagy by inhibiting SesB activity. All together, these data demonstrate that SesB is a novel negative regulator of autophagic flux during *Drosophila* mid-oogenesis and its levels are reduced following starvation in a Dcp-1 dependent manner.

4.1. Discussion

The *Drosophila* genome encodes 7 caspases, and to date only the initiator caspase Dronc and the effector caspase Drice have been shown to localize to the mitochondria (Dorstyn et al., 2002). In mammalian cells, caspases have been detected at the mitochondria during apoptosis (Chandra and Tang, 2003; Krajewski et al., 1999; Susin et al., 1999), however the role of caspases at the mitochondria, especially under

Figure 4.7 Dcp-1 and SesB interact genetically.

(A) Ovaries from nutrient deprived control *SesB^{Org}/FM7a;Dcp-1^{Prev1}/Dcp-1^{Prev1}* flies contained degenerating mid-stage egg chambers with persisting nurse cell nuclei and an increase in Ref(2)P. n=117 ovarioles examined. **(B)** Degenerating mid-stage egg chambers from well fed *SesB^{Org};Dcp-1^{Prev1}* flies contained condensed and fragmented nurse cell nuclei and no accumulation of Ref(2)P. n=156 ovarioles examined. Scale bars, 25μm, zoomed images, 10μm.

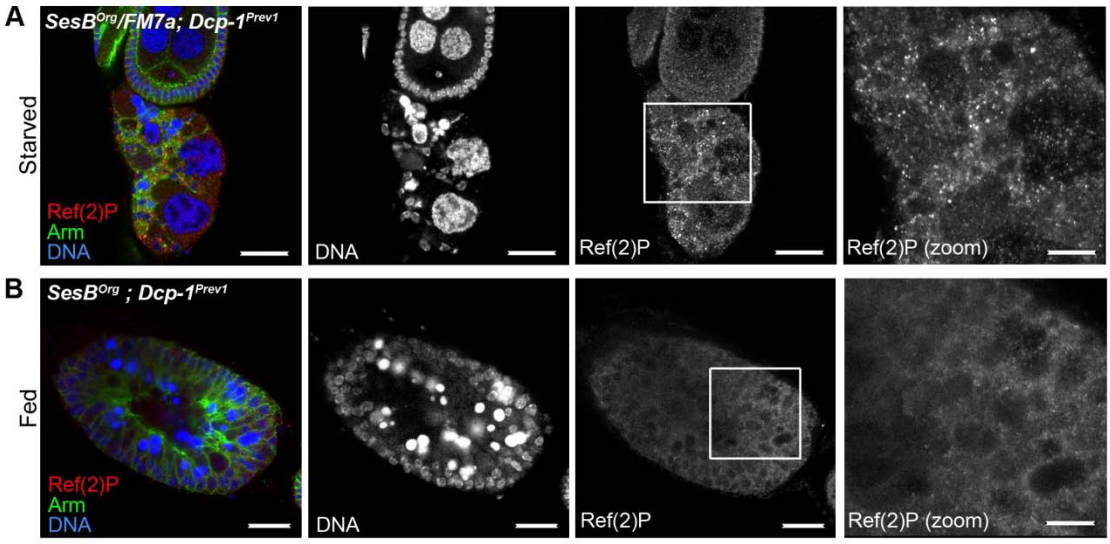
A
SesB^Org/FM7a; Dcp-1^Prev1
Starved
Ref(2)P
Arm
DNA
DNA
Ref(2)P
Ref(2)P (zoom)
B
SesB^Org ; Dcp-1^Prev1
Fed
Ref(2)P
Arm
DNA
DNA
Ref(2)P
Ref(2)P (zoom)

non-apoptotic conditions, is poorly understood. Our results demonstrate that Dcp-1 localizes to the mitochondria and functions to maintain the mitochondrial network morphology. Under nutrient rich conditions, non-degenerating mid-stage egg chambers from *Dcp-1*^{Prev1} flies contained mitochondria that appeared elongated and overly connected, uncovering a novel role of an effector caspase in the maintenance of the mitochondrial network. Consistent with these findings, overexpression of the caspase inhibitor p35 in the amnioserosa suppressed the transition of mitochondria from a tubular to a fragmented state during delamination (Muliyil et al., 2011) further suggesting that inhibition of caspases hinders normal mitochondrial dynamics.

Dcp-1 acts to finely tune the apoptotic process and cell death only occurs when caspase activity reaches a certain apoptotic threshold (Florentin and Arama, 2012). Our data shows that Dcp-1 is present in both its pro-form and processed form under well fed conditions with no associated increase in cell death suggesting that Dcp-1 primarily functions non-apoptotically under these baseline conditions. Furthermore, the expression of Dcp-1 inversely correlates with cell viability following starvation further indicating that Dcp-1 is not the main executor of starvation-induced cell death. Effector caspases may be restricted in time or space to regulate caspase activity (Florentin and Arama, 2012; Kaplan et al., 2010). As Dcp-1 has auto-catalytic activity (Song et al., 2000b), Dcp-1 may be sequestered in mitochondria to prevent its full activation and thereby limiting the induction of apoptosis. S-nitrosylation of caspases, including mitochondrial localized mammalian pro-Caspase 3 and 9, in their catalytic active site leads to the inhibition of their activity (Jiang et al., 2009; Mannick et al., 2001). S-nitrosylation of mitochondrial Dcp-1 could be an additional regulatory mechanism to limit Dcp-1's pro-apoptotic and pro-autophagic activity.

Dcp-1 is a positive regulator of autophagic flux in degenerating mid-stage egg chambers, and one mechanism of Dcp-1 induced autophagic flux is mediated through SesB. SesB, an adenine nucleotide translocase (ANT), catalyzes the electrogenic exchange of ATP^{4-} and ADP^{3-} across the inner mitochondrial membrane. ATP is exported from the mitochondrial matrix to the intermembrane space, whereas ADP is imported from the intermembrane space to the matrix (Pfaff and Klingenberg, 1968; Pfaff et al., 1969). SesB was originally characterized as a stress-sensitive mutant that is reversibly paralytic following mechanical stress (Homyk and Sheppard, 1977; Zhang et al., 1999) and SesB stress-sensitivity has been attributed to defects in energy metabolism (Zhang et al., 1999). Females carrying homozygous germline clones of SesB are sterile and show defects in late oogenesis, including late nurse cell degeneration (Perrimon et al., 1984). Mutations of SesB lead to reduced cytoplasmic ATP and it was shown that SesB is required to provide a continuous supply of mitochondrial ATP for Dynamin-mediated synaptic transmission (Rikhy et al., 2003). There are two adenine nucleotide translocases in *Drosophila*, SesB (ANT1), and ANT2, that are transcribed from a common promoter and show high sequence identity (78% amino acid identity) (Zhang et al., 1999). SesB is ubiquitously expressed but is virtually absent from testis, whereas ANT2 is testis-specific (Terhzaz et al., 2010). In humans, there are four mitochondrial adenine nucleotide translocase (ANT) isoforms, each with a tissue specific distribution and different roles in apoptosis. ANT1 and ANT3 were proposed to be pro-apoptotic, whereas ANT2 and ANT4 were shown to be anti-apoptotic (Brenner et al., 2010). Mitochondrial ANTs have been shown to interact with Bcl-2 family members including Bcl-2 and Bax. Bcl-2 was shown to enhance the exchange of ADP/ATP, whereas during apoptosis, Bax was shown to displace Bcl-2 from ANT and block the exchange of ADP/ATP (Belzacq et al., 2003). In addition, ANTs have also

been proposed as components of the mitochondrial permeability transition pore complex (PTPC) (Zoratti and Szabò, 1995), a large conductance channel that increases the permeability of mitochondria ultimately leading to cell death (Brenner et al., 2010). However, more recent studies using ANT1/ANT2 knockout mice revealed little involvement of ANTs in PTPC (Kokoszka et al., 2004).

Although many studies have examined the role of ANTs in apoptosis, the role of mammalian or *Drosophila* ANT proteins in autophagy has yet to be characterized. The data presented in this chapter indicate that SesB is required to suppress autophagic flux during mid-oogenesis even under nutrient rich conditions, and the levels of SesB are reduced following starvation in a Dcp-1 dependent manner to promote autophagic flux. This is the first report suggesting an adenine nucleotide translocase functions as a negative regulator of autophagic flux. Examination of the interaction between SesB and Dcp-1 revealed that only the pro-form of Dcp-1, and not the processed active form of Dcp-1, interacts with SesB. Moreover, loss of SesB in $Dcp\text{-}1^{Prev1}$ flies rescued the apoptotic and autophagic defect during mid-oogenesis indicating that Dcp-1 and SesB interact genetically. Like $SesB^{Org}$ degenerating mid-stage egg chambers, I suspect that the degenerating mid-stage egg chambers from $SesB^{Org};Dcp\text{-}1^{Prev1}$ double mutant flies are TUNEL positive, but that will need to be verified. These findings indicate that pro-Dcp-1 may affect SesB stability and uncover a novel role for a pro-caspase. However, we cannot rule out the possibility that very low levels of active Dcp-1 interact with SesB and are undetectable by western blot.

Effector caspases are the main executioners of apoptotic cell death; however it is becoming increasingly evident that caspases have non-apoptotic functions in differentiation, proliferation, cytokine production and cell survival (Galluzzi et al., 2012;

Kuranaga and Miura, 2007). For example, Caspase 3 was shown to regulate tumour cell repopulation *in vitro* and *in vivo* (Huang et al., 2011), and it was also shown to be required for skeletal muscle (Fernando et al., 2002) and macrophage differentiation (Sordet et al., 2002). Our results show that Dcp-1 also has a non-apoptotic role during oogenesis, where it is required to maintain mitochondrial physiology under basal conditions. Loss of Dcp-1 alters this physiology, leading to increased SesB and ATP levels that in part prevent the induction of autophagic flux following starvation. This data supports the notion that caspases play a much more diverse role than previously known, and that the underlying mechanisms should be better understood to appreciate the full impact of apoptosis pathway modulation for treatment in human pathologies.

5. Conclusions

5.1. Summary and significance of the study

In this thesis, I set out to (1) investigate the role of Dcp-1 in starvation-induced autophagic flux during mid-oogenesis, (2) characterize and validate the role of candidate Dcp-1 interacting partners and substrates in autophagy, and (3) examine the mechanism by which Dcp-1 promotes autophagic flux. I anticipated that the results from this study would provide insights into how an effector of cell death positively regulates a cell survival pathway.

Drosophila mid-oogenesis has been a powerful model system to study the crosstalk between autophagy and apoptosis. Using GFP-mCherry-Atg8a and Ref(2)P distribution analyses to examine autophagic flux during *Drosophila* oogenesis, I confirmed that autophagic flux occurs in both non-degenerating and degenerating mid-stage egg chambers in response to starvation. Importantly, the catalytic activity of Dcp-1 is required for autophagic flux specifically in degenerating mid-stage egg chambers. Moreover, well fed flies overexpressing Dcp-1 in the germline resulted in increased autophagic flux in both non-degenerating and degenerating mid-stage egg chambers indicating that Dcp-1 is both necessary and sufficient for autophagic flux during *Drosophila* mid-oogenesis.

Data obtained from a previous Dcp-1 immunoprecipitation and mass spectrometry (IP-MS) assay was utilized to not only screen and identify novel regulators

of starvation-induced autophagy, but also to better understand the mechanism of Dcp-1 mediated autophagy. Thirteen novel negative regulators of starvation-induced autophagy, as measured by LTG, were identified including the heat shock proteins Hsc70-4, Hsp70Aa, Hsp60 and Hsp83, translation initiation factor eIF-4a, the chromatin remodeler Mi-2, the ribosomal constituent Sta, the AAA^+ ATPase Ter94, the chloride intracellular protein Clic, the proteasome activator REG, and the mitochondrial proteins ATPsynthase-β, Blw and SesB. Since interpretations of LTG-based assays are limited, further *in vitro* assays confirming the role of these candidates in autophagic flux, including *in vitro* GFP-mCherry-Atg8a analyses, are required. However, this RNAi screen has provided a foundation for future studies to examine the role of these candidates in starvation-induced autophagy *in vivo.* Moreover, these data, incorporated with further biochemical and genetic analyses including *in vitro* cleavage assays and epistasis analyses, will contribute to a better understanding of the mechanism of Dcp-1 mediated autophagy.

The identification of four mitochondrial proteins, ATPsyn-β, Blw, SesB and Hsp60, in the IP-MS study led us to uncover a novel mitochondrial-associated role for Dcp-1 in the regulation of autophagy. Dcp-1 localizes to the mitochondria where it functions to regulate the mitochondrial network morphology, ATP levels, and the levels of the adenine nucleotide translocase (ANT) SesB. Moreover, I found that SesB negatively regulates autophagic flux in mid-stage egg chambers, identifying a novel role of a mitochondrial ANT in the regulation of autophagy. I found that the pro-form of Dcp-1, but not the processed active form of Dcp-1, interacts with SesB in a non-proteolytic manner. Perhaps the pro-form of Dcp-1 has low activity that promotes autophagy rather than apoptosis. Emerging evidence now indicates that pro-caspases are not latent

enzymes. It was shown that following phosphorylation, mammalian pro-caspase-8 promotes cell migration in a non-apoptotic, non-catalytic manner (Barbero et al., 2008; Senft et al., 2007), and *Drosophila* Dronc was shown to bind Numb independently of its caspase activation recruitment domain (CARD) to attenuate ectopic neuroblast formation in a non-apoptotic, non-catalytic manner. It is possible, however, that SesB is a proteolytic target of Drice, and that low levels of processed Dcp-1 interact with SesB but is undetectable by western blot. However, using genetics and epistasis analyses, I have determined that Dcp-1 acts upstream of SesB in the regulation of autophagy. I propose a model where in response to starvation, Dcp-1 negatively regulates the levels of SesB in a non-proteolytic manner resulting in the reduction of ATP levels and an increase in autophagic flux (Figure 5.1). Further studies are required to determine the exact mechanism of Dcp-1-mediated regulation of SesB levels.

Further *in vivo* analyses of two candidate Dcp-1 interacting proteins, Clic and Hsp83, identified as negative regulators of LTG following starvation, revealed that they negatively regulate starvation-induced autophagic flux during mid-oogenesis. Nutrient deprived *Clic*-RNAi flies and *Hsp83* trans-heterozygous flies contained an increase in the percentage of degenerating mid-stage egg chambers that stained positively for LTR and had reduced Ref(2)P, indicating that Clic and Hsp83 function to restrain autophagy in mid-stage egg chambers following starvation. Analyzing the role of Clic and Hsp83 in additional tissues would be beneficial to better distinguish the role of these proteins in autophagy and apoptosis. The interaction between Dcp-1 and Hsp83 was further characterized, and although we confirmed that pro-Dcp-1 interacts with Hsp83, it does so in a non-proteolytic manner. Given that pro-Dcp-1 localizes to the mitochondria, I suspect that the Dcp-1-Hsp83 interaction occurs within the mitochondria. In a large scale

co-affinity purification assay coupled with mass spectrometry, Hsp83 was found to interact with the mitochondrial proteins Blw, Porin and ATPsyn-β (Guruharsha et al., 2011), further indicating that a fraction of Hsp83 may reside in the mitochondria. In mammalian cells, mitochondrial Hsp60 and Hsp10 were shown to interact with mitochondrial pro-Caspase 3 where they function to accelerate pro-Caspase 3 activation following the induction of apoptosis (Samali et al., 1999). Activation of Caspase 3 led to its dissociation from Hsp60 and Hsp10, followed by its translocation from the mitochondria into the cytosol (Samali et al., 1999). Perhaps Dcp-1's association with *Drosophila* Hsp60, identified in the IP-MS study, accelerates the activation of Dcp-1 in response to stress. Conversely, Dcp-1's interaction with Hsp83 may prevent its ability to become fully activated in the mitochondria. Thus, these Hsps may act as upstream regulators of Dcp-1. Although Hsp83 trans-heterozygous flies did not have an autophagy phenotype under fed conditions, I hypothesize that starvation signals leads to enhanced activation of Dcp-1 in the absence of Hsp83, resulting in an increase in the percentage of degenerating mid-stage egg chambers undergoing autophagic flux (Figure 5.1). This is consistent with our data, as overexpression of Dcp-1 resulted in increased degenerating mid-stage egg chambers undergoing autophagic flux (Figure 3.1 H-I and Hou et al., 2008).

In summary, we have confirmed that Dcp-1 is a positive regulator of starvation induced autophagic flux in degenerating mid-stage egg chambers. We have successfully identified three novel regulators of starvation-induced autophagy *in vivo* during *Drosophila* oogenesis, SesB, Clic and Hsp83. Moreover, we have uncovered a novel mitochondrial-associated role of Dcp-1 in the regulation of autophagy. Significantly, we have found that Dcp-1 localizes to the mitochondria where it regulates

mitochondrial dynamics and the levels of ATP and SesB in a non-apoptotic, non-proteolytic manner. I propose a model where in response to starvation, Dcp-1 negatively regulates the levels of SesB in a non-proteolytic manner, resulting in a reduction in ATP levels and an increase in autophagic flux (Figure 5.1).

5.2. Strengths and limitations of the study, and future research avenues

To identify candidate substrates and interaction partners of Dcp-1 by IP-MS, a catalytically inactive construct of Dcp-1 (Dcp-$1^{C<A}$) was utilized to stabilize the caspase-substrate complex (Hou et al., unpublished). A similar study was previously described using modified mammalian Caspase 3 as bait in a yeast two-hybrid screen (Kamada et al., 1998). This method has been beneficial as it has identified novel regulators of starvation induced autophagy. Moreover, our list of candidate interacting partners and substrates of Dcp-1 identified both potential substrates of Dcp-1 (ie. Stubarista), and interacting partners of Dcp-1 (ie. Hsp83 and SesB). Subsequently, we have also been able to demonstrate that SesB functions as a downstream mediator of Dcp-1-induced autophagy.

To better understand the role of Dcp-1 candidate substrates and interactors in starvation-induced autophagy, an RNAi based approach was used in combination with LTG analyses. However, due to incomplete knockdown, functional redundancy, or a long half life of the protein, our RNAi screen may not have identified all regulators of starvation-induced autophagy. To confirm that the observed increase in LTG levels following RNAi treatment and starvation is representative of an increase in autophagic

Figure 5.1 A model of Dcp-1 mediated autophagy

A schematic representation depicting the role of Dcp-1 in autophagy. We propose that in response to starvation, Dcp-1 negatively regulates the levels of SesB. This in turn reduces the levels of ATP and increases autophagic flux. Of note, Dcp-1 regulates the levels of SesB even under well fed conditions. Potential upstream regulators of Dcp-1, including Hsp60 and Hsp83, need to be validated and are shown by hatched lines.

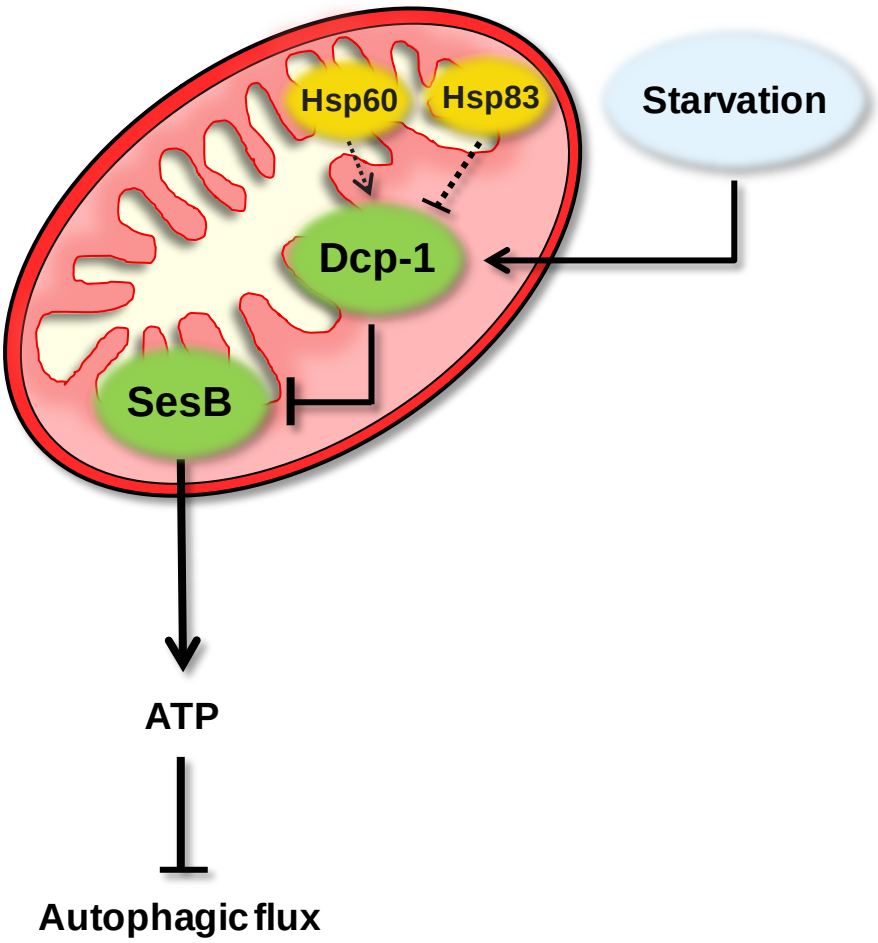
Hsp60
Hsp83
Starvation
Dcp-1
SesB
ATP
Autophagic flux

flux, *in vitro* autophagic flux assays, including analysis of GFP-RFP-Atg8a, must be performed. It is possible that substrates of Dcp-1 require an activating cleavage event, rather than a degradative cleavage event, to carry out their roles in autophagy. Our RNAi approach did not take possible activating cleavage events into consideration due to the fact that RNAi depletes target mRNA and protein, thereby removing the possibility of Dcp-1 mediated cleavage and activation of its substrate. Therefore, it is possible that those candidates identified in the LTG assay as *not significant* may actually regulate starvation induced autophagy. To identify substrates of Dcp-1 that require an activating cleavage event, two-dimensional PAGE (2D-PAGE), coupling orthogonal isoelectric focusing and SDS-PAGE, can be used (Bredemeyer et al., 2004; Demon et al., 2009). The resulting 2D-PAGE protein spots of Dcp-1 overexpressing cells can be compared to that of control cells, and any new spots that may represent stable cleavage fragments can be identified by mass spectrometry (Demon et al., 2009).

An *in vivo* RNAi approach was also used to confirm the role of candidate Dcp-1 interactors and substrates in starvation-induced autophagy. However, this approach was unsuccessful at determining the role of Ter94, Hsc70-4, Sta, eIF-4a and Hsp83 in starvation-induced autophagy in the germline as RNAi-mediated knockdown of these candidates led to rudimentary, agametic ovaries. Ananlysis of hypomorphic alleles, analysis of RNAi lines using GAL80, or RNAi-mediated knockdown of these candidates in alternate tissues may help to unveil the role of these candidates in starvation-induced autophagy *in vivo.* In addition, validation of the remaining candidates in starvation-induced autophagy *in vivo* during *Drosophila* oogenesis or in other tissues will be valuable. Finally, epistasis analyses of candidate genes with Dcp-1 will provide additional information on the mechanism of Dcp-1 mediated autophagy in *Drosophila*.

One interesting area of research will be to identify the functional homolog of Dcp-1. Although Dcp-1 has similar substrate specificity as mammalian Caspase 3 (Song et al., 1997), and both pro-Caspase 3 and active Caspase 3 have been shown previously to reside in the mitochondria (Chandra and Tang, 2003; Mancini et al., 1998), there have been no studies to date, to the best of my knowledge, examining a non-apoptotic role of pro-Caspase 3 and active Caspase 3 in the mitochondria. Like Dcp-1, mammalian Caspase 6 also has auto-catalytic activity (Klaiman et al., 2008; Song et al., 2000; Wang et al., 2010), indicating that Caspase 6 may also function like Dcp-1. Activation of Caspase 6 does not necessarily lead to cell death in HEK293T cells (Klaiman et al., 2008), and Caspase 6 was shown to immunoprecipitate Hsp60, a mitochondrial protein, in an *in vitro* system (Xanthoudakis et al., 1999) suggesting Caspase 6 may be an interesting candidate to test as well.

Dcp-1^{Prev1} flies are homozygous viable, and Dcp-1 was shown to regulate mitochondrial network morphology, SesB and ATP levels independently of a starvation signal suggesting that Dcp-1 may function similarly in other tissues. Like *Dcp-1*^{Prev1} flies, Caspase $6^{-/-}$ mice are homozygous viable and fertile. Until recently, it was thought that Caspase $6^{-/-}$ mice develop normally, however it was shown that Caspase $6^{-/-}$ mice undergo age-dependent behavioral and neuroanatomical changes (Uribe et al., 2012). Neuronal degeneration of axons, dendrites and synaptic connections occurs during normal development and in response to injury, stress and disease (Keller et al., 2011). Recently, Dcp-1 was shown to be necessary and sufficient for motor neuron degeneration. Overexpression of Dcp-1 in motor neurons induced axonal and nerve terminal degeneration (Keller et al., 2011). Similarily, Caspase 6 has been shown to be required for developmental and stress-induced axonal degeneration (Nikolaev et al.,

2009). Sympathetic neurons from Caspase $6^{-/-}$ mice show protection against axonal degeneration following nerve growth factor (NGF) deprivation, and Caspase $6^{-/-}$ medium spiny neurons (MSNs) were protected from NMDA receptor-mediated excitotoxicity (induces cell death due to excess activation) (Uribe et al., 2012). Importantly, Caspase $6^{-/-}$ MSNs had a significant increase in ATP levels and a significant reduction in TUNEL staining post NMDA-treatment (Uribe et al., 2012). Perhaps overexpression of Dcp-1 in motor neurons leads to reduced ATP levels in a SesB dependent manner, resulting in motor neuron degeneration. The role of Dcp-1 in motor neurons and its implications in neuronal degeneration may be an exciting new avenue of research.

5.3. Potential applications of research

Recent data has implicated both mammalian Hsp90, the homologue of *Drosophila* Hsp83, and mammalian Clic4 in autophagy regulation; however, the role of ANT family members in autophagy has yet to be tested. Hsp90 is an abundantly expressed molecular chaperone that promotes the correct folding and functionality of its client proteins including several protein kinases, steroid hormone receptors, anti-apoptotic proteins, and oncogenes (Wu et al., 2012). As inhibition of Hsp90 leads to degradation of its client proteins, targeting Hsp90 with small molecular inhibitors has emerged as an anti-cancer therapy (Whitesell and Lindquist, 2005). However, to date only few studies have shown a clear clinical response (Hong et al., 2012) indicating that perhaps a better understanding of Hsp90 at the molecular level is required. Specifically in cancer cells, and unlike most normal counterparts, Hsp90 is localized to the mitochondria where it functions to antagonize mitochondrial permeability transition, characterized by permeability of the inner mitochondrial membrane resulting in release

of apoptotic factors and cell death (Kang et al., 2007), and maintain organelle proteostasis (Siegelin et al., 2011). Inhibition of Hsp90 specifically in the mitochondria leads to phosphorylation and activation of AMPK, inhibition of mTOR complex 1, and induction of autophagy (Chae et al., 2012b). As induction of autophagy following chemotherapy treatment is thought to promote tumour cell survival (Amaravadi et al., 2007; Degenhardt et al., 2006), perhaps Hsp90 inhibitors in combination with autophagy inhibition will better sensitize cancer cells to cell death. Consistent with this, treatment with the Hsp90 inhibitor 17DMAG in combination with the autophagy inhibitor 3-methyladenine (3-MA) facilitated Cytochrome c release and caspase activation in multiple myeloma cells (Palacios et al., 2010). Our data is consistent with the notion that inhibition of Hsp90 enhances autophagy. Further studies are required to understand the function of Hsp90 at the molecular level to develop better therapeutic strategies.

The Clic family of proteins were first identified based on their chloride intracellular channel activity; however it is now clear that they function in signal transduction, differentiation and stress induced apoptosis (Fernández-Salas et al., 2002; Shukla et al., 2009; Suh et al., 2007). Specifically, Clic4, the most extensively studied Clic family member, has been shown to translocate from the cytoplasm to the nucleus in response to various cellular stresses, including etoposide and cyclohexamide, to accelerate apoptosis in keratinocytes (Suh et al., 2004). Clic4 expression is reduced in renal, ovarian, and breast cancers and Clic4 protein is excluded from the nucleus in cancer cells (Suh et al., 2004). Moreover, the extent to which Clic4 expression level is reduced is associated with progression of squamous tumours from benign to malignant, implicating Clic4 as a suppressor of squamous tumour development (Suh et al., 2012). Not only does starvation induce autophagy in glioma cancer cells, but it also increases

the expression of Clic4 and induces its nuclear translocation, suggesting that Clic4 acts as a responder of starvation-induced autophagy (Zhong et al., 2012). However, RNAi-mediated knockdown of Clic4 enhanced autophagy and apoptosis following starvation in a glioma cancer cell line (Zhong et al., 2012) suggesting that the levels of Clic4, in addition to its localization, may play a critical role in the outcome of the cell. We showed that RNAi mediated knockdown of Clic in the germline in *Drosophila* enhanced the percentage of degenerating mid-stage egg chambers undergoing autophagic flux following starvation. Based on this data and the data from Zhong *et al*., perhaps low levels of Clic4 in the tumour promote cytoprotective autophagy, leading to increased survival and progression of tumour cells. However, further studies are required to determine the autophagy status in cancers with low levels of Clic4.

There are 4 human ANT isoforms (ANT1-4), each with a specific expression depending on the tissue, cell type and proliferation status (Chevrollier et al., 2011). ANT1 and ANT3 are pro-apoptotic (Jang et al., 2008; Zamora et al., 2004), whereas ANT2 and ANT4 are anti-apoptotic (Gallerne et al., 2010; Jang et al., 2010). Specifically in cancer patients, ANT2 and ANT3 have been shown to be up-regulated, whereas ANT1 has been shown to be down-regulated (Sharaf el dein et al., 2011). ANT2 shRNA in breast cancer cells restored their susceptibility to TRAIL-induced apoptosis by activating the JNK signaling pathway (Jang et al., 2010), and ANT2 shRNA significantly reduced tumour growth in an *in vivo* breast cancer xenograft model (Jang et al., 2008) further suggesting that ANT2 acts anti-apoptotically in cancer. Our results show that loss of SesB function enhances autophagic flux and cell death in degenerating mid-stage egg chambers, indicating that SesB may function more like ANT2 or ANT4 than ANT1 or ANT3. Currently, there are several small molecule inhibitors of ANT function under

current investigation as anti-cancer therapies (reviewed in Sharaf el dein et al., 2011). As the induction of autophagy has been shown to play a cytoprotective role in established tumours (Amaravadi et al., 2007; Degenhardt et al., 2006), it may be worthwhile investigating the role of ANT proteins in autophagy. Perhaps combining ANT and autophagy inhibition may be a more effective treatment than ANT inhibition alone.

In summary, our study has identified candidate genes involved in starvation induced autophagy *in vitro*, and has confirmed the role of three candidates, Clic, Hsp83 and SesB, in starvation induced autophagy during mid-oogenesis. Moreover, I have uncovered a novel connection between an effector caspase and the regulation of mitochondrial dynamics and function. This study has provided insights into the connection between autophagy and apoptosis in *Drosophila*, and provides a foundation for future studies examining the role of Dcp-1 and its interactors in starvation-induced autophagy.

References

Ahlberg, J., and Glaumann, H. (1985). Uptake--microautophagy--and degradation of exogenous proteins by isolated rat liver lysosomes. Effects of pH, ATP, and inhibitors of proteolysis. Exp. Mol. Pathol. *42*, 78–88.

Amaravadi, R.K., Yu, D., Lum, J.J., Bui, T., Christophorou, M.A., Evan, G.I., Thomas-Tikhonenko, A., and Thompson, C.B. (2007). Autophagy inhibition enhances therapy-induced apoptosis in a Myc-induced model of lymphoma. Journal of Clinical Investigation *117*, 326–336.

Amaravadi, R.K., Lippincott-Schwartz, J., Yin, X.-M., Weiss, W.A., Takebe, N., Timmer, W., DiPaola, R.S., Lotze, M.T., and White, E. (2011). Principles and Current Strategies for Targeting Autophagy for Cancer Treatment. Clin Cancer Res *17*, 654–666.

Andersen, R.O., Turnbull, D.W., Johnson, E.A., and Doe, C.Q. (2012). Sgt1 acts via an LKB1/AMPK pathway to establish cortical polarity in larval neuroblasts. Dev. Biol. *363*, 258–265.

Arama, E., Agapite, J., and Steller, H. (2003). Caspase Activity and a Specific Cytochrome C Are Required for Sperm Differentiation in Drosophila. Developmental Cell *4*, 687–697.

Arstila, A.U., and Trump, B.F. (1968). Studies on cellular autophagocytosis. The formation of autophagic vacuoles in the liver after glucagon administration. Am. J. Pathol. *53*, 687–733.

Ashford, T.P., and Porter, K.R. (1962). Cytoplasmic Components in Hepatic Cell Lysosomes. J Cell Biol *12*, 198–202.

Axe, E.L., Walker, S.A., Manifava, M., Chandra, P., Roderick, H.L., Habermann, A., Griffiths, G., and Ktistakis, N.T. (2008). Autophagosome formation from membrane compartments enriched in phosphatidylinositol 3-phosphate and dynamically connected to the endoplasmic reticulum. J Cell Biol *182*, 685–701.

Baba, M., Takeshige, K., Baba, N., and Ohsumi, Y. (1994). Ultrastructural analysis of the autophagic process in yeast: detection of autophagosomes and their characterization. J. Cell Biol. *124*, 903–913.

Baehrecke, E.H. (2002). How death shapes life during development. Nat. Rev. Mol. Cell Biol. *3*, 779–787.

Bahadorani, S., Hur, J.H., Lo, T., Vu, K., and Walker, D.W. (2010). Perturbation of mitochondrial complex V alters the response to dietary restriction in Drosophila. Aging Cell *9*, 100–103.

Baker, M.J., Tatsuta, T., and Langer, T. (2011). Quality Control of Mitochondrial Proteostasis. Cold Spring Harb Perspect Biol *3*.

Barbero, S., Barilà, D., Mielgo, A., Stagni, V., Clair, K., and Stupack, D. (2008). Identification of a critical tyrosine residue in caspase 8 that promotes cell migration. J. Biol. Chem. *283*, 13031–13034.

Barth, J.M.I., Szabad, J., Hafen, E., and Kohler, K. (2011). Autophagy in Drosophila ovaries is induced by starvation and is required for oogenesis. Cell Death Differ *18*, 915–924.

Bartlett, B.J., Isakson, P., Lewerenz, J., Sanchez, H., Kotzebue, R.W., Cumming, R.C., Harris, G.L., Nezis, I.P., Schubert, D.R., Simonsen, A., et al. (2011). p62, Ref(2)P and ubiquitinated proteins are conserved markers of neuronal aging, aggregate formation and progressive autophagic defects. Autophagy *7*, 572–583.

Bartolomeo, S.D., Corazzari, M., Nazio, F., Oliverio, S., Lisi, G., Antonioli, M., Pagliarini, V., Matteoni, S., Fuoco, C., Giunta, L., et al. (2010). The dynamic interaction of AMBRA1 with the dynein motor complex regulates mammalian autophagy. J Cell Biol *191*, 155–168.

Baum, J.S., Arama, E., Steller, H., and McCall, K. (2007). The Drosophila caspases Strica and Dronc function redundantly in programmed cell death during oogenesis. Cell Death Differ. *14*, 1508–1517.

Belzacq, A.-S., Vieira, H.L.A., Verrier, F., Vandecasteele, G., Cohen, I., Prévost, M.-C., Larquet, E., Pariselli, F., Petit, P.X., Kahn, A., et al. (2003). Bcl-2 and Bax modulate adenine nucleotide translocase activity. Cancer Res. *63*, 541–546.

Berry, D.L., and Baehrecke, E.H. (2007). Growth Arrest and Autophagy Are Required for Salivary Gland Cell Degradation in Drosophila. Cell *131*, 1137–1148.

Boatright, K.M., and Salvesen, G.S. (2003). Mechanisms of caspase activation. Curr. Opin. Cell Biol. *15*, 725–731.

Boatright, K.M., Renatus, M., Scott, F.L., Sperandio, S., Shin, H., Pedersen, I.M., Ricci, J.E., Edris, W.A., Sutherlin, D.P., Green, D.R., et al. (2003). A unified model for apical caspase activation. Mol. Cell *11*, 529–541.

Bodmer, J.-L., Holler, N., Reynard, S., Vinciguerra, P., Schneider, P., Juo, P., Blenis, J., and Tschopp, J. (2000). TRAIL receptor-2 signals apoptosis through FADD and caspase-8. Nature Cell Biology *2*, 241–243.

Bredemeyer, A.J., Lewis, R.M., Malone, J.P., Davis, A.E., Gross, J., Townsend, R.R., and Ley, T.J. (2004). A proteomic approach for the discovery of protease substrates. PNAS *101*, 11785–11790.

Brenner, C., Subramaniam, K., Pertuiset, C., and Pervaiz, S. (2010). Adenine nucleotide translocase family: four isoforms for apoptosis modulation in cancer. Oncogene *30*, 883–895.

Bursch, W., Ellinger, A., Kienzl, H., Török, L., Pandey, S., Sikorska, M., Walker, R., and Hermann, R.S. (1996). Active Cell Death Induced by the Anti-Estrogens Tamoxifen and ICI 164 384 in Human Mammary Carcinoma Cells (MCF-7) in Culture: The Role of Autophagy. Carcinogenesis *17*, 1595–1607.

Calamita, P., and Fanto, M. (2011). Slimming down fat makes neuropathic hippo: the Fat/Hippo tumor suppressor pathway protects adult neurons through regulation of autophagy. Autophagy *7*, 907–909.

Carmona-Gutierrez, D., Eisenberg, T., Büttner, S., Meisinger, C., Kroemer, G., and Madeo, F. (2010). Apoptosis in yeast: triggers, pathways, subroutines. Cell Death Differ *17*, 763–773.

Chae, Y.C., Caino, M.C., Lisanti, S., Ghosh, J.C., Dohi, T., Danial, N.N., Villanueva, J., Ferrero, S., Vaira, V., Santambrogio, L., et al. (2012a). Control of tumor bioenergetics and survival stress signaling by mitochondrial HSP90s. Cancer Cell *22*, 331–344.

Chae, Y.C., Caino, M.C., Lisanti, S., Ghosh, J.C., Dohi, T., Danial, N.N., Villanueva, J., Ferrero, S., Vaira, V., Santambrogio, L., et al. (2012b). Control of tumor bioenergetics and survival stress signaling by mitochondrial HSP90s. Cancer Cell *22*, 331–344.

Chai, J., Wu, Q., Shiozaki, E., Srinivasula, S.M., Alnemri, E.S., and Shi, Y. (2001). Crystal structure of a procaspase-7 zymogen: mechanisms of activation and substrate binding. Cell *107*, 399–407.

Chai, J., Yan, N., Huh, J.R., Wu, J.-W., Li, W., Hay, B.A., and Shi, Y. (2003). Molecular mechanism of Reaper-Grim-Hid-mediated suppression of DIAP1-dependent Dronc ubiquitination. Nature Structural & Molecular Biology *10*, 892–898.

Chandra, D., and Tang, D.G. (2003). Mitochondrially localized active caspase-9 and caspase-3 result mostly from translocation from the cytosol and partly from caspase-mediated activation in the organelle. Lack of evidence for Apaf-1-mediated procaspase-9 activation in the mitochondria. J. Biol. Chem. *278*, 17408–17420.

Chang, Y.-Y., and Neufeld, T.P. (2010). Autophagy takes flight in Drosophila. FEBS Lett. *584*, 1342–1349.

Chen, H., and Chan, D.C. (2009). Mitochondrial dynamics-fusion, fission, movement, and mitophagy-in neurodegenerative diseases. Human Molecular Genetics *18*, R169–R176.

Chen, Y., and Klionsky, D.J. (2011). The regulation of autophagy – unanswered questions. J Cell Sci *124*, 161–170.

Chen, P., Nordstrom, W., Gish, B., and Abrams, J.M. (1996). grim, a novel cell death gene in Drosophila. Genes Dev. *10*, 1773–1782.

Chen, Y., Azad, M.B., and Gibson, S.B. (2009). Superoxide is the major reactive oxygen species regulating autophagy. Cell Death Differ. *16*, 1040–1052.

Chevrollier, A., Loiseau, D., Reynier, P., and Stepien, G. (2011). Adenine nucleotide translocase 2 is a key mitochondrial protein in cancer metabolism. Biochim. Biophys. Acta *1807*, 562–567.

Chiang, H.L., Terlecky, S.R., Plant, C.P., and Dice, J.F. (1989). A role for a 70-kilodalton heat shock protein in lysosomal degradation of intracellular proteins. Science *246*, 382–385.

Cho, D.-H., Jo, Y.K., Hwang, J.J., Lee, Y.M., Roh, S.A., and Kim, J.C. (2009). Caspase-mediated cleavage of ATG6/Beclin-1 links apoptosis to autophagy in HeLa cells. Cancer Letters *274*, 95–100.

Clark, S.L. (1957). CELLULAR DIFFERENTIATION IN THE KIDNEYS OF NEWBORN MICE STUDIED WITH THE ELECTRON MICROSCOPE. J Biophys Biochem Cytol *3*, 349–362.

Clavería, C., Caminero, E., Martínez-A, C., Campuzano, S., and Torres, M. (2002). GH3, a novel proapoptotic domain in Drosophila Grim, promotes a mitochondrial death pathway. EMBO J. *21*, 3327–3336.

Colussi, P.A., Quinn, L.M., Huang, D.C., Coombe, M., Read, S.H., Richardson, H., and Kumar, S. (2000). Debcl, a proapoptotic Bcl-2 homologue, is a component of the Drosophila melanogaster cell death machinery. J. Cell Biol. *148*, 703–714.

Conradt, B., and Horvitz, H.R. (1998). The C. elegans protein EGL-1 is required for programmed cell death and interacts with the Bcl-2-like protein CED-9. Cell *93*, 519–529.

Cox, R.T., and Spradling, A.C. (2003). A Balbiani Body and the Fusome Mediate Mitochondrial Inheritance During Drosophila Oogenesis. Development *130*, 1579–1590.

Crawford, E.D., and Wells, J.A. (2011). Caspase Substrates and Cellular Remodeling. Annual Review of Biochemistry *80*, 1055–1087.

Cuervo, A.M., and Dice, J.F. (1996). A receptor for the selective uptake and degradation of proteins by lysosomes. Science *273*, 501–503.

Cuervo, A.M., Dice, J.F., and Knecht, E. (1997). A population of rat liver lysosomes responsible for the selective uptake and degradation of cytosolic proteins. J. Biol. Chem. *272*, 5606–5615.

Cumming, R.C., Simonsen, A., and Finley, K.D. (2008). Quantitative analysis of autophagic activity in Drosophila neural tissues by measuring the turnover rates of pathway substrates. Meth. Enzymol. *451*, 639–651.

Degenhardt, K., Sundararajan, R., Lindsten, T., Thompson, C., and White, E. (2002). Bax and Bak Independently Promote Cytochrome cRelease from Mitochondria. J. Biol. Chem. *277*, 14127–14134.

Degenhardt, K., Mathew, R., Beaudoin, B., Bray, K., Anderson, D., Chen, G., Mukherjee, C., Shi, Y., Gélinas, C., Fan, Y., et al. (2006). Autophagy promotes tumor cell survival and restricts necrosis, inflammation, and tumorigenesis. Cancer Cell *10*, 51–64.

Demon, D., Van Damme, P., Vanden Berghe, T., Vandekerckhove, J., Declercq, W., Gevaert, K., and Vandenabeele, P. (2009). Caspase substrates: easily caught in deep waters? Trends Biotechnol. *27*, 680–688.

Denton, D., Shravage, B., Simin, R., Mills, K., Berry, D.L., Baehrecke, E.H., and Kumar, S. (2009). Autophagy, not apoptosis, is essential for midgut cell death in Drosophila. Curr. Biol. *19*, 1741–1746.

Dezelee, S., Bras, F., Contamine, D., Lopez-Ferber, M., Segretain, D., and Teninges, D. (1989). Molecular analysis of ref(2)P, a Drosophila gene implicated in sigma rhabdovirus multiplication and necessary for male fertility. The EMBO Journal *8*, 3437–3446.

Díaz-Troya, S., Pérez-Pérez, M.E., Florencio, F.J., and Crespo, J.L. (2008). The role of TOR in autophagy regulation from yeast to plants and mammals. Autophagy *4*, 851–865.

Donepudi, M., Mac Sweeney, A., Briand, C., and Grütter, M.G. (2003). Insights into the regulatory mechanism for caspase-8 activation. Mol. Cell *11*, 543–549.

Dorstyn, L., Read, S., Cakouros, D., Huh, J.R., Hay, B.A., and Kumar, S. (2002). The role of cytochrome c in caspase activation in Drosophila melanogaster cells. J Cell Biol *156*, 1089–1098.

Doumanis, J., Dorstyn, L., and Kumar, S. (2007). Molecular determinants of the subcellular localization of the Drosophila Bcl-2 homologues DEBCL and BUFFY. Cell Death Differ *14*, 907–915.

Drummond-Barbosa, D., and Spradling, A.C. (2001). Stem cells and their progeny respond to nutritional changes during Drosophila oogenesis. Dev. Biol. *231*, 265–278.

Dunn, W.A., Jr (1990). Studies on the mechanisms of autophagy: formation of the autophagic vacuole. J. Cell Biol. *110*, 1923–1933.

De Duve, C., and Wattiaux, R. (1966). Functions of Lysosomes. Annual Review of Physiology *28*, 435–492.

DE DUVE, C. (1963). The lysosome. Sci. Am. *208*, 64–72.

Eisenberg-Lerner, A., Bialik, S., Simon, H.-U., and Kimchi, A. (2009). Life and death partners: apoptosis, autophagy and the cross-talk between them. Cell Death & Differentiation *16*, 966–975.

Ellis, H.M., and Horvitz, H.R. (1986). Genetic control of programmed cell death in the nematode C. elegans. Cell *44*, 817–829.

Etchegaray, J.I., Timmons, A.K., Klein, A.P., Pritchett, T.L., Welch, E., Meehan, T.L., Li, C., and McCall, K. (2012). Draper acts through the JNK pathway to control synchronous engulfment of dying germline cells by follicular epithelial cells. Development *139*, 4029–4039.

Fernández-Salas, E., Suh, K.S., Speransky, V.V., Bowers, W.L., Levy, J.M., Adams, T., Pathak, K.R., Edwards, L.E., Hayes, D.D., Cheng, C., et al. (2002). mtCLIC/CLIC4, an organellular chloride channel protein, is increased by DNA damage and participates in the apoptotic response to p53. Mol. Cell. Biol. *22*, 3610–3620.

Fernando, P., Kelly, J.F., Balazsi, K., Slack, R.S., and Megeney, L.A. (2002). Caspase 3 activity is required for skeletal muscle differentiation. Proc. Natl. Acad. Sci. U.S.A. *99*, 11025–11030.

Filkins, J.P. (1970). Lysosomes and hepatic regression during fasting. Am. J. Physiol. *219*, 923–927.

Florentin, A., and Arama, E. (2012). Caspase Levels and Execution Efficiencies Determine the Apoptotic Potential of the Cell. J Cell Biol *196*, 513–527.

Foley, K., and Cooley, L. (1998). Apoptosis in Late Stage Drosophila Nurse Cells Does Not Require Genes Within the H99 Deficiency. Development *125*, 1075–1082.

Fred Dice, J. (1990). Peptide sequences that target cytosolic proteins for lysosomal proteolysis. Trends in Biochemical Sciences *15*, 305–309.

Fujita, N., Itoh, T., Omori, H., Fukuda, M., Noda, T., and Yoshimori, T. (2008). The Atg16L complex specifies the site of LC3 lipidation for membrane biogenesis in autophagy. Mol. Biol. Cell *19*, 2092–2100.

Funderburk, S.F., Wang, Q.J., and Yue, Z. (2010). The Beclin 1–VPS34 complex – at the crossroads of autophagy and beyond. Trends in Cell Biology *20*, 355–362.

Gallerne, C., Touat, Z., Chen, Z.X., Martel, C., Mayola, E., Sharaf el dein, O., Buron, N., Le Bras, M., Jacotot, E., Borgne-Sanchez, A., et al. (2010). The fourth isoform of the adenine nucleotide translocator inhibits mitochondrial apoptosis in cancer cells. Int. J. Biochem. Cell Biol. *42*, 623–629.

Galluzzi, L., Kepp, O., Trojel-Hansen, C., and Kroemer, G. (2012). Non-apoptotic functions of apoptosis-regulatory proteins. EMBO Reports *13*, 322–330.

Ganley, I.G., Lam, D.H., Wang, J., Ding, X., Chen, S., and Jiang, X. (2009). ULK1·ATG13·FIP200 Complex Mediates mTOR Signaling and Is Essential for Autophagy. J Biol Chem *284*, 12297–12305.

Garay-Malpartida, H.M., Occhiucci, J.M., Alves, J., and Belizário, J.E. (2005). CaSPredictor: a new computer-based tool for caspase substrate prediction. Bioinformatics *21 Suppl 1*, i169–176.

Geetha, T., and Wooten, M.W. (2002). Structure and functional properties of the ubiquitin binding protein p62. FEBS Lett. *512*, 19–24.

Geisbrecht, E.R., and Montell, D.J. (2004). A Role for Drosophila IAP1-Mediated Caspase Inhibition in Rac-Dependent Cell Migration. Cell *118*, 111–125.

Gingras, A.-C., Gstaiger, M., Raught, B., and Aebersold, R. (2007). Analysis of protein complexes using mass spectrometry. Nature Reviews Molecular Cell Biology *8*, 645–654.

Giorgi, F., and Deri, P. (1976). Cell death in ovarian chambers of Drosophila melanogaster. Journal of Embryology and Experimental Morphology *35*, 521 –533.

Gleason, C.E., Lu, D., Witters, L.A., Newgard, C.B., and Birnbaum, M.J. (2007). The Role of AMPK and mTOR in Nutrient Sensing in Pancreatic B-Cells. J. Biol. Chem. *282*, 10341–10351.

Gomes, L.C., Benedetto, G.D., and Scorrano, L. (2011). During autophagy mitochondria elongate, are spared from degradation and sustain cell viability. Nature Cell Biology *13*, 589–598.

Goyal, L., McCall, K., Agapite, J., Hartwieg, E., and Steller, H. (2000). Induction of apoptosis by Drosophila reaper, hid and grim through inhibition of IAP function. EMBO J. *19*, 589–597.

Grether, M.E., Abrams, J.M., Agapite, J., White, K., and Steller, H. (1995). The head involution defective gene of Drosophila melanogaster functions in programmed cell death. Genes Dev. *9*, 1694–1708.

Gumienny, T.L., Lambie, E., Hartwieg, E., Horvitz, H.R., and Hengartner, M.O. (1999). Genetic control of programmed cell death in the Caenorhabditis elegans hermaphrodite germline. Development *126*, 1011–1022.

Guruharsha, K.G., Rual, J.-F., Zhai, B., Mintseris, J., Vaidya, P., Vaidya, N., Beekman, C., Wong, C., Rhee, D.Y., Cenaj, O., et al. (2011). A Protein Complex Network of Drosophila melanogaster. Cell *147*, 690–703.

Hailey, D.W., Rambold, A.S., Satpute-Krishnan, P., Mitra, K., Sougrat, R., Kim, P.K., and Lippincott-Schwartz, J. (2010). Mitochondria Supply Membranes for Autophagosome Biogenesis during Starvation. Cell *141*, 656–667.

Haining, W.N., Carboy-Newcomb, C., Wei, C.L., and Steller, H. (1999). The proapoptotic function of Drosophila Hid is conserved in mammalian cells. Proc. Natl. Acad. Sci. U.S.A. *96*, 4936–4941.

Hanada, T., Noda, N.N., Satomi, Y., Ichimura, Y., Fujioka, Y., Takao, T., Inagaki, F., and Ohsumi, Y. (2007). The Atg12-Atg5 Conjugate Has a Novel E3-like Activity for Protein Lipidation in Autophagy. J. Biol. Chem. *282*, 37298–37302.

Handler, D., Olivieri, D., Novatchkova, M., Gruber, F.S., Meixner, K., Mechtler, K., Stark, A., Sachidanandam, R., and Brennecke, J. (2011). A systematic analysis of Drosophila TUDOR domain-containing proteins identifies Vreteno and the Tdrd12 family as essential primary piRNA pathway factors. The EMBO Journal *30*, 3977–3993.

Hara, T., and Mizushima, N. (2009). Role of ULK-FIP200 complex in mammalian autophagy: FIP200, a counterpart of yeast Atg17? Autophagy *5*, 85–87.

Harding, T.M., Morano, K.A., Scott, S.V., and Klionsky, D.J. (1995). Isolation and characterization of yeast mutants in the cytoplasm to vacuole protein targeting pathway. J. Cell Biol. *131*, 591–602.

Harding, T.M., Hefner-Gravink, A., Thumm, M., and Klionsky, D.J. (1996). Genetic and Phenotypic Overlap between Autophagy and the Cytoplasm to Vacuole Protein Targeting Pathway. J. Biol. Chem. *271*, 17621–17624.

Harrop, S.J., DeMaere, M.Z., Fairlie, W.D., Reztsova, T., Valenzuela, S.M., Mazzanti, M., Tonini, R., Qiu, M.R., Jankova, L., Warton, K., et al. (2001). Crystal Structure of a Soluble Form of the Intracellular Chloride Ion Channel CLIC1 (NCC27) at 1.4-Å Resolution. J. Biol. Chem. *276*, 44993–45000.

Hawkins, C.J., Yoo, S.J., Peterson, E.P., Wang, S.L., Vernooy, S.Y., and Hay, B.A. (2000). The Drosophila Caspase DRONC Cleaves following Glutamate or Aspartate and Is Regulated by DIAP1, HID, and GRIM. J. Biol. Chem. *275*, 27084–27093.

Hay, B.A., and Guo, M. (2006). Caspase-Dependent Cell Death in Drosophila. Annual Review of Cell and Developmental Biology *22*, 623–650.

Hengartner, M.O., and Horvitz, H.R. (1994). C. elegans cell survival gene ced-9 encodes a functional homolog of the mammalian proto-oncogene bcl-2. Cell *76*, 665–676.

Hennig, K.M., Colombani, J., and Neufeld, T.P. (2006). TOR coordinates bulk and targeted endocytosis in the Drosophila melanogaster fat body to regulate cell growth. J. Cell Biol. *173*, 963–974.

Homyk, T., and Sheppard, D.E. (1977). Behavioral Mutants of Drosophila Melanogaster. I. Isolation and Mapping of Mutations Which Decrease Flight Ability. Genetics *87*, 95–104.

Hong, D.S., Banerji, U., Tavana, B., George, G.C., Aaron, J., and Kurzrock, R. (2012). Targeting the molecular chaperone heat shock protein 90 (HSP90): Lessons learned and future directions. Cancer Treat. Rev.

Hosokawa, N., Hara, T., Kaizuka, T., Kishi, C., Takamura, A., Miura, Y., Iemura, S., Natsume, T., Takehana, K., Yamada, N., et al. (2009). Nutrient-dependent mTORC1 Association with the ULK1–Atg13–FIP200 Complex Required for Autophagy. Mol. Biol. Cell *20*, 1981–1991.

Hou, W., Han, J., Lu, C., Goldstein, L.A., and Rabinowich, H. (2010). Autophagic degradation of active caspase-8: A crosstalk mechanism between autophagy and apoptosis. Autophagy *6*, 891–900.

Hou, Y.-C.C., Chittaranjan, S., Barbosa, S.G., McCall, K., and Gorski, S.M. (2008). Effector caspase Dcp-1 and IAP protein Bruce regulate starvation-induced autophagy during Drosophila melanogaster oogenesis. J Cell Biol *182*, 1127–1139.

Høyer-Hansen, M., and Jäättelä, M. (2008). Autophagy: An emerging target for cancer therapy. Autophagy *4*, 574–580.

Huang, Q., Li, F., Liu, X., Li, W., Shi, W., Liu, F.-F., O'Sullivan, B., He, Z., Peng, Y., Tan, A.-C., et al. (2011). Caspase 3-mediated stimulation of tumor cell repopulation during cancer radiotherapy. Nature Medicine *17*, 860–866.

Hubbard, V.M., Valdor, R., Patel, B., Singh, R., Cuervo, A.M., and Macian, F. (2010). Macroautophagy regulates energy metabolism during effector T cell activation. J. Immunol. *185*, 7349–7357.

Huh, J.R., Vernooy, S.Y., Yu, H., Yan, N., Shi, Y., Guo, M., and Hay, B.A. (2003). Multiple Apoptotic Caspase Cascades Are Required in Nonapoptotic Roles for Drosophila Spermatid Individualization. PLoS Biol *2*, e15.

Huh, J.R., Guo, M., and Hay, B.A. (2004). Compensatory proliferation induced by cell death in the Drosophila wing disc requires activity of the apical cell death caspase Dronc in a nonapoptotic role. Curr. Biol. *14*, 1262–1266.

Ichimura, Y., Kirisako, T., Takao, T., Satomi, Y., Shimonishi, Y., Ishihara, N., Mizushima, N., Tanida, I., Kominami, E., Ohsumi, M., et al. (2000). A ubiquitin-like system mediates protein lipidation. Nature *408*, 488–492.

Itakura, E., and Mizushima, N. (2010). Characterization of autophagosome formation site by a hierarchical analysis of mammalian Atg proteins. Autophagy *6*, 764–776.

Jang, J.-Y., Choi, Y., Jeon, Y.-K., Aung, K.C.Y., and Kim, C.-W. (2008). Over-expression of adenine nucleotide translocase 1 (ANT1) induces apoptosis and tumor regression in vivo. BMC Cancer *8*, 160.

Jang, J.-Y., Jeon, Y.-K., Choi, Y., and Kim, C.-W. (2010). Short-hairpin RNA-induced suppression of adenine nucleotide translocase-2 in breast cancer cells restores their susceptibility to TRAIL-induced apoptosis by activating JNK and modulating TRAIL receptor expression. Molecular Cancer *9*, 262.

Jiang, X., and Wang, X. (2000). Cytochrome c promotes caspase-9 activation by inducing nucleotide binding to Apaf-1. J. Biol. Chem. *275*, 31199–31203.

Jiang, Z.L., Fletcher, N.M., Diamond, M.P., Abu-Soud, H.M., and Saed, G.M. (2009). S-nitrosylation of caspase-3 is the mechanism by which adhesion fibroblasts manifest lower apoptosis. Wound Repair Regen *17*, 224–229.

Joo, J.H., Dorsey, F.C., Joshi, A., Hennessy-Walters, K.M., Rose, K.L., McCastlain, K., Zhang, J., Iyengar, R., Jung, C.H., Suen, D.-F., et al. (2011). Hsp90-Cdc37 Chaperone Complex Regulates Ulk1- and Atg13-Mediated Mitophagy. Molecular Cell *43*, 572–585.

Juhasz, G., and Neufeld, T.P. (2008). Experimental Control and Characterization of Autophagy in Drosophila. In Autophagosome and Phagosome, V. Deretic, ed. (Totowa, NJ: Humana Press), pp. 125–133.

Juhász, G., Érdi, B., Sass, M., and Neufeld, T.P. (2007). Atg7-Dependent Autophagy Promotes Neuronal Health, Stress Tolerance, and Longevity but Is Dispensable for Metamorphosis in Drosophila. Genes Dev. *21*, 3061–3066.

Juhász, G., Hill, J.H., Yan, Y., Sass, M., Baehrecke, E.H., Backer, J.M., and Neufeld, T.P. (2008). The class III PI(3)K Vps34 promotes autophagy and endocytosis but not TOR signaling in Drosophila. J Cell Biol *181*, 655–666.

Jung, C.H., Jun, C.B., Ro, S.-H., Kim, Y.-M., Otto, N.M., Cao, J., Kundu, M., and Kim, D.-H. (2009). ULK-Atg13-FIP200 Complexes Mediate mTOR Signaling to the Autophagy Machinery. Mol. Biol. Cell *20*, 1992–2003.

Kabeya, Y., Mizushima, N., Ueno, T., Yamamoto, A., Kirisako, T., Noda, T., Kominami, E., Ohsumi, Y., and Yoshimori, T. (2000). LC3, a mammalian homologue of yeast Apg8p, is localized in autophagosome membranes after processing. EMBO J. *19*, 5720–5728.

Kamada, S., Kusano, H., Fujita, H., Ohtsu, M., Koya, R.C., Kuzumaki, N., and Tsujimoto, Y. (1998). A cloning method for caspase substrates that uses the yeast two-hybrid system: Cloning of the antiapoptotic gene gelsolin. Proc Natl Acad Sci U S A *95*, 8532–8537.

Kamada, Y., Funakoshi, T., Shintani, T., Nagano, K., Ohsumi, M., and Ohsumi, Y. (2000). Tor-Mediated Induction of Autophagy via an Apg1 Protein Kinase Complex. J Cell Biol *150*, 1507–1513.

Kamada, Y., Yoshino, K., Kondo, C., Kawamata, T., Oshiro, N., Yonezawa, K., and Ohsumi, Y. (2010). Tor Directly Controls the Atg1 Kinase Complex To Regulate Autophagy. Mol. Cell. Biol. *30*, 1049–1058.

Kanda, H., and Miura, M. (2004). Regulatory Roles of JNK in Programmed Cell Death. J Biochem *136*, 1–6.

Kang, B.H., Plescia, J., Dohi, T., Rosa, J., Doxsey, S.J., and Altieri, D.C. (2007). Regulation of tumor cell mitochondrial homeostasis by an organelle-specific Hsp90 chaperone network. Cell *131*, 257–270.

Kanuka, H., Sawamoto, K., Inohara, N., Matsuno, K., Okano, H., and Miura, M. (1999). Control of the cell death pathway by Dapaf-1, a Drosophila Apaf-1/CED-4-related caspase activator. Mol. Cell *4*, 757–769.

Kanzawa, T., Kondo, Y., Ito, H., Kondo, S., and Germano, I. (2003). Induction of autophagic cell death in malignant glioma cells by arsenic trioxide. Cancer Res. *63*, 2103–2108.

Kaplan, Y., Gibbs-Bar, L., Kalifa, Y., Feinstein-Rotkopf, Y., and Arama, E. (2010). Gradients of a ubiquitin E3 ligase inhibitor and a caspase inhibitor determine differentiation or death in spermatids. Dev. Cell *19*, 160–173.

Karkoulis, P.K., Stravopodis, D.J., Margaritis, L.H., and Voutsinas, G.E. (2010). 17-Allylamino-17-demethoxygeldanamycin induces downregulation of critical Hsp90 protein clients and results in cell cycle arrest and apoptosis of human urinary bladder cancer cells. BMC Cancer *10*, 481.

Kawamata, T., Kamada, Y., Kabeya, Y., Sekito, T., and Ohsumi, Y. (2008). Organization of the pre-autophagosomal structure responsible for autophagosome formation. Mol. Biol. Cell *19*, 2039–2050.

Keller, L.C., Cheng, L., Locke, C.J., Müller, M., Fetter, R.D., and Davis, G.W. (2011). Glial-derived prodegenerative signaling in the Drosophila neuromuscular system. Neuron *72*, 760–775.

Kerr, J.F.R., Wyllie, A.H., and Currie, A.R. (1972). Apoptosis: A Basic Biological Phenomenon with Wide-ranging Implications in Tissue Kinetics. Br J Cancer *26*, 239–257.

Kihara, A., Kabeya, Y., Ohsumi, Y., and Yoshimori, T. (2001). Beclin–phosphatidylinositol 3-kinase complex functions at the trans-Golgi network. EMBO Rep *2*, 330–335.

Kim, J., Kundu, M., Viollet, B., and Guan, K.-L. (2011). AMPK and mTOR regulate autophagy through direct phosphorylation of Ulk1. Nature Cell Biology *13*, 132–141.

Kim, Y.-I., Ryu, T., Lee, J., Heo, Y.-S., Ahnn, J., Lee, S.-J., and Yoo, O. (2010). A genetic screen for modifiers of Drosophila caspase Dcp-1 reveals caspase involvement in autophagy and novel caspase-related genes. BMC Cell Biology *11*, 9.

Kimura, S., Noda, T., and Yoshimori, T. (2007). Dissection of the autophagosome maturation process by a novel reporter protein, tandem fluorescent-tagged LC3. Autophagy *3*, 452–460.

King, R.C. (1970). Ovarian development in Drosophila melanogaster (Academic Press).

Kischkel, F.C., Hellbardt, S., Behrmann, I., Germer, M., Pawlita, M., Krammer, P.H., and Peter, M.E. (1995). Cytotoxicity-dependent APO-1 (Fas/CD95)-associated proteins form a death-inducing signaling complex (DISC) with the receptor. EMBO J *14*, 5579–5588.

Kischkel, F.C., Lawrence, D.A., Chuntharapai, A., Schow, P., Kim, K.J., and Ashkenazi, A. (2000). Apo2L/TRAIL-Dependent Recruitment of Endogenous FADD and Caspase-8 to Death Receptors 4 and 5. Immunity *12*, 611–620.

Klaiman, G., Petzke, T.L., Hammond, J., and LeBlanc, A.C. (2008). Targets of Caspase-6 Activity in Human Neurons and Alzheimer Disease. Mol Cell Proteomics *7*, 1541–1555.

Klionsky, D.J., Cregg, J.M., Dunn, W.A., Jr, Emr, S.D., Sakai, Y., Sandoval, I.V., Sibirny, A., Subramani, S., Thumm, M., Veenhuis, M., et al. (2003). A unified nomenclature for yeast autophagy-related genes. Dev. Cell *5*, 539–545.

Klionsky, D.J., Baehrecke, E.H., Brumell, J.H., Chu, C.T., Codogno, P., Cuervo, A.M., Debnath, J., Deretic, V., Elazar, Z., Eskelinen, E.-L., et al. (2011). A comprehensive glossary of autophagy-related molecules and processes (2nd edition). Autophagy *7*, 1273–1294.

Klionsky, D.J., Abdalla, F.C., Abeliovich, H., Abraham, R.T., Acevedo-Arozena, A., Adeli, K., Agholme, L., Agnello, M., Agostinis, P., Aguirre-Ghiso, J.A., et al. (2012). Guidelines for the use and interpretation of assays for monitoring autophagy. Autophagy *8*, 445–544.

Kokoszka, J.E., Waymire, K.G., Levy, S.E., Sligh, J.E., Cai, J., Jones, D.P., MacGregor, G.R., and Wallace, D.C. (2004). The ADP/ATP translocator is not essential for the mitochondrial permeability transition pore. Nature *427*, 461–465.

Krajewski, S., Krajewska, M., Ellerby, L.M., Welsh, K., Xie, Z., Deveraux, Q.L., Salvesen, G.S., Bredesen, D.E., Rosenthal, R.E., Fiskum, G., et al. (1999). Release of caspase-9 from mitochondria during neuronal apoptosis and cerebral ischemia. PNAS *96*, 5752–5757.

Krieser, R.J., and White, K. (2009). Inside an enigma: do mitochondria contribute to cell death in Drosophila? Apoptosis *14*, 961–968.

Kuranaga, E., and Miura, M. (2007). Nonapoptotic functions of caspases: caspases as regulatory molecules for immunity and cell-fate determination. Trends in Cell Biology *17*, 135–144.

Landry, D., Sullivan, S., Nicolaides, M., Redhead, C., Edelman, A., Field, M., al-Awqati, Q., and Edwards, J. (1993). Molecular cloning and characterization of p64, a chloride channel protein from kidney microsomes. J. Biol. Chem. *268*, 14948–14955.

Landry, D.W., Akabas, M.H., Redhead, C., Edelman, A., Cragoe, E.J., Jr, and Al-Awqati, Q. (1989). Purification and reconstitution of chloride channels from kidney and trachea. Science *244*, 1469–1472.

Laundrie, B., Peterson, J.S., Baum, J.S., Chang, J.C., Fileppo, D., Thompson, S.R., and McCall, K. (2003). Germline cell death is inhibited by P-element insertions disrupting the dcp-1/pita nested gene pair in Drosophila. Genetics *165*, 1881–1888.

Lee, C.Y., and Baehrecke, E.H. (2001). Steroid Regulation of Autophagic Programmed Cell Death During Development. Development *128*, 1443–1455.

Legros, F., Lombès, A., Frachon, P., and Rojo, M. (2002). Mitochondrial Fusion in Human Cells Is Efficient, Requires the Inner Membrane Potential, and Is Mediated by Mitofusins. Mol. Biol. Cell *13*, 4343–4354.

Levine, B., and Kroemer, G. (2008). Autophagy in the Pathogenesis of Disease. Cell *132*, 27–42.

Li, H., Zhu, H., Xu, C.J., and Yuan, J. (1998). Cleavage of BID by caspase 8 mediates the mitochondrial damage in the Fas pathway of apoptosis. Cell *94*, 491–501.

Liang, C., Lee, J., Inn, K.-S., Gack, M.U., Li, Q., Roberts, E.A., Vergne, I., Deretic, V., Feng, P., Akazawa, C., et al. (2008). Beclin1-binding UVRAG targets the class C Vps complex to coordinate autophagosome maturation and endocytic trafficking. Nat Cell Biol *10*, 776–787.

Lisacek, F. (2006). Web-based MS/MS Data Analysis. PROTEOMICS *6*, 22–32.

Littler, D.R., Harrop, S.J., Brown, L.J., Pankhurst, G.J., Mynott, A.V., Luciani, P., Mandyam, R.A., Mazzanti, M., Tanda, S., Berryman, M.A., et al. (2008). Comparison of vertebrate and invertebrate CLIC proteins: The crystal structures of Caenorhabditis elegans EXC-4 and Drosophila melanogaster DmCLIC. Proteins: Structure, Function, and Bioinformatics *71*, 364–378.

Madeo, F., Fröhlich, E., and Fröhlich, K.U. (1997). A yeast mutant showing diagnostic markers of early and late apoptosis. J. Cell Biol. *139*, 729–734.

Madeo, F., Herker, E., Maldener, C., Wissing, S., Lächelt, S., Herlan, M., Fehr, M., Lauber, K., Sigrist, S.J., Wesselborg, S., et al. (2002). A caspase-related protease regulates apoptosis in yeast. Mol. Cell *9*, 911–917.

Maiuri, M.C., Zalckvar, E., Kimchi, A., and Kroemer, G. (2007a). Self-eating and self-killing: crosstalk between autophagy and apoptosis. Nature Reviews Molecular Cell Biology *8*, 741–752.

Maiuri, M.C., Toumelin, G.L., Criollo, A., Rain, J.-C., Gautier, F., Juin, P., Tasdemir, E., Pierron, G., Troulinaki, K., Tavernarakis, N., et al. (2007b). Functional and physical interaction between Bcl-XL and a BH3-like domain in Beclin-1. The EMBO Journal *26*, 2527–2539.

Mancini, M., Nicholson, D.W., Roy, S., Thornberry, N.A., Peterson, E.P., Casciola-Rosen, L.A., and Rosen, A. (1998). The caspase-3 precursor has a cytosolic and mitochondrial distribution: implications for apoptotic signaling. J. Cell Biol. *140*, 1485–1495.

Mannick, J.B., Schonhoff, C., Papeta, N., Ghafourifar, P., Szibor, M., Fang, K., and Gaston, B. (2001). S-Nitrosylation of mitochondrial caspases. J. Cell Biol. *154*, 1111–1116.

Margolis, J., and Spradling, A. (1995). Identification and behavior of epithelial stem cells in the Drosophila ovary. Development *121*, 3797–3807.

Marzella, L., Ahlberg, J., and Glaumann, H. (1980). In vitro uptake of particles by lysosomes. Experimental Cell Research *129*, 460–466.

Mathew, R., Kongara, S., Beaudoin, B., Karp, C.M., Bray, K., Degenhardt, K., Chen, G., Jin, S., and White, E. (2007). Autophagy suppresses tumor progression by limiting chromosomal instability. Genes Dev. *21*, 1367–1381.

Matsunaga, K., Saitoh, T., Tabata, K., Omori, H., Satoh, T., Kurotori, N., Maejima, I., Shirahama-Noda, K., Ichimura, T., Isobe, T., et al. (2009). Two Beclin 1-binding proteins, Atg14L and Rubicon, reciprocally regulate autophagy at different stages. Nature Cell Biology *11*, 385–396.

Mazzoni, C., Herker, E., Palermo, V., Jungwirth, H., Eisenberg, T., Madeo, F., and Falcone, C. (2005). Yeast caspase 1 links messenger RNA stability to apoptosis in yeast. EMBO Rep. *6*, 1076–1081.

McPhee, C.K., and Baehrecke, E.H. (2009). Autophagy in Drosophila melanogaster. Biochimica Et Biophysica Acta (BBA) - Molecular Cell Research *1793*, 1452–1460.

Meier, P., Silke, J., Leevers, S.J., and Evan, G.I. (2000). The Drosophila caspase DRONC is regulated by DIAP1. The EMBO Journal *19*, 598–611.

Meléndez, A., and Neufeld, T.P. (2008). The cell biology of autophagy in metazoans: a developing story. Development *135*, 2347–2360.

Mijaljica, D., Prescott, M., and Devenish, R.J. (2011). Microautophagy in mammalian cells: Revisiting a 40-year-old conundrum. Autophagy *7*, 673–682.

Mizushima, N. (2007). Autophagy: process and function. Genes Dev. *21*, 2861–2873.

Mizushima, N., Yoshimori, T., and Ohsumi, Y. (2011). The Role of Atg Proteins in Autophagosome Formation. Annual Review of Cell and Developmental Biology *27*, 107–132.

Mohseni, N., McMillan, S.C., Chaudhary, R., Mok, J., and Reed, B.H. (2009). Autophagy promotes caspase-dependent cell death during Drosophila development. Autophagy *5*, 329–338.

Moscat, J., and Diaz-Meco, M.T. (2009). p62 at the Crossroads of Autophagy, Apoptosis, and Cancer. Cell *137*, 1001–1004.

Muliyil, S., Krishnakumar, P., and Narasimha, M. (2011). Spatial, temporal and molecular hierarchies in the link between death, delamination and dorsal closure. Development *138*, 3043–3054.

Muro, I., Monser, K., and Clem, R.J. (2004). Mechanism of Dronc activation in Drosophila cells. J. Cell. Sci. *117*, 5035–5041.

Muzio, M., Salvesen, G.S., and Dixit, V.M. (1997). FLICE induced apoptosis in a cell-free system. Cleavage of caspase zymogens. J. Biol. Chem. *272*, 2952–2956.

Nargund, A.M., Pellegrino, M.W., Fiorese, C.J., Baker, B.M., and Haynes, C.M. (2012). Mitochondrial import efficiency of ATFS-1 regulates mitochondrial UPR activation. Science *337*, 587–590.

Nezis, I.P., Stravopodis, D.J., Papassideri, I., Robert-Nicoud, M., and Margaritis, L.H. (2000). Stage-specific apoptotic patterns during Drosophila oogenesis. Eur. J. Cell Biol. *79*, 610–620.

Nezis, I.P., Stravopodis, D.J., Papassideri, I., Robert-Nicoud, M., and Margaritis, L.H. (2002). Dynamics of apoptosis in the ovarian follicle cells during the late stages of Drosophila oogenesis. Cell Tissue Res. *307*, 401–409.

Nezis, I.P., Simonsen, A., Sagona, A.P., Finley, K., Gaumer, S., Contamine, D., Rusten, T.E., Stenmark, H., and Brech, A. (2008). Ref(2)P, the Drosophila melanogaster homologue of mammalian p62, is required for the formation of protein aggregates in adult brain. The Journal of Cell Biology *180*, 1065 –1071.

Nezis, I.P., Lamark, T., Velentzas, A.D., Rusten, T.E., Bjørkøy, G., Johansen, T., Papassideri, I.S., Stravopodis, D.J., Margaritis, L.H., Stenmark, H., et al. (2009). Cell death during Drosophila melanogaster early oogenesis is mediated through autophagy. Autophagy *5*, 298–303.

Nezis, I.P., Shravage, B.V., Sagona, A.P., Lamark, T., Bjørkøy, G., Johansen, T., Rusten, T.E., Brech, A., Baehrecke, E.H., and Stenmark, H. (2010). Autophagic degradation of dBruce controls DNA fragmentation in nurse cells during late Drosophila melanogaster oogenesis. The Journal of Cell Biology *190*, 523 –531.

Nicholson, D.W. (1999). Caspase structure, proteolytic substrates, and function during apoptotic cell death. , Published Online: 24 November 1999; | Doi:10.1038/sj.cdd.44005986.

Nikolaev, A., McLaughlin, T., O'Leary, D.D.M., and Tessier-Lavigne, M. (2009). APP binds DR6 to trigger axon pruning and neuron death via distinct caspases. Nature *457*, 981–989.

Nimmanapalli, R., O'Bryan, E., Kuhn, D., Yamaguchi, H., Wang, H.-G., and Bhalla, K.N. (2003). Regulation of 17-AAG—induced apoptosis: role of Bcl-2, Bcl-xL, and Bax downstream of 17-AAG—mediated down-regulation of Akt, Raf-1, and Src kinases. Blood *102*, 269–275.

Oberst, A., Pop, C., Tremblay, A.G., Blais, V., Denault, J.-B., Salvesen, G.S., and Green, D.R. (2010). Inducible Dimerization and Inducible Cleavage Reveal a Requirement for Both Processes in Caspase-8 Activation. J Biol Chem *285*, 16632–16642.

Olson, M.R., Holley, C.L., Gan, E.C., Colón-Ramos, D.A., Kaplan, B., and Kornbluth, S. (2003). A GH3-like domain in reaper is required for mitochondrial localization and induction of IAP degradation. J. Biol. Chem. *278*, 44758–44768.

Ouyang, Y., Petritsch, C., Wen, H., Jan, L., Jan, Y.N., and Lu, B. (2011). Dronc Caspase Exerts a Non-Apoptotic Function to Restrain Phospho-Numb-Induced Ectopic Neuroblast Formation in Drosophila. Development *138*, 2185–2196.

Palacios, C., Martín-Pérez, R., López-Pérez, A.I., Pandiella, A., and López-Rivas, A. (2010). Autophagy inhibition sensitizes multiple myeloma cells to 17-dimethylaminoethylamino-17-demethoxygeldanamycin-induced apoptosis. Leuk. Res. *34*, 1533–1538.

Pankiv, S., Clausen, T.H., Lamark, T., Brech, A., Bruun, J.-A., Outzen, H., Øvervatn, A., Bjørkøy, G., and Johansen, T. (2007). p62/SQSTM1 Binds Directly to Atg8/LC3 to Facilitate Degradation of Ubiquitinated Protein Aggregates by Autophagy. J. Biol. Chem. *282*, 24131–24145.

Pattingre, S., Tassa, A., Qu, X., Garuti, R., Liang, X.H., Mizushima, N., Packer, M., Schneider, M.D., and Levine, B. (2005). Bcl-2 antiapoptotic proteins inhibit Beclin 1-dependent autophagy. Cell *122*, 927–939.

Perrimon, N., Engstrom, L., and Mahowald, A.P. (1984). The effects of zygotic lethal mutations on female germ-line functions in Drosophila. Developmental Biology *105*, 404–414.

Peterson, J.S., Bass, B.P., Jue, D., Rodriguez, A., Abrams, J.M., and McCall, K. (2007). Noncanonical cell death pathways act during Drosophila oogenesis. Genesis *45*, 396–404.

Petiot, A., Ogier-Denis, E., Blommaart, E.F.C., Meijer, A.J., and Codogno, P. (2000). Distinct Classes of Phosphatidylinositol 3′-Kinases Are Involved in Signaling Pathways That Control Macroautophagy in HT-29 Cells. J. Biol. Chem. *275*, 992–998.

Pfaff, E., and Klingenberg, M. (1968). Adenine Nucleotide Translocation of Mitochondria. European Journal of Biochemistry *6*, 66–79.

Pfaff, E., Heldt, H.W., and Klingenberg, M. (1969). Adenine Nucleotide Translocation of Mitochondria. European Journal of Biochemistry *10*, 484–493.

Pircs, K., Nagy, P., Varga, A., Venkei, Z., Erdi, B., Hegedus, K., and Juhasz, G. (2012). Advantages and limitations of different p62-based assays for estimating autophagic activity in Drosophila. PLoS ONE *7*, e44214.

Pop, C., and Salvesen, G.S. (2009). Human Caspases: Activation, Specificity, and Regulation. J. Biol. Chem. *284*, 21777–21781.

Prasad, S., Soldatenkov, V.A., Srinivasarao, G., and Dritschilo, A. (1998). Identification of keratins 18, 19 and heat-shock protein 90 beta as candidate substrates of proteolysis during ionizing radiation-induced apoptosis of estrogen-receptor negative breast tumor cells. International Journal of Oncology *13*, 757.

Pyo, J.-O., Jang, M.-H., Kwon, Y.-K., Lee, H.-J., Jun, J.-I., Woo, H.-N., Cho, D.-H., Choi, B., Lee, H., Kim, J.-H., et al. (2005). Essential Roles of Atg5 and FADD in Autophagic Cell Death DISSECTION OF AUTOPHAGIC CELL DEATH INTO VACUOLE FORMATION AND CELL DEATH. J. Biol. Chem. *280*, 20722–20729.

Qu, X., Yu, J., Bhagat, G., Furuya, N., Hibshoosh, H., Troxel, A., Rosen, J., Eskelinen, E.-L., Mizushima, N., Ohsumi, Y., et al. (2003). Promotion of tumorigenesis by heterozygous disruption of the beclin 1 autophagy gene. Journal of Clinical Investigation *112*, 1809–1820.

Quinn, L., Coombe, M., Mills, K., Daish, T., Colussi, P., Kumar, S., and Richardson, H. (2003). Buffy, a Drosophila Bcl-2 protein, has anti-apoptotic and cell cycle inhibitory functions. EMBO J *22*, 3568–3579.

Rabinowitz, J.D., and White, E. (2010). Autophagy and metabolism. Science *330*, 1344–1348.

Radoshevich, L., Murrow, L., Chen, N., Fernandez, E., Roy, S., Fung, C., and Debnath, J. (2010). ATG12 conjugation to ATG3 regulates mitochondrial homeostasis and cell death. Cell *142*, 590–600.

Ravikumar, B., Moreau, K., Jahreiss, L., Puri, C., and Rubinsztein, D.C. (2010). Plasma membrane contributes to the formation of pre-autophagosomal structures. Nat. Cell Biol. *12*, 747–757.

Ren, C., Finkel, S.E., and Tower, J. (2009). Conditional inhibition of autophagy genes in adult Drosophila impairs immunity without compromising longevity. Exp. Gerontol. *44*, 228–235.

Riedl, S.J., and Shi, Y. (2004). Molecular mechanisms of caspase regulation during apoptosis. Nature Reviews Molecular Cell Biology *5*, 897–907.

Rikhy, R., Ramaswami, M., and Krishnan, K.S. (2003). A Temperature-Sensitive Allele of Drosophila sesB Reveals Acute Functions for the Mitochondrial Adenine Nucleotide Translocase in Synaptic Transmission and Dynamin Regulation. Genetics *165*, 1243–1253.

Romanov, J., Walczak, M., Ibiricu, I., Schüchner, S., Ogris, E., Kraft, C., and Martens, S. (2012). Mechanism and functions of membrane binding by the Atg5–Atg12/Atg16 complex during autophagosome formation. The EMBO Journal *31*, 4304–4317.

Rongo, C., and Lehmann, R. (1996). Regulated synthesis, transport and assembly of the Drosophila germ plasm. Trends Genet. *12*, 102–109.

Rosenfeldt, M.T., and Ryan, K.M. (2009). The role of autophagy in tumour development and cancer therapy. Expert Rev Mol Med *11*.

Roy, S., and Debnath, J. (2010). Autophagy and Tumorigenesis. Seminars in Immunopathology *32*, 383–396.

Rubinstein, A.D., Eisenstein, M., Ber, Y., Bialik, S., and Kimchi, A. (2011). The autophagy protein Atg12 associates with antiapoptotic Bcl-2 family members to promote mitochondrial apoptosis. Mol. Cell *44*, 698–709.

Rusten, T.E., Lindmo, K., Juhász, G., Sass, M., Seglen, P.O., Brech, A., and Stenmark, H. (2004). Programmed Autophagy in the Drosophila Fat Body Is Induced by Ecdysone through Regulation of the PI3K Pathway. Developmental Cell *7*, 179–192.

Saleh, A., Srinivasula, S.M., Acharya, S., Fishel, R., and Alnemri, E.S. (1999). Cytochrome c and dATP-mediated Oligomerization of Apaf-1 Is a Prerequisite for Procaspase-9 Activation. J. Biol. Chem. *274*, 17941–17945.

Salt, I.P., Johnson, G., Ashcroft, S.J., and Hardie, D.G. (1998). AMP-activated protein kinase is activated by low glucose in cell lines derived from pancreatic beta cells, and may regulate insulin release. Biochem J *335*, 533–539.

Samali, A., Cai, J., Zhivotovsky, B., Jones, D.P., and Orrenius, S. (1999). Presence of a pre-apoptotic complex of pro-caspase-3, Hsp60 and Hsp10 in the mitochondrial fraction of jurkat cells. EMBO J. *18*, 2040–2048.

Scherz-Shouval, R., Shvets, E., Fass, E., Shorer, H., Gil, L., and Elazar, Z. (2007). Reactive oxygen species are essential for autophagy and specifically regulate the activity of Atg4. EMBO J *26*, 1749–1760.

Schworer, C.M., and Mortimore, G.E. (1979). Glucagon-induced autophagy and proteolysis in rat liver: mediation by selective deprivation of intracellular amino acids. Proc Natl Acad Sci U S A *76*, 3169–3173.

Scott, R.C., Schuldiner, O., and Neufeld, T.P. (2004). Role and Regulation of Starvation-Induced Autophagy in the Drosophila Fat Body. Developmental Cell *7*, 167–178.

Scott, R.C., Juhász, G., and Neufeld, T.P. (2007). Direct Induction of Autophagy by Atg1 Inhibits Cell Growth and Induces Apoptotic Cell Death. Current Biology *17*, 1–11.

Senft, J., Helfer, B., and Frisch, S.M. (2007). Caspase-8 Interacts with the p85 Subunit of Phosphatidylinositol 3-Kinase to Regulate Cell Adhesion and Motility. Cancer Res *67*, 11505–11509.

Sharaf el dein, O., Mayola, E., Chopineau, J., and Brenner, C. (2011). The Adenine Nucleotide Translocase 2, a Mitochondrial Target for Anticancer Biotherapy. Current Drug Targets *12*, 894–901.

Shelly, S., Lukinova, N., Bambina, S., Berman, A., and Cherry, S. (2009). Autophagy plays an essential anti-viral role in Drosophila against Vesicular Stomatitis virus. Immunity *30*, 588–598.

Sheng, Z.-H., and Cai, Q. (2012). Mitochondrial transport in neurons: impact on synaptic homeostasis and neurodegeneration. Nature Reviews Neuroscience.

Shi, Y. (2002). Mechanisms of Caspase Activation and Inhibition during Apoptosis. Molecular Cell *9*, 459–470.

Shintani, T., Mizushima, N., Ogawa, Y., Matsuura, A., Noda, T., and Ohsumi, Y. (1999). Apg10p, a novel protein-conjugating enzyme essential for autophagy in yeast. EMBO J. *18*, 5234–5241.

Shukla, A., Malik, M., Cataisson, C., Ho, Y., Friesen, T., Suh, K.S., and Yuspa, S.H. (2009). TGF-beta signalling is regulated by Schnurri-2-dependent nuclear translocation of CLIC4 and consequent stabilization of phospho-Smad2 and 3. Nat. Cell Biol. *11*, 777–784.

Siegelin, M.D., Dohi, T., Raskett, C.M., Orlowski, G.M., Powers, C.M., Gilbert, C.A., Ross, A.H., Plescia, J., and Altieri, D.C. (2011). Exploiting the mitochondrial unfolded protein response for cancer therapy in mice and human cells. J. Clin. Invest. *121*, 1349–1360.

Simonsen, A., Cumming, R.C., Brech, A., Isakson, P., Schubert, D.R., and Finley, K.D. (2008). Promoting basal levels of autophagy in the nervous system enhances longevity and oxidant resistance in adult Drosophila. Autophagy *4*, 176–184.

Song, Z., McCall, K., and Steller, H. (1997). DCP-1, a Drosophila Cell Death Protease Essential for Development. Science *275*, 536–540.

Song, Z., Guan, B., Bergman, A., Nicholson, D.W., Thornberry, N.A., Peterson, E.P., and Steller, H. (2000). Biochemical and Genetic Interactions betweenDrosophila Caspases and the Proapoptotic Genesrpr, hid, and grim. Mol. Cell. Biol. *20*, 2907–2914.

Sordet, O., Rébé, C., Plenchette, S., Zermati, Y., Hermine, O., Vainchenker, W., Garrido, C., Solary, E., and Dubrez-Daloz, L. (2002). Specific involvement of caspases in the differentiation of monocytes into macrophages. Blood *100*, 4446–4453.

Spowart, J.E., Townsend, K.N., Huwait, H., Eshragh, S., West, N.R., Ries, J.N., Kalloger, S., Anglesio, M., Gorski, S.M., Watson, P.H., et al. (2012). The Autophagy Protein LC3A Correlates with Hypoxia and is a Prognostic Marker of Patient Survival in Clear Cell Ovarian Cancer. J. Pathol.

Srinivasula, S.M., Datta, P., Kobayashi, M., Wu, J.-W., Fujioka, M., Hegde, R., Zhang, Z., Mukattash, R., Fernandes-Alnemri, T., Shi, Y., et al. (2002). sickle, a Novel Drosophila Death Gene in the reaper/hid/grim Region, Encodes an IAP-Inhibitory Protein. Curr Biol *12*, 125–130.

Staab, S., and Steinmann-Zwicky, M. (1996). Female germ cells of Drosophila require zygotic ovo and otu product for survival in larvae and pupae respectively. Mech. Dev. *54*, 205–210.

Stennicke, H.R., Jürgensmeier, J.M., Shin, H., Deveraux, Q., Wolf, B.B., Yang, X., Zhou, Q., Ellerby, H.M., Ellerby, L.M., Bredesen, D., et al. (1998). Pro-caspase-3 Is a Major Physiologic Target of Caspase-8. J. Biol. Chem. *273*, 27084–27090.

Van der Straten, A., Rommel, C., Dickson, B., and Hafen, E. (1997). The heat shock protein 83 (Hsp83) is required for Raf-mediated signalling in Drosophila. EMBO J. *16*, 1961–1969.

Suh, K.S., Mutoh, M., Nagashima, K., Fernandez-Salas, E., Edwards, L.E., Hayes, D.D., Crutchley, J.M., Marin, K.G., Dumont, R.A., Levy, J.M., et al. (2004). The organellular chloride channel protein CLIC4/mtCLIC translocates to the nucleus in response to cellular stress and accelerates apoptosis. J. Biol. Chem. *279*, 4632–4641.

Suh, K.S., Mutoh, M., Mutoh, T., Li, L., Ryscavage, A., Crutchley, J.M., Dumont, R.A., Cheng, C., and Yuspa, S.H. (2007). CLIC4 mediates and is required for Ca2+-induced keratinocyte differentiation. J. Cell. Sci. *120*, 2631–2640.

Suh, K.S., Malik, M., Shukla, A., Ryscavage, A., Wright, L., Jividen, K., Crutchley, J.M., Dumont, R.A., Fernandez-Salas, E., Webster, J.D., et al. (2012). CLIC4 is a tumor suppressor for cutaneous squamous cell cancer. Carcinogenesis *33*, 986–995.

Sulston, J.E., Schierenberg, E., White, J.G., and Thomson, J.N. (1983). The embryonic cell lineage of the nematode Caenorhabditis elegans. Developmental Biology *100*, 64–119.

Susin, S.A., Lorenzo, H.K., Zamzami, N., Marzo, I., Brenner, C., Larochette, N., Prévost, M.-C., Alzari, P.M., and Kroemer, G. (1999). Mitochondrial Release of Caspase-2 and -9 during the Apoptotic Process. J Exp Med *189*, 381–394.

Tait, S.W.G., and Green, D.R. (2010). Mitochondria and cell death: outer membrane permeabilization and beyond. Nat. Rev. Mol. Cell Biol. *11*, 621–632.

Tanida, I., Ueno, T., and Kominami, E. (2004a). LC3 conjugation system in mammalian autophagy. Int. J. Biochem. Cell Biol. *36*, 2503–2518.

Tanida, I., Sou, Y., Ezaki, J., Minematsu-Ikeguchi, N., Ueno, T., and Kominami, E. (2004b). HsAtg4B/HsApg4B/Autophagin-1 Cleaves the Carboxyl Termini of Three Human Atg8 Homologues and Delipidates Microtubule-associated Protein Light Chain 3- and GABAA Receptor-associated Protein-Phospholipid Conjugates. J. Biol. Chem. *279*, 36268–36276.

Tanner, E.A., Blute, T.A., Brachmann, C.B., and McCall, K. (2011). Bcl-2 proteins and autophagy regulate mitochondrial dynamics during programmed cell death in the Drosophila ovary. Development *138*, 327–338.

Tavosanis, G., and Gonzalez, C. (2003). γ-Tubulin function during female germ-cell development and oogenesis in Drosophila. PNAS *100*, 10263–10268.

Tenev, T., Zachariou, A., Wilson, R., Ditzel, M., and Meier, P. (2005). IAPs are functionally non-equivalent and regulate effector caspases through distinct mechanisms. Nat. Cell Biol. *7*, 70–77.

Terhzaz, S., Cabrero, P., Chintapalli, V.R., Davies, S.-A., and Dow, J.A.T. (2010). Mislocalization of Mitochondria and Compromised Renal Function and Oxidative Stress Resistance in Drosophila SesB Mutants. Physiol. Genomics *41*, 33–41.

Tettamanti, G., Malagoli, D., Marchesini, E., Congiu, T., Eguileor, M., and Ottaviani, E. (2006). Oligomycin A induces autophagy in the IPLB-LdFB insect cell line. Cell and Tissue Research *326*, 179–186.

Thomenius, M., Freel, C.D., Horn, S., Krieser, R., Abdelwahid, E., Cannon, R., Balasundaram, S., White, K., and Kornbluth, S. (2011). Mitochondrial fusion is regulated by Reaper to modulate Drosophila programmed cell death. Cell Death Differ *18*, 1640–1650.

Thornberry, N.A., Rano, T.A., Peterson, E.P., Rasper, D.M., Timkey, T., Garcia-Calvo, M., Houtzager, V.M., Nordstrom, P.A., Roy, S., Vaillancourt, J.P., et al. (1997). A Combinatorial Approach Defines Specificities of Members of the Caspase Family and Granzyme B FUNCTIONAL RELATIONSHIPS ESTABLISHED FOR KEY MEDIATORS OF APOPTOSIS. J. Biol. Chem. *272*, 17907–17911.

Tresse, E., Salomons, F.A., Vesa, J., Bott, L.C., Kimonis, V., Yao, T.-P., Dantuma, N.P., and Taylor, J.P. (2010). VCP/p97 is essential for maturation of ubiquitin-containing autophagosomes and this function is impaired by mutations that cause IBMPFD. Autophagy *6*, 217–227.

Tsukada, M., and Ohsumi, Y. (1993). Isolation and characterization of autophagy-defective mutants of Saccharomyces cerevisiae. FEBS Lett. *333*, 169–174.

Twig, G., Elorza, A., Molina, A.J.A., Mohamed, H., Wikstrom, J.D., Walzer, G., Stiles, L., Haigh, S.E., Katz, S., Las, G., et al. (2008). Fission and selective fusion govern mitochondrial segregation and elimination by autophagy. EMBO J. *27*, 433–446.

Uribe, V., Wong, B.K.Y., Graham, R.K., Cusack, C.L., Skotte, N.H., Pouladi, M.A., Xie, Y., Feinberg, K., Ou, Y., Ouyang, Y., et al. (2012). Rescue from excitotoxicity and axonal degeneration accompanied by age-dependent behavioral and neuroanatomical alterations in caspase-6-deficient mice. Hum. Mol. Genet. *21*, 1954–1967.

Vanhaesebroeck, B., Guillermet-Guibert, J., Graupera, M., and Bilanges, B. (2010). The emerging mechanisms of isoform-specific PI3K signalling. Nature Reviews Molecular Cell Biology *11*, 329–341.

Velentzas, A.D., Nezis, I.P., Stravopodis, D.J., Papassideri, I.S., and Margaritis, L.H. (2007). Mechanisms of programmed cell death during oogenesis in Drosophila virilis. Cell Tissue Res. *327*, 399–414.

Wang, S.H., and Elgin, S.C.R. (2011). Drosophila Piwi functions downstream of piRNA production mediating a chromatin-based transposon silencing mechanism in female germ line. Proc. Natl. Acad. Sci. U.S.A. *108*, 21164–21169.

Wang, S.L., Hawkins, C.J., Yoo, S.J., Müller, H.A., and Hay, B.A. (1999). The Drosophila caspase inhibitor DIAP1 is essential for cell survival and is negatively regulated by HID. Cell *98*, 453–463.

Wang, X.-J., Cao, Q., Liu, X., Wang, K.-T., Mi, W., Zhang, Y., Li, L.-F., LeBlanc, A.C., and Su, X.-D. (2010). Crystal structures of human caspase 6 reveal a new mechanism for intramolecular cleavage self-activation. EMBO Rep. *11*, 841–847.

White, E., and DiPaola, R.S. (2009). The Double-Edged Sword of Autophagy Modulation in Cancer. Clin Cancer Res *15*, 5308–5316.

White, K., Tahaoglu, E., and Steller, H. (1996). Cell killing by the Drosophila gene reaper. Science *271*, 805–807.

Whitesell, L., and Lindquist, S.L. (2005). HSP90 and the chaperoning of cancer. Nature Reviews Cancer *5*, 761–772.

Wilson, R., Goyal, L., Ditzel, M., Zachariou, A., Baker, D.A., Agapite, J., Steller, H., and Meier, P. (2002). The DIAP1 RING finger mediates ubiquitination of Dronc and is indispensable for regulating apoptosis. Nature Cell Biology *4*, 445–450.

Wirawan, E., Vande Walle, L., Kersse, K., Cornelis, S., Claerhout, S., Vanoverberghe, I., Roelandt, R., De Rycke, R., Verspurten, J., Declercq, W., et al. Caspase-mediated cleavage of Beclin-1 inactivates Beclin-1-induced autophagy and enhances apoptosis by promoting the release of proapoptotic factors from mitochondria. Cell Death and Dis *1*, e18.

Witkowski, W.A., and Hardy, J.A. (2009). L2′ loop is critical for caspase7 active site formation. Protein Sci *18*, 1459–1468.

Wójcik, C., Yano, M., and DeMartino, G.N. (2004). RNA interference of valosin-containing protein (VCP/p97) reveals multiple cellular roles linked to ubiquitin/proteasome-dependent proteolysis. J Cell Sci *117*, 281–292.

Wu, H., Wang, M.C., and Bohmann, D. (2009). JNK protects Drosophila from oxidative stress by trancriptionally activating autophagy. Mechanisms of Development *126*, 624–637.

Wu, Z., Moghaddas Gholami, A., and Kuster, B. (2012). Systematic identification of the HSP90 candidate regulated proteome. Mol. Cell Proteomics *11*, M111.016675.

Wyers, F., Dru, P., Simonet, B., and Contamine, D. (1993). Immunological cross-reactions and interactions between the Drosophila melanogaster ref(2)P protein and sigma rhabdovirus proteins. J Virol *67*, 3208–3216.

Xanthoudakis, S., Roy, S., Rasper, D., Hennessey, T., Aubin, Y., Cassady, R., Tawa, P., Ruel, R., Rosen, A., and Nicholson, D.W. (1999). Hsp60 accelerates the maturation of pro-caspase-3 by upstream activator proteases during apoptosis. EMBO J. *18*, 2049–2056.

Xu, D., Wang, Y., Willecke, R., Chen, Z., Ding, T., and Bergmann, A. (2006). The effector caspases drICE and dcp-1 have partially overlapping functions in the apoptotic pathway in Drosophila. Cell Death & Differentiation *13*, 1697–1706.

Xue, D., Shaham, S., and Horvitz, H.R. (1996). The Caenorhabditis elegans cell-death protein CED-3 is a cysteine protease with substrate specificities similar to those of the human CPP32 protease. Genes Dev. *10*, 1073–1083.

Yang, Z., and Klionsky, D.J. (2010). Eaten alive: a history of macroautophagy. Nature Cell Biology *12*, 814–822.

Yoneda, M., Miyatake, T., and Attardi, G. (1994). Complementation of mutant and wild-type human mitochondrial DNAs coexisting since the mutation event and lack of complementation of DNAs introduced separately into a cell within distinct organelles. Mol Cell Biol *14*, 2699–2712.

Yoo, B.H., Wu, X., Li, Y., Haniff, M., Sasazuki, T., Shirasawa, S., Eskelinen, E.-L., and Rosen, K.V. (2010). Oncogenic ras-induced down-regulation of autophagy mediator Beclin-1 is required for malignant transformation of intestinal epithelial cells. J. Biol. Chem. *285*, 5438–5449.

Yoo, S.J., Huh, J.R., Muro, I., Yu, H., Wang, L., Wang, S.L., Feldman, R.M.R., Clem, R.J., Müller, H.-A.J., and Hay, B.A. (2002). Hid, Rpr and Grim negatively regulate DIAP1 levels through distinct mechanisms. Nat. Cell Biol. *4*, 416–424.

Youle, R.J., and van der Bliek, A.M. (2012). Mitochondrial fission, fusion, and stress. Science *337*, 1062–1065.

Yousefi, S., Perozzo, R., Schmid, I., Ziemiecki, A., Schaffner, T., Scapozza, L., Brunner, T., and Simon, H.-U. (2006). Calpain-mediated cleavage of Atg5 switches autophagy to apoptosis. Nat Cell Biol *8*, 1124–1132.

Yu, L., Wan, F., Dutta, S., Welsh, S., Liu, Z., Freundt, E., Baehrecke, E.H., and Lenardo, M. (2006). Autophagic programmed cell death by selective catalase degradation. PNAS *103*, 4952–4957.

Yuan, J., Shaham, S., Ledoux, S., Ellis, H.M., and Horvitz, H.R. (1993). The C. elegans cell death gene ced-3 encodes a protein similar to mammalian interleukin-1 beta-converting enzyme. Cell *75*, 641–652.

Yuan, S., Yu, X., Topf, M., Dorstyn, L., Kumar, S., Ludtke, S.J., and Akey, C.W. (2011). Structure of the Drosophila apoptosome at 6.9 å resolution. Structure *19*, 128–140.

Yue, L., Karr, T.L., Nathan, D.F., Swift, H., Srinivasan, S., and Lindquist, S. (1999). Genetic analysis of viable Hsp90 alleles reveals a critical role in Drosophila spermatogenesis. Genetics *151*, 1065–1079.

Zamora, M., Granell, M., Mampel, T., and Viñas, O. (2004). Adenine nucleotide translocase 3 (ANT3) overexpression induces apoptosis in cultured cells. FEBS Lett. *563*, 155–160.

Zhang, Y.Q., Roote, J., Brogna, S., Davis, A.W., Barbash, D.A., Nash, D., and Ashburner, M. (1999). stress sensitive B Encodes an Adenine Nucleotide Translocase in Drosophila melanogaster. Genetics *153*, 891–903.

Zhong, J., Kong, X., Zhang, H., Yu, C., Xu, Y., Kang, J., Yu, H., Yi, H., Yang, X., and Sun, L. (2012). Inhibition of CLIC4 enhances autophagy and triggers mitochondrial and ER stress-induced apoptosis in human glioma U251 cells under starvation. PLoS ONE *7*, e39378.

Zhu, Y., Zhao, L., Liu, L., Gao, P., Tian, W., Wang, X., Jin, H., Xu, H., and Chen, Q. (2010). Beclin 1 cleavage by caspase-3 inactivates autophagy and promotes apoptosis. Protein Cell *1*, 468–477.

Zoratti, M., and Szabò, I. (1995). The mitochondrial permeability transition. Biochim. Biophys. Acta *1241*, 139–176.

Zou, H., Henzel, W.J., Liu, X., Lutschg, A., and Wang, X. (1997). Apaf-1, a human protein homologous to C. elegans CED-4, participates in cytochrome c-dependent activation of caspase-3. Cell *90*, 405–413.